2007:241 CIV

MASTER'S THESIS

# Temperature effects in overcoring stress measurements

Rebecca Bertilsson

Luleå University of Technology

MSc Programmes in Engineering
Engineering Physics
Department of Civil and Environmental Engineering
Division of Rock Mechanics

2007:241 CIV - ISSN: 1402-1617 - ISRN: LTU-EX--07/241--SE

# Abstract

Overcoring is a measurement method used for estimating the state of stress in a rock mass. The method is based on measuring the strains that develop when a sample of rock, by drilling with a hollow core bit, is released from the surrounding rock and the stresses acting upon it.

During the current work to find a site suitable for a future underground repository for final disposal of spent nuclear fuel in Sweden, the overcoring stress measurement method was used in the site investigation programme. In some of these tests temperature effects have been noted, which affect the reliability of the results. The causes and consequences of these effects have not been investigated though. This thesis work was conducted to address part of the issue of temperature effects during overcoring.

The main part of the thesis consisted of a study of which of the parameters (i) logger, (ii) glue, (iii) strain gauges and (iv) material type that were most sensitive to temperature effects during overcoring. The temperature sensitivity was determined by measuring the strains recorded by the logger when heating each object in different test cases.

All of the factors logger, glue and material showed a response dependent on temperature. The response of the logger was so small in magnitude that it could be neglected on basis of the small magnitude of the absolute error it caused on calculated stresses.

The glue showed a response of fairly great magnitude regarding temperature change when not fully cured. When subjected to temperature increase, the curing of the glue was reactivated, causing shrinkage of the material and affecting strain readings to seem smaller in magnitude than the true value.

The rock cores tested showed a temperature response of great magnitude. The response was not that of an ideal material as the cores did not expand and contract as expected when subjected to temperature change. The response could thus not be quantified based on the tests performed

It is not known if these factors are independent or dependent of each other and hence it is hard to tell which factor that is most sensitive to temperature increase during an actual overcoring. The temperature effects of the glue and rock were difficult to quantify and thus also difficult to compensate for. Therefore they should be avoided by minimizing the temperature increase caused by overcoring. This can be done by better flushing and temperature control, by a larger overcoring diameter or possibly by a different overcoring feed speed or different drill bit.

# Sammanfattning

Överborrning är en mätmetod som används för att uppskatta spänningstillståndet i berg med. Metoden baseras på att mäta de töjningar som utbildas då ett stycke berg, genom borrning med en ihålig borrkrona, friläggs från omgivande berg och de spänningar som verkar på det.

Vid platsundersökningarna under det pågående arbetet med att hitta en lämplig plats för ett framtida, underjordiskt slutförvar av kärnbränsle i Sverige användes överborrningsmetoden. I vissa av de här testerna noterades temperatureffekter, vilket påverkar resultatens tillförlitlighet. Orsakerna och konsekvenserna av de här effekterna har dock inte undersökts. Det här examensarbetet utfördes för att belysa en del av problemet med temperatureffekter vid överborrning.

Huvuddelen av arbetet utgjordes av en undersökning av vilken av parametrarna (i) logger, (ii) lim, (iii) töjningsgivare och (iv) materialtyp som var mest känslig för temperatureffekter vid överborrning. Temperaturkänsligheten undersöktes genom att mäta de töjningar som registrerades av loggern när varje föremål värmdes i olika testfall.

Alla faktorerna logger, lim och material visade en temperaturberoende respons. Loggerns respons var av så liten storleksordning att den kunde försummas på grund av det lilla absolutfel den orsakade på beräknade spänningar.

Då limmet inte var helt härdat visade det en relativt stor respons med avseende på temperaturförändring. När det utsattes för en temperaturhöjning återaktiverades härdningsprocessen vilket orsakade krympning av materialet och fick töjningarna att förefalla mindre i storleksorning än det verkliga värdet.

Bergkärnorna som testades visade en betydande temperaturrespons. Responsen var inte den från ett idealt material eftersom kärnorna inte expanderade och kontraherade som förväntat när de utsattes för temperaturförändring. Responsen kunde inte kvantifieras grundat på de test som utfördes.

Det är inte känt om de här faktorerna är oberoende eller beroende av varandra och därför är det svårt att avgöra vilken faktor som är mest känslig för temperaturhöjning vid en verklig överborrning. Temperatureffekterna som limmet och berget visade var svåra att kvantifiera och därför även svåra att kompensera för. De bör därför undvikas genom att minimera temperaturökning orsakad av överborrning. Detta kan uppnås genom bättre spolning och temperaturkontroll, genom större överborrningsdiameter och möjligtvis genom annan borrhastighet eller borrkrona.

# Table of contents

# 1 Introduction

## 1.1 Problem description

SKB (Swedish Nuclear Fuel and Waste Management Company) is the company assigned to manage and dispose of the radioactive waste from Swedish nuclear power plants. Current work is to find a site suitable for a future underground repository for final disposal of spent nuclear fuel. The two places of choice are narrowed down to Forsmark and Oskarshamn. To determine which place is more suitable, site investigations have been performed in order to get as much knowledge as possible about the local conditions in the bedrock and ambient environment.

During the site investigations, among other tests (www.skb.se), overcoring stress measurements were performed. The overcoring stress measurement method is based on measuring the strains that develop when a sample of rock, by drilling with a hollow core bit, is released from the rock and the stresses acting upon it. Some tests have shown temperature effects which affect the reliability of these results (Lindfors et al., 2007). The temperature effects are displayed as a rapid increase in strain during overcoring, followed by subsiding strains once the cell has been overcored and the temperature decreases. It also appears that this temperature effect is more pronounced at Forsmark, in particular in boreholes KFM07C and KFM02B, compared to Oskarshamn (cf. Lindfors et al., 2007 and Sjöberg & Perman, 2005). In Figure 1.1 and Figure 1.2 examples of strain data readings during overcoring are shown, the first with temperature effects and the second without.

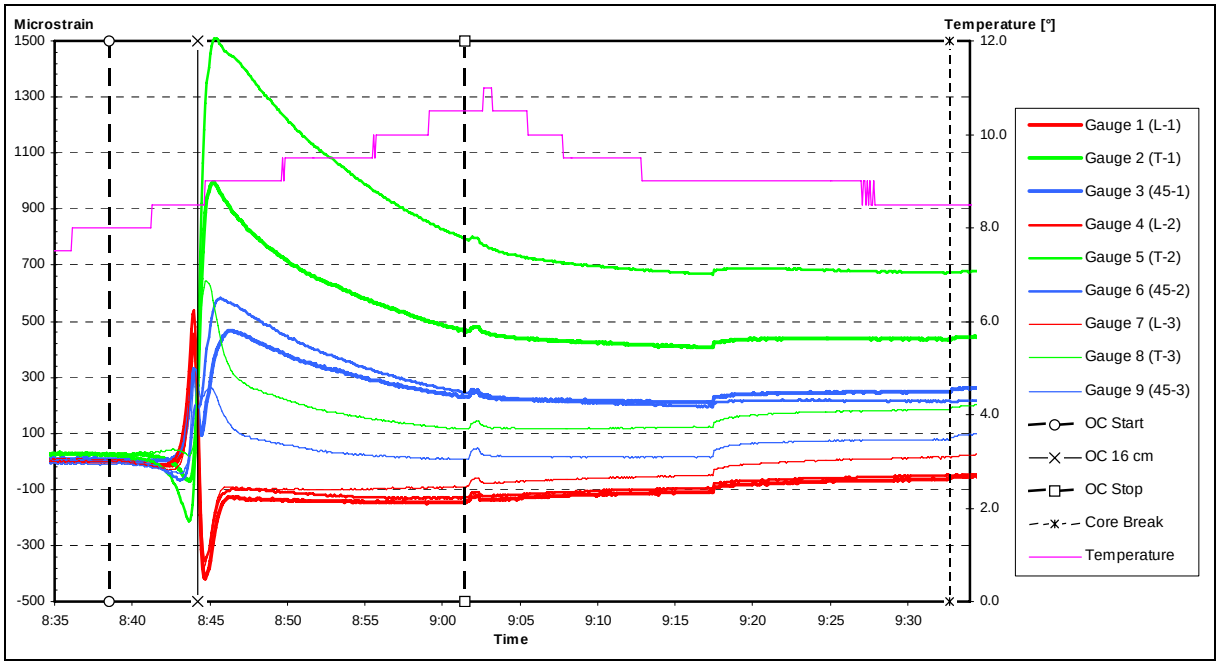


**Figure 1.1 Strain data reading with temperature effects. From Forsmark, borehole KFM07C test no. 2:9:1 (Lindfors et al., 2007).**

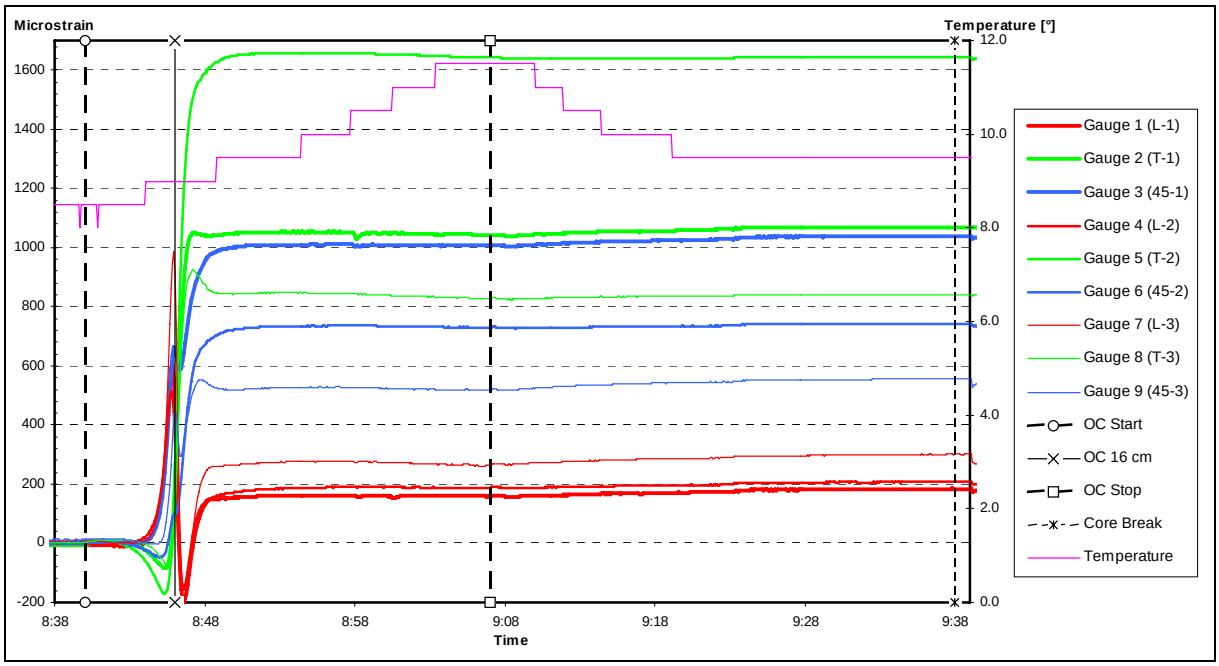


**Figure 1.2 Strain data reading without temperature effects. From Forsmark, borehole KFM01B test no. 1:4:1 (Sjöberg, 2004).**

## 1.2 Objective and scope

Temperature effects have been noted in overcoring stress measurement results but the causes and consequences of these have not been investigated. This thesis work was conducted to address part of the issue of temperature effects during overcoring. The work was performed for SKB at the Luleå University of Technology through supervision by Vattenfall Power Consultant.

The main part of the thesis consists of a study of which of the parameters (i) logger, (ii) glue, (iii) strain gauges, (iv) glue + strain gauges, (v) material type and (vi) the system logger + glue + strain gauges + rock that are most sensitive to temperature effects during overcoring and a quantification of these effects in terms of strain and stress values.

The report opens with the general theory of overcoring and core drilling discussed in Chapter 2 together with a summary of previous knowledge in the field of temperature effects during overcoring and an introduction to polymer materials. Chapter 3 presents the outcome of a numerical simulation made in an attempt to estimate the temperature that the strain gauges might be exposed to during overcoring. Following, in Chapter 4, are laboratory experiments where the temperature sensitivity of the factors mentioned above was examined. Finally the thesis is concluded in Chapter 5 with an evaluation of the results achieved, and recommendations of how to handle temperature effects for both conducted and future measurements in Chapter 6.

## 1.3 Rock mechanic basics

The rock mass is defined as a larger volume of intact rock together with discontinuities such as joints and faults. The state of stress in a rock mass is usually divided into primary and secondary stresses. Primary stresses are the undisturbed stresses that exist in a rock mass before any interference of man, and secondary stresses are the disturbed stresses that exist after interference of man. The primary state of stress in a rock mass depends mainly on gravity and tectonics. It can in many cases be described with one vertical principal stress and

two horizontal stress components. The vertical stress component is often assumed to be purely gravitational, caused by the weight of the overburden and described as

$$\sigma_z \text{ [Pa]} = \rho \cdot g \cdot z, \quad (1.1)$$

where
$\sigma_z$ [Pa] = vertical stress,
$\rho$ [kg/m$^3$] = density of the rock mass,
g [m/s$^2$] = gravitational acceleration,
z [m] = depth below rock surface.

The minor and major horizontal stresses are named $\sigma_h$ and $\sigma_H$ respectively. In old shield regions, the major horizontal stress is generally larger than the vertical stress. In Scandinavia the state of stress can roughly be described as (Nordlund, Rådberg & Sjöberg, 1998)

$$\sigma_z \text{ [MPa]} = 0.027 \cdot z, \quad (1.2)$$
$$\sigma_H \text{ [MPa]} = 2.8 + 0.04 \cdot z, \quad (1.3)$$
$$\sigma_h \text{ [MPa]} = 2.2 + 0.024 \cdot z \quad (1.4)$$

assuming that $\rho = 2700$ kg/m$^3$.

## 1.4 Rock drilling basics

The most common methods of rock drilling can be divided into:

- Rotary percussive drilling, where a piston moves forth and back, pounding on the drill bit under simultaneous rotation.
- Rotary crushing drilling, where the drill bit is pressed against the rock and simultaneously rotated.
- Rotary cutting drilling, where the procedure is similar to drilling in metal or wood with a twisted drill bit.
- Rotary abrasive drilling, also called core drilling, where a hollow drill bit is used, enabling a sample to be retrieved instead of just fragments of rock as in the other three cases (Bergteknik, 1985).

Friction generates heat at the contact surface between rock and drill bit and to some extent also between rock and drill string. Flushing water is thus needed not only to remove drill dust and cuttings but also to prevent the drill bit from damage due to overheating (Lummus & Azar, 1986). The flushing water circulates from inside the drill string, under and through holes in the drill bit and out between the hole wall and the drill string (Bergteknik, 1985). This causes the heat generated near the bottom of the drill hole to warm the outgoing flushing water to a higher temperature than the ingoing (Tuomas, 2004).

The energy flow during drilling can be described by looking at a system consisting of the drill hole, the drill bit and the drill string as in Figure 1.3 below. Ingoing energy is the mechanical energy from the drill bit and drill string. The mechanical energy is consumed either in fracturing the rock or transformed to heat. The heat is either absorbed by the flushing water or dissipated into the rock (Tuomas, 2004).

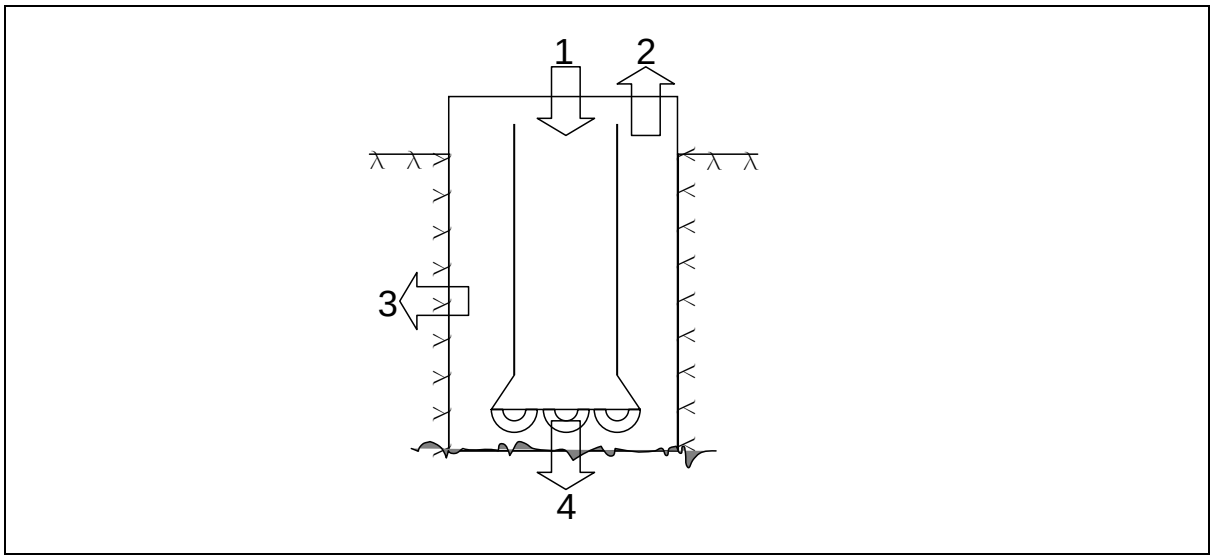


**Figure 1.3 Energy flow during drilling. 1) Ingoing mechanical energy. 2) Outgoing heat transported by the flushing water. 3) Outgoing heat dissipated into the rock. 4) Energy consumed in fracturing the rock.**

# 2 Overcoring — theory, core drilling, temperature effects and polymers

## 2.1 Overcoring theory and the *Borre* cell

One way to estimate the primary stress state in rock is through the overcoring method. In this method the procedure starts with drilling a large-diameter hole down to the level where measurements are to be taken (Figure 3(a)). From the bottom of this hole a smaller pilot hole is drilled with its length axis concentrical with the large-diameter hole (Figure 3(b)). Inside the smaller pilot hole a strain measuring instrument is installed. In the final step the large-diameter hole is resumed and the rock sample is overcored (Figure 3(c)).

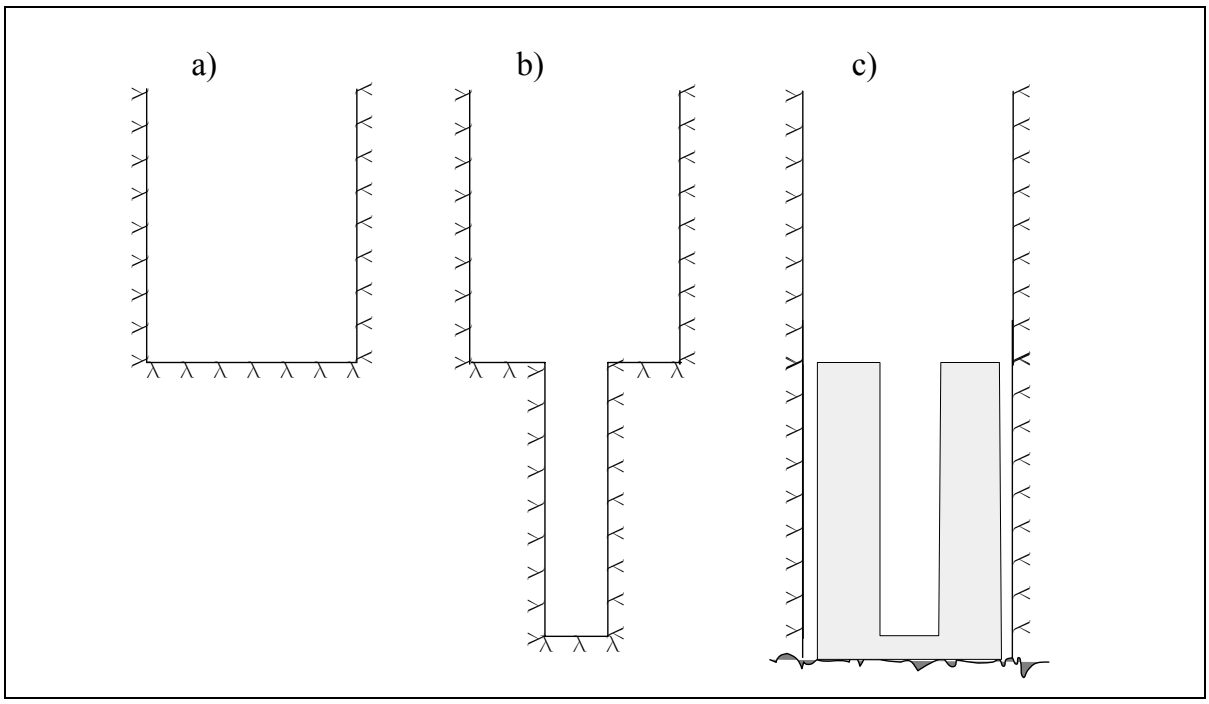


**Figure 2.1 Steps commonly followed in overcoring stress measurements. a) Drilling of large-diameter hole. b) Drilling of small-diameter hole. c) Overcoring.**

The stresses are calculated from the strains that develop when the sample of rock is released from the rock mass and the stresses acting upon it. These calculations are made under the assumption that the rock behaves as a continuous, homogeneous, isotropic and linear-elastic (so called CHILE) material. This assumption is a basic requirement of the overcoring method; however, certain forms of anisotropy may also be considered. Often the third step is followed by a biaxial pressure test of the achieved cylindrical, hollow core to determine its elastic properties (Amadei & Stephansson, 1997).

SKB have used the *Borre* probe for overcoring stress measurements within the site investigation programme at Forsmark and Oskarshamn. A picture of the probe is shown in Figure 2.2. The strain logger is situated at the bottom of the large-diameter hole, connected to three strain gauge rosettes glued onto the rock, 160 mm down the smaller pilot hole.

The strain gauges are mounted on the yellow cantilever arms and situated under the protective cone in Figure 2.2. Before installation the cantilever arms are attached to the gauge holder and

the strain gauges connected to the logger. The strain gauges are covered with a 2-3 mm thick layer of glue and then covered with the protective cone. A two component epoxy that cures under water is used as adhesive. The probe is then lowered down into the large-diameter hole. When the logger reaches the bottom of the hole, the protective cone is automatically pushed further into the pilot hole and the cantilever arms and the strain gauges are pressed outwards against the bore hole wall. The pressure is maintained during curing which typically lasts overnight. Since the bore holes often are filled with water, the strain gauge connection sockets are protected from water and short circuits by a coat of Vaseline.

The strain gauge rosettes are equally separated around the bore hole wall, each measuring strains in the directions 0, 45 and 90º to the bore hole axis. When using the *Borre* probe the pilot hole diameter is 36 mm and the overcoring diameter 76 mm, producing a hollow cylinder with an outer diameter of 61.7 mm (Sjöberg & Klasson, 2003).

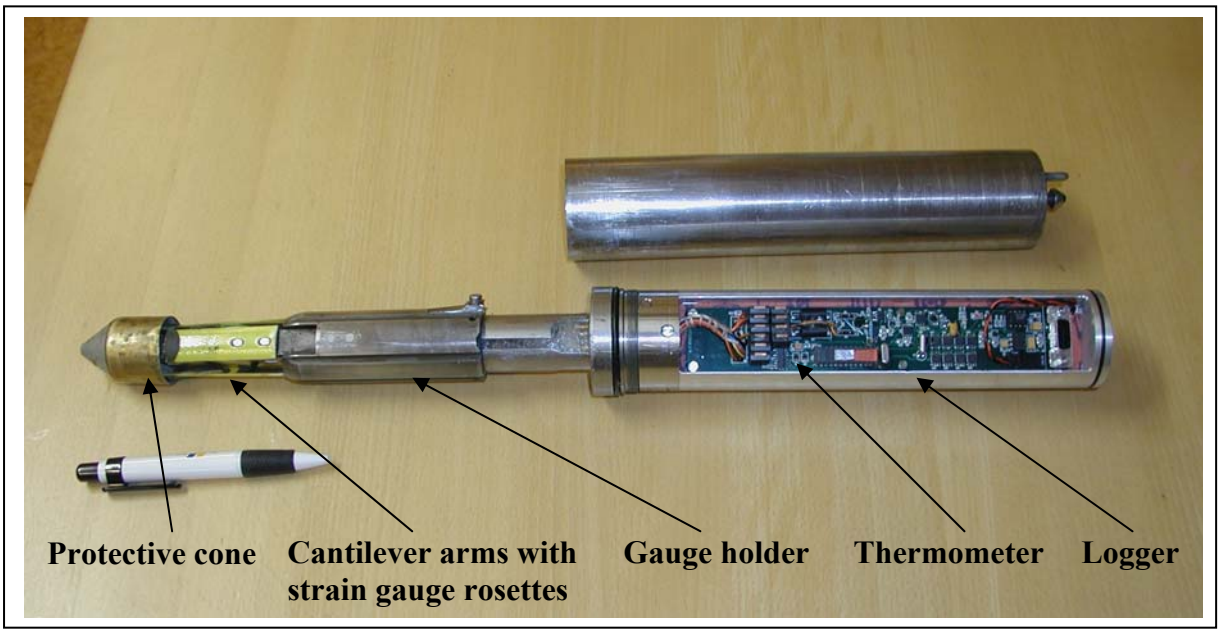


**Figure 2.2 The *Borre* probe.**

## 2.2 Core drilling

Core drilling is the type of drilling used in overcoring. It involves using a hollow drill bit and retrieving a cylindrical sample. The aim is thus not to make a hole but to retrieve a sample. In comparison, "ordinary" drilling uses a solid drill bit and all material retrieved is ground to fragments.

Two different techniques are common in core drilling — the conventional and the wireline technique. The difference lies in how the core sample is retrieved to the surface. In the conventional technique the core is collected within the drill string. To get the core to the surface the entire drill string has to be removed from the hole. To do this, the drill string has to be disassembled into separate rods. Retrieving the rods from the hole one at a time is evidently time-consuming. In the wireline technique the core sample is collected inside an inner tube, inside the drill string. This allows the inner tube, together with the core, to be removed from the hole, leaving the drill string in place for the next session and thus saving a lot of production time (http://toolboxes.flexiblelearning.net.au/demosites).

The number of core barrels used is dependent on the required quality of the core sample. A single tube core barrel, as in the conventional core drilling technique, is used when the core quality is less important (http://www.welltech.se). Since the flushing water is in direct contact with the whole length of the core during the drilling it might cause erosive damage to it and reduce the quality.

A double-tube core barrel is used when requirements on the core quality is higher. Inside the drill string a tube is contained in which the core sample is collected. The core is thus not exposed to damage caused by the flushing water since the water passes between the outer and inner barrel (Heinz, 1989). When retrieved to the surface the core is pushed out of the tube which then might cause damage to it and degrade the quality.

Triple-tube core barrels are used when drilling in very soft or fractured rock and when the core quality is very important. Inside the first inner tube a second one is contained in which the core sample now is collected. When retrieved to the surface the second inner tube is pushed out of the first. Since the second inner tube is split lengthwise it is possible for one half of the tube to be removed to unveil the core and hence further reducing the risk of damaging the core sample (http://www.boartlongyear.com).

In addition to this, there is the option of standard or thin-walled drill bits. Nowadays the thin-walled drill bit is more commonly used than the standard. The main arguments for choosing the thin-walled drill bit to the standard drill bit are the smaller cutting face that requires less feed force, hence a smaller energy consumption, the higher penetration rate and the lighter drill strings that are easier and more ergonomical to work with. The possible temperature effect on the core sample is not considered when choosing type of drill bit and no opinion has been stated whether the heating/cooling effect differs between the two types of drill bits (Drillcon, 2007; Protek Norr, 2007; Rockma, 2007).

When overcoring with the *Borre* cell for the SKB site investigation programme, the wireline technique with triple-tubes was applied for the small-diameter pilot hole while the actual overcoring was performed with the conventional technique (Lindfors, 2007). Overcoring a 76 mm hole with the wireline technique would create a rock core with an outer diameter as small as 50 mm, compared to 61.7 mm with the conventional technique. The smaller outer diameter would increase the risk of damage and microcracks in the core. Applying the wireline technique to a larger hole and hence also a larger outer diameter of the rock core would be more expensive than the conventional technique and also require more development and capacity of present equipment. (Sjöberg, 2007). In Forsmark only thin-walled coring bits were used (Nilsson, 2007).

## 2.3 Temperature effects in overcoring

Discussions in the field of, or closely related to, temperature effects in overcoring have previously been presented by:

- Garritty, Irvin and Farmer (1985) who state that errors due to temperature changes within the overcore are of neglectable magnitude when the overcoring has been performed at moderate or great depths. However, when performed on shallow depths where the magnitude of the stress state is low, the strains induced by temperature changes have adverse effects on results since they comprise a bigger portion of the total strain measured.

- Thompson, Lang and Sneider (1986) who state that the main reason a temperature controlled drill water system was installed for the overcoring stress measurements in the AECL's (Atomic Energy of Canada Limited) stress measurement program at the URL (Underground Research Laboratory) was to keep temperature changes to a minimum on both instrument and rock. Warm and cold drill water was usually mixed and kept at a steady temperature of 1 ºC below ambient rock temperature. During a typical overcoring test, the cell temperature was between the two temperature curves of the ingoing and the outgoing water. The temperature difference between ingoing and outgoing water was approximately 2 ºC. Corresponding typical drill data was:
  - Torque: 55 Nm
  - Thrust force: 60 kN
  - Rotation speed: 180 RPM
  - Penetration speed: 12 mm/min.

Corresponding site typical values from Forsmark are presented in Section 4.2.

- Leijon (1988) claims that strains induced by temperature changes, using the LUT (Luleå University of Technology)-gauge, caused an error corresponding to at most ±1 MPa during typical field conditions. (compare to the calculated principal stresses from Forsmark, borehole KFM07C: test no. 2:9:1 were $\sigma_1$ = 24 MPa, $\sigma_2$ = 9 MPa and $\sigma_3$ = 4 MPa) Hence, the relative error is larger at shallow depths.

- Martin and Christiansson (1991) that point out the importance to keep the temperature at the strain gauges relatively constant during the overcoring process to minimize the effect on the results. They present the data described in Table 2.1 below, showing how a temperature increase affects the calculated principal stress magnitudes and orientations.

**Table 2.1 The affect on magnitude and orientation on calculated principal stresses caused by temperature increase. (from Martin & Christiansson, 1991)**

| Temperature increase [ºC] | Change in principal stress magnitude, $\sigma_1$ [%] | Change in principal stress magnitude, $\sigma_3$ [%] | Change in principal stress orientation, $\sigma_1$ [%] | Change in principal stress orientation, $\sigma_3$ [%] |
|---|---|---|---|---|
| **2** | No significant change | No significant change | No significant change | No significant change |
| **8** | 11 | 23 | -10 | 4 |
| **15** | 22 | 59 | -14 | 6 |

- Cai and Thomas (1993) tell that the temperature-induced strains recorded during their test showed great dependence on rock type and measuring cell. For example the CSIR (South African Council of Scientific and Industrial Research) cell gave a response of -19 microstrain/ºC for sandstone and 23 microstrain/ºC for marble while the USBM (U.S. Bureau of Mines) cell gave the corresponding values of 7 respectively 2 microstrain/ºC.

- Martino et al. (1997) refer to Thompson, Lang and Sneider (1986) above and like Martin and Christiansson (1991) also point out the importance of keeping the rock and cell temperature relatively constant to minimize the effect on calculated stresses. In the same paper it is also stated that core drilling during overcoring can result in a temperature rise of up to 15 ºC. However it is not explained how this temperature was estimated.

- Hakala (2006) refers to the statement of Martino et al. (1997) and suggests that in the case when temperature change cannot be controlled, strain readings are to be taken, with and without flushing on, before and after overcoring. This is to get two strain difference values for each strain gauge. If the measurements are made in stable temperatures, the two difference values would be close to each other.

- When looking into previously conducted overcoring and biaxial pressure test data from Vattenfall's overcoring stress measurements at Odenplan in 2007, the test conditions for test no. 2:2:2 and 2:6:1 were similar except from the biaxial pressure test temperature (23 °C respectively 15-17.5 °C). The difference in Young's modulus (E = 92.3 GPa respectively E = 82.6 GPa) could not be attributed to the different ambient test temperatures. However, for other old measurements, temperature was often judged to be of little importance, and complete temperature records are often not available.

- The *Borre* cell is constructed with the thermometer positioned in the logger unit in the large-diameter hole and not at the position of the strain gauges. Hence the temperature registered by the *Borre* cell is closer to the temperature of the flushing water around the logger unit than the temperatures the strain gauges are exposed to (Sjöberg, 2007).

- (http://www.hbm.com/uploads/faqs/FAQ03_037_en.pdf) states that a temperature increase causes thermal expansion of the rock as well as of the strain gauge in addition to change in resistance of the strain gauge. None of these effects show a strictly linear dependence on temperature but is compensated for when a half or full bridge circuit is used or can be compensated for mathematically when a quarter bridge circuit is used.

- (www.hbm.com/data/softdoc/hbm/data/s1265.pdf) tell that strain gauge rosettes with three measuring grids, such as RY91 used for the *Borre* cell, are connected each in a quarter bridge circuit.

To summarize, it can be said that thought has been given to the fact that temperature increase during overcoring affects the strain readings and hence the importance to keep the temperature at the strain gauges relatively constant during the overcoring process to minimize this effect on the results. Except for the controlled drill water temperature test, no practical attempt to control the temperature has been made, or is currently systematically used in the overcoring drill process.

Since it has been stated that different strain measuring cells give different results concerning temperature-induced strains, it is motivated to investigate the temperature response of the *Borre* cell to enable compensation for temperature-induced strains in a proper way.

It would also be desirable to investigate what temperature the strain gauges are exposed to during overcoring since the thermometer, in the case of the *Borre* cell, is located in the logger in the large-diameter hole and not at the position of the strain gauges. This should be investigated to show whether strain measurements after overcoring are taken at the same temperature as the strain measurements before overcoring, and enable to compensate for the possible temperature raise in a proper way.

## 2.4 Polymers

Polymers can be divided into one of the two main groups thermoplastics or cross-linked polymers as described in Figure 2.3. The principal difference between the groups is that thermoplastics are meltable whereas cross-linked polymers only can be softened once cured. Thermoplastics consist of polymer chains held together by intermolecular forces like van der Waals, dipole and hydrogen bonds. In the structure of cross-linked polymers the polymer chains are mainly bonded together with intramolecular covalent bonds - cross-linked. The bond energy is much higher for covalent bonds than for van der Waals, dipole and hydrogen bonds. The higher bond energy for covalent bonds is the explanation to why cross-linked polymers can not be melted or dissolved.

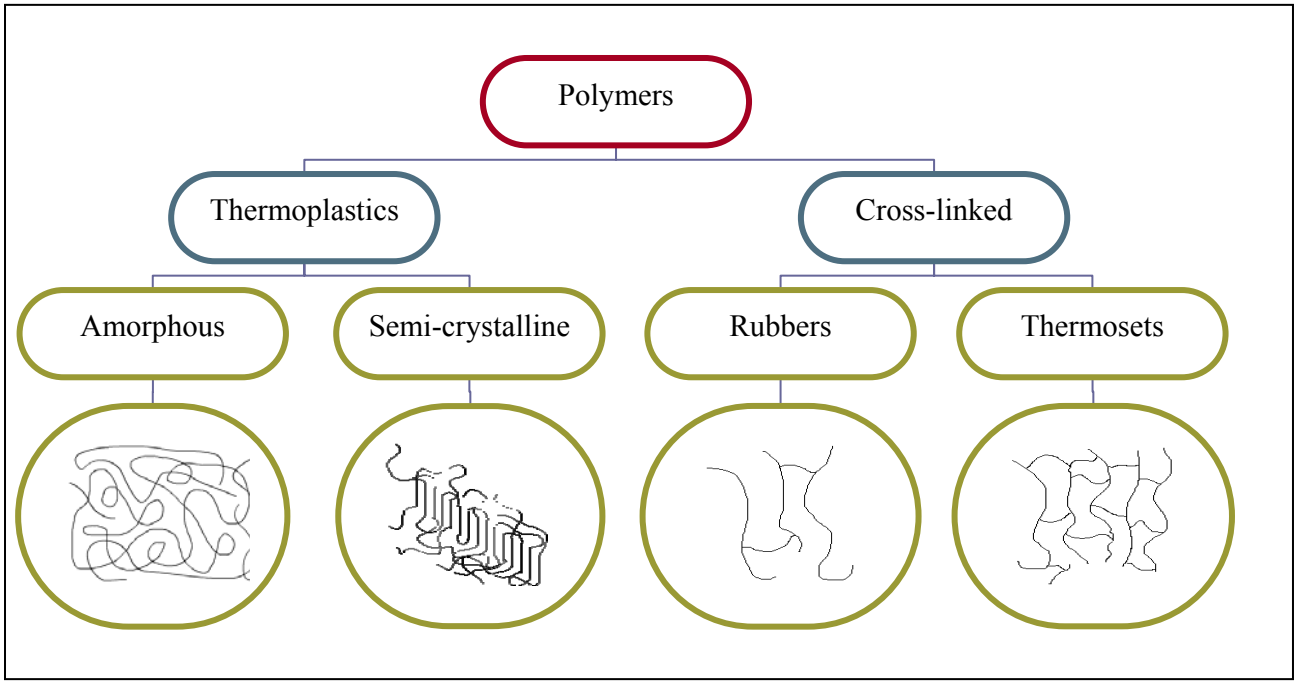


**Figure 2.3 Classification of polymers and sketches of molecular structure.**

At low temperatures the polymer molecules have low relative mobility and the material is stiff or even brittle. Essentially the polymer is in a solid state known as the glassy state. At a certain temperature interval where the midpoint is called the glass transition temperature, $T_g$, the intermolecular bonds start to break and the mobility of the molecules increase. When short segments of the molecule chain move easily the material has entered the rubbery state. This is valid for both thermoplastics and cross-linked polymers. At even higher temperatures when even more intermolecular bonds have broken and the chain segments easily slip past each other, thermoplastics go into a viscous state at $T_m$ as shown in Figure 2.4.

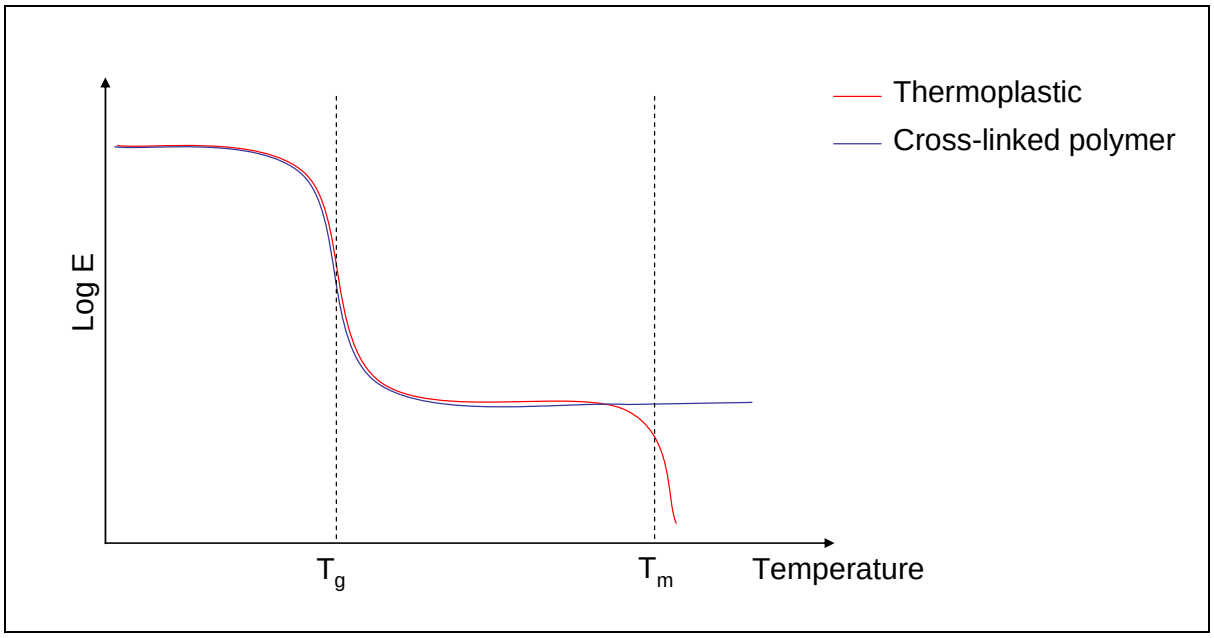


**Figure 2.4 The effect of temperature on the elastic modulus.**

Epoxy glue belongs to the class of thermosets under cross-linked polymers. When the two components of epoxy glue are mixed, the curing reaction starts. In the curing process, cross-links are formed and the material enters a solid state (the rubbery state) at some point. As cross-linking restricts the motion of the chain segments the glass transition temperature increases as cross-links are formed. When the glass transition temperature reaches the curing temperature, the formation of new cross-links is stopped since no chain mobility is possible and the polymer goes into the glassy state. In this way the glue might enter the glassy state without being fully cured. If heated above the curing temperature the reaction is resumed and the forming of new cross-links continues until the glass transition temperature again has reached the curing temperature. This course of events can proceed until a temperature is reached where all reactions possible can take place (Berglund, 1997).

# 3 Numerical simulations

To estimate the temperature the strain gauges are exposed to during overcoring, a numerical simulation of the heat transfer during overcoring was performed. The simulation also provided comprehension of the heat transfer process and what factors that affect and are important to it.

## 3.1 COMSOL Multiphysics

For the simulations the program COMSOL Multiphysics, formerly named FEMLAB, was used (www.comsol.com). It is a program based on the finite element method, suitable for problems that can be described by partial differential equations, like heat transfer (Wernersson, 1994).

## 3.2 Model assumptions

The small-diameter pilot hole, the *Borre* cell, the drill string and part of the ambient rock were included in the model. The geometry of the hole together with assumed boundary conditions allowed an axisymmetric, 2D-model to be used. The model geometry was the one shown in Figure 3.1 and Figure 3.2 below where the red line at the centre of the borehole is the symmetry axis. The model size was selected to be large enough for the boundary conditions not to affect the outcome of events occurring within the domains. Figure 3.1 shows a figure to scale and Figure 3.2 shows one with different length and height scale to enlarge and clarify details.

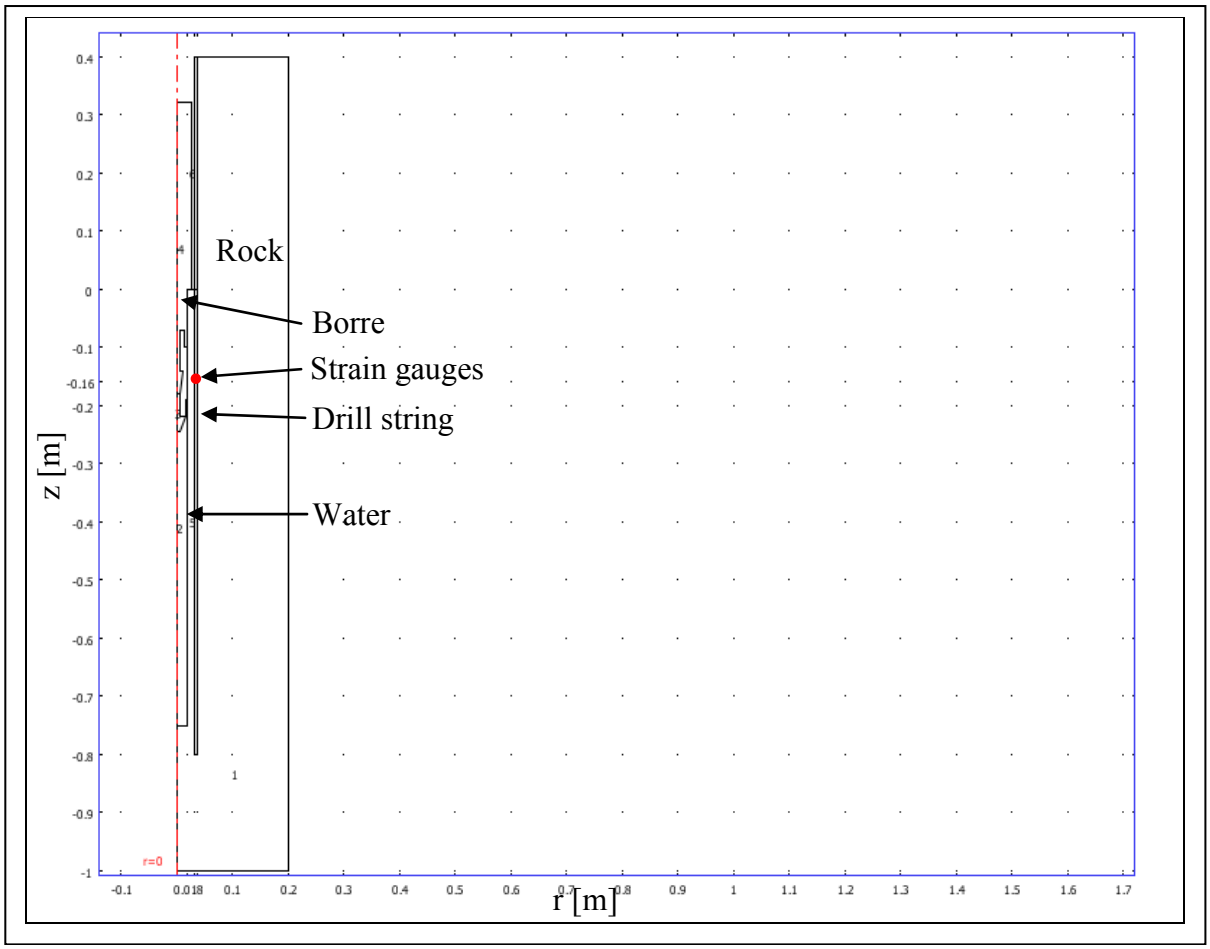


**Figure 3.1 The model used in the numerical heat transfer simulation. Figure to scale.**

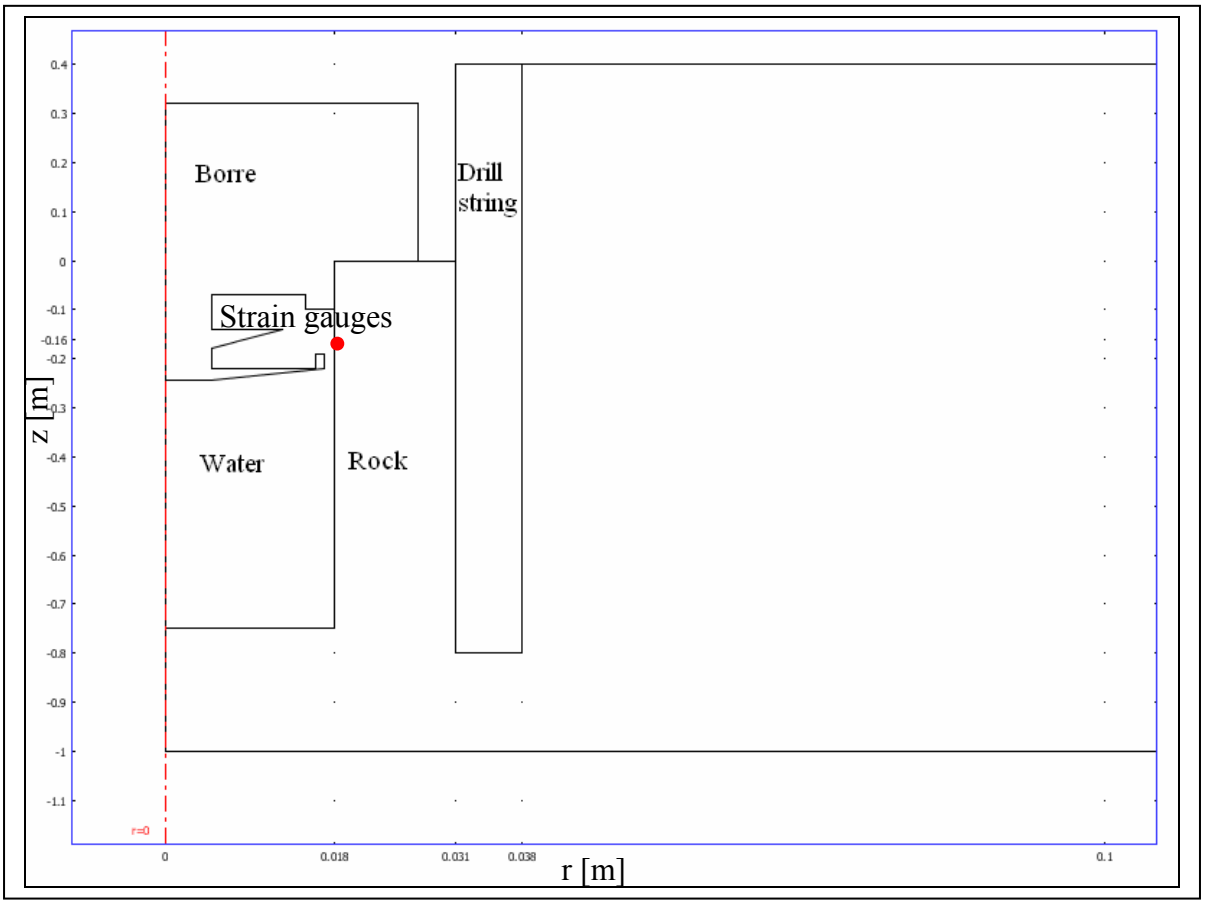


**Figure 3.2 The model used in the numerical heat transfer simulation. Figure with different length and height scale.**

The material properties used in the model are presented in Table 3.1 below.

**Table 3.1 Material properties used in the numerical heat transfer simulation.**

| | λ [W/(m·K)] | c [J/(kg·K)] | ρ [kg/m$^3$] |
|---|---|---|---|
| **Rock** | 3 | 850 | 2700 |
| **Water** | 0.6 | 4190 | 997 |
| **Stainless steel** | 14 | 475 | 8000 |
| **Steel (AISI 4340)** | 44.5 | 475 | 7850 |

The rock mass was assumed to be homogeneous and isotropic. Flushing water in the large-diameter drill hole was simulated as a boundary temperature that varied linearly from 8-11 ºC as overcoring drilling proceeded and after overcoring stopped, cooled down at the same rate. The temperature registered by the *Borre* cell (corresponding to the temperature of the flushing water in the large-diameter hole) in conducted measurements from Forsmark, borehole KFM07C, often showed a behaviour similar to this. In the pilot hole, the water was assumed only to transfer heat through conduction. The entire *Borre* cell was assumed to be made of stainless steel to simplify voids and different materials in the printed circuit board. The drill bit as well as the drill string was assumed to be made of steel. All sub-domains were assumed to have initial temperatures of 7 ºC.

When simulation of overcoring started, the drill bit was assumed to be at position z = 0. The material properties of the drill string domain were those for steel above the drill bit and those for rock below it. As overcoring proceeded and the drill bit penetrated the rock, the properties of the drill string domain changed from rock to steel.

The total energy input was calculated with drill data from the bore hole KFM02B at the Forsmark site in accordance with the energy calculation in Tuomas (2004). The heat generating energy input was calculated as

$$P = M \cdot \omega + F \cdot v, \tag{4.1}$$

where
P [W] = energy input,
M [Nm] = mechanical torque acting on drill bit,
ω [rad/s] = angular velocity of drill bit,
F [N] = feed force,
v [m/s] = feed speed,

with site typical values chosen as

M = 1400 Nm,
ω = 52 rad/s,
F = 25 kN,
v = $5 \cdot 10^{-4}$ m/s = 3 cm/min,

which gave a typical energy input value of P = 75 kW.

The mechanical properties of the drill bit change at approximately 300 ºC and since no such changes have been detected, this is the maximum possible temperature at the drill bit front during overcoring (Nilsson, 2007).

## 3.3 Simulation with continuous heat flow from the drill string — assumptions and output

In this simulation the drill bit was set as the heat generating domain. The energy input value was chosen so the temperature at the drill bit was approximately 300 ºC. All heat released during overcoring was supposed to be generated at the 0.01 m in the very front of the drill bit, see Appendix A. No compensation for the flushing water around the drill bit was made and in that way an overcoring without flushing water was simulated. With no flushing water a direct conductive heat flow from the drill bit and drill string to the ambient rock was assumed.

A temperature-time plot for the strain gauge positions can be seen in Figure 3.3. The drill bit was at level with the strain gauges at 320 s (5 min) and about 90 s later they experienced their maximum temperature value of a little more than 150 ºC. Overcoring stopped at 1600 s (27 min) and 1800 s (30 min) afterwards the strain gauges had cooled down to 35 ºC. In Figure 3.4 the temperature distribution just after the strain gauges were exposed to their maximum temperature is shown.

Until the drill bit passed the strain gauges they did not experience almost any temperature change. As the drill bit passed, they were exposed to a rapid increase and immediately afterwards the temperature subsided quite fast.

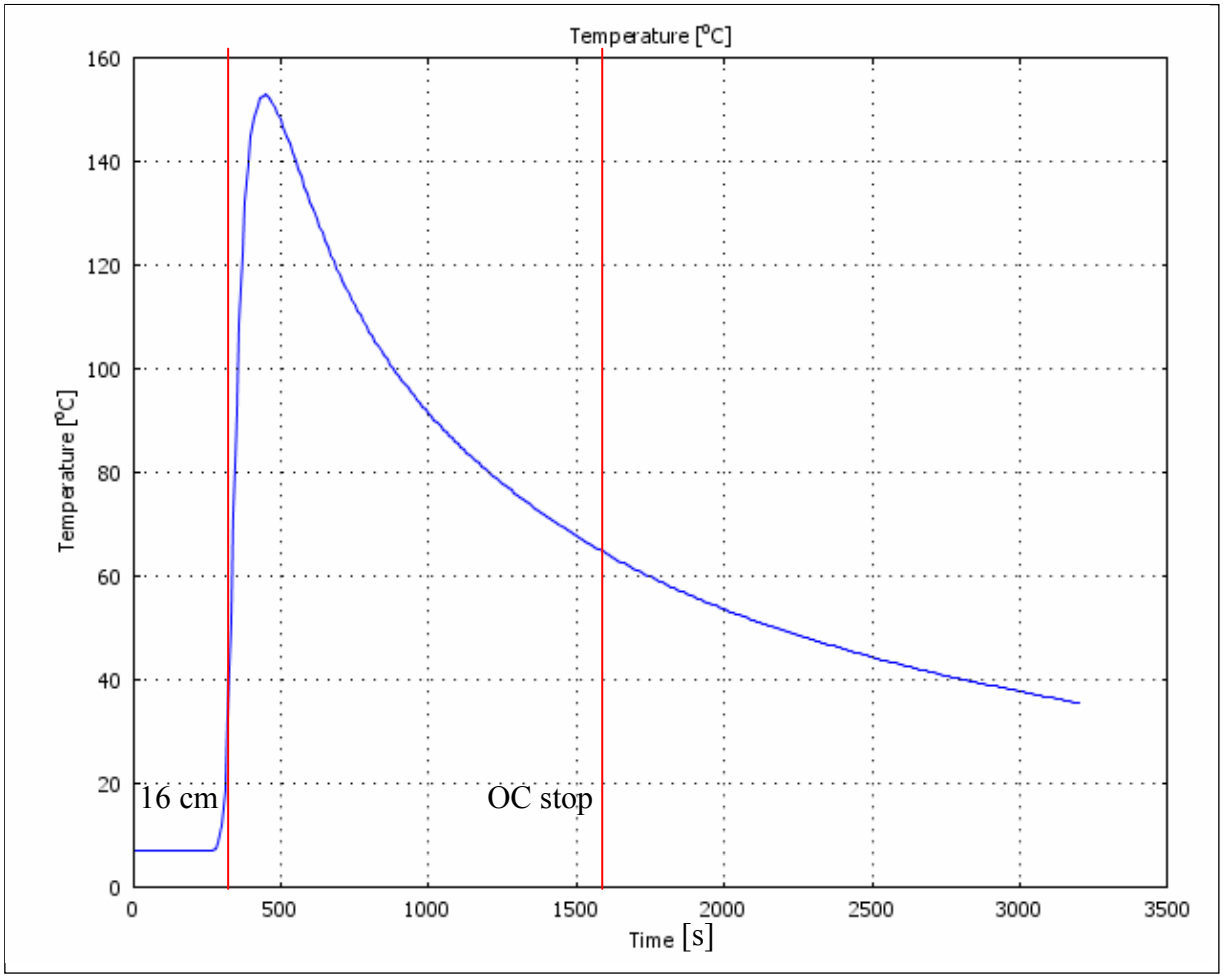


**Figure 3.3 Simulation with continuous heat flow from the drill string. Temperature-time plot for the strain gauge positions. Point r=0.018, z=-0.16 in the model. (cf. Figure 3.2) Assuming 300 °C at the drill bit front.**

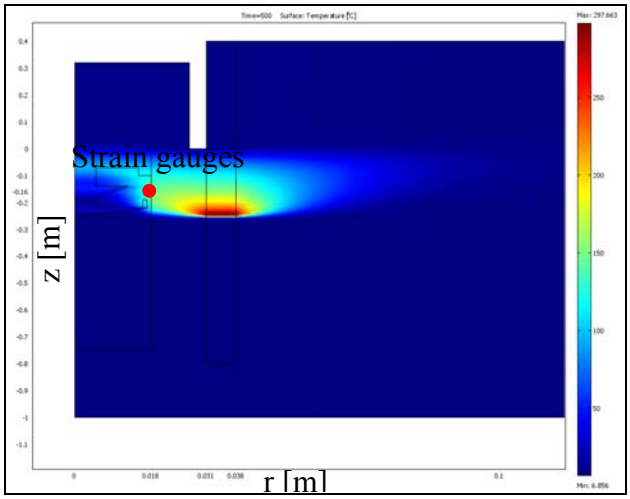


**Figure 3.4 Simulation with continuous heat flow from the drill string. Temperature distribution just after the strain gauges were exposed to their maximum temperature. Assuming 300 °C at the drill bit front.**

Vaseline is used during overcoring to protect the strain gauge connection sockets from water and short circuits. Vaseline melts in water between 55 and 60 ºC and during field measurements no indication of dissolved Vaseline has been detected. Assuming that the temperature distribution in the pilot hole was homogeneous, this was the maximum temperature the strain gauges were exposed to. Adapting the input energy to give a maximum temperature at the position of the strain gauges to between 55 and 60 ºC corresponded to a temperature of 110 ºC at the drill bit. The changed temperature profile is shown in Figure 3.5 below. 1800 s (30 min) after overcoring stopped the temperature was a little less than 20 ºC.

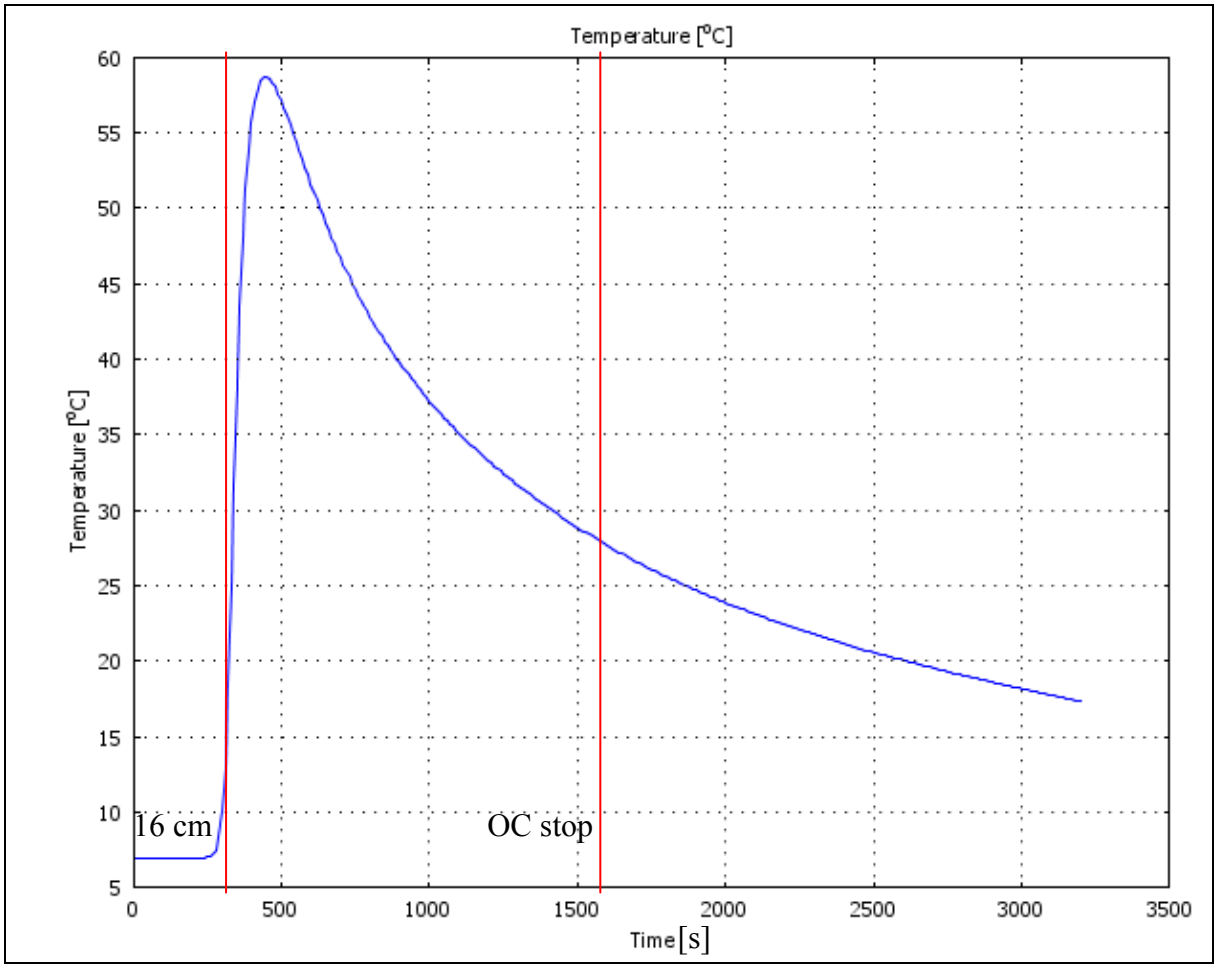


**Figure 3.5 Simulation with continuous heat flow from the drill string. Temperature-time plot for the strain gauge positions. Point r=0.018, z=-0.16 in the model. (cf. Figure 3.2) Assuming 60 ºC as maximum temperature at the strain gauge positions.**

## 3.4 Simulation with fixed temperature boundary condition on the drill string — assumptions and output

In this simulation the temperature of the flushing water outside the drill string was set as the heat generating domain. The domain corresponding to the drill bit was replaced by a fixed temperature set as boundary condition on the drill string. The domain corresponding to the drill bit was thus numerically isolated in this boundary condition and hence had no role in the heat generating process. Initially the flushing water temperature was set to 7 ºC and as the drill bit advanced it varied linearly from the temperature of the flushing water in the large-diameter hole to 100 ºC at the depth where overcoring stopped. It was thus assumed that the flushing water turned warmer the further the drill bit penetrated the rock. 100 ºC was set to be

the upper limit of the flushing water temperature as it was not believed that the water evaporates at the drill bit and then again condensates on its way to the surface.

The temperature-time plot for the strain gauge positions can be seen in Figure 3.6 below. The drill bit was at level with the strain gauges at 320 s (5 min) just as in the previous simulation, but the temperature profile was quite different. The temperature steadily increased after the drill bit had passed the level of the strain gauges at 320 s (5 min). Around 500 s (8 min) when the drill bit had penetrated 0.25 m, the curve flattened out. The maximum temperature the strain gauges were exposed to was slightly less than 30 ºC as overcoring stopped.

In Figure 3.7 the temperature distribution just before the strain gauges were exposed to their maximum temperature is shown.

Due to time constraints no simulation of the temperature at the strain gauges after overcoring stopped was conducted.

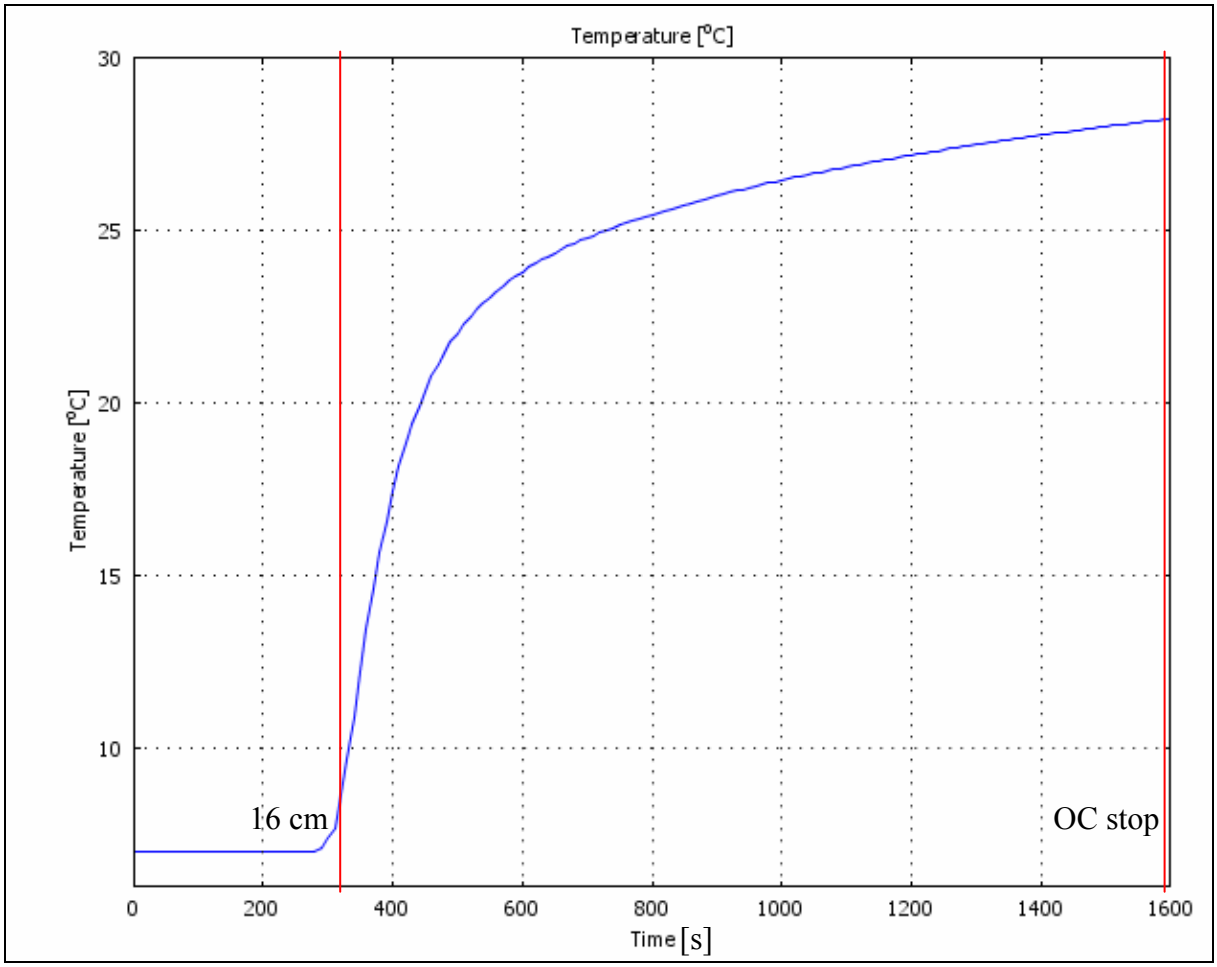


**Figure 3.6 Simulation with fixed temperature boundary condition on the drill bit with fixed temperature boundary condition on the drill string. Temperature-time plot for the strain gauge positions. Point r=0.018, z=-0.16 in the model. (cf. Figure 3.2)**

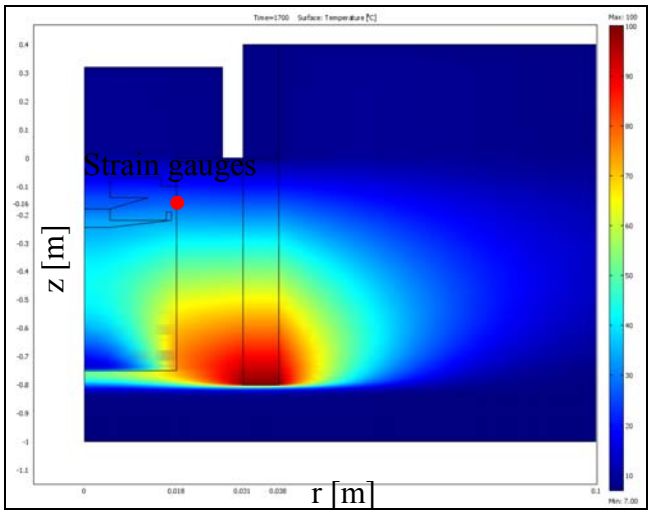


**Figure 3.7 Simulation with fixed temperature boundary condition on the drill string. Temperature distribution just before the strain gauges were exposed to their maximum temperature.**

In Appendix A several plots of temperature distributions during different time steps are shown.

## 3.5 Discussion

With the assumptions in the simulation with continuous heat flow from the drill bit, the achieved temperature values at the position of the strain gauges can be seen as maximum values. Considering that part of the heat generated at the drill bit is dissipated by the flushing water around it, it is reasonable to believe that the temperatures during field conditions are lower than the ones achieved in this simulation. Also considering that the drill bit during operation probably not is on the boarder to experience the extreme temperatures where its mechanical properties are about to change seconds the assumption that temperatures probably are lower during field conditions.

With the assumptions from the simulation with continuous heat flow from the drill bit, a temperature at the drill front of 300 ºC corresponds to a heat release of 1800 W ($120 \cdot 10^6$ W/m$^3$) from the drill bit, i.e. 2 % of the generated energy is transformed to heat into the rock, while the remaining 98 % is consumed in fracturing the rock. A temperature at the drill front of 110 ºC corresponds to a heat release of 700 W ($45 \cdot 10^6$ W/m$^3$) from the drill bit, i.e. 1 % of the generated energy is transformed to heat into the rock, while the remaining 99 % is consumed in fracturing the rock. In a real situation with flushing water the distribution between energy consumed in fracturing the rock, absorbed by the flushing water and dissipated into the rock might be different.

With the assumptions in the simulation with a fixed temperature boundary condition on the drill bit, the values achieved cannot be said to be minimum values. If the flushing water temperature varies linearly, a maximum value of 100ºC might be an exaggeration. It might also be the case that the flushing water temperature does not vary linearly at all but instead quite fast reaches a peak value that is kept relatively constant during the entire overcoring. It is also possible that the heat generated at the drill bit, spreading from underneath and out is underestimated in this simulation since the heat generated at the drill bit is numerically isolated within the drill string boundary conditions.

A drawback in the first simulation is lack of consideration for flushing water influence around the drill bit. For the second simulation the drawback is the numerical isolation of the domain corresponding to the drill bit due to the fixed temperature set as boundary condition as well as the type of temperature boundary condition. It is desirable to have the option to simulate a temperature boundary condition or convective heat flow above the drill bit and continuous conductive heat flow below it.

To get a more accurate value, closer to field conditions, further work in calculating and simulating the energy distribution between fracturing the rock, the amount of heat absorbed by the flushing water contra the amount of heat dissipated by the rock is needed. In addition, more data on actual temperature during field work would be required to better calibrate the model to real conditions.

One factor affecting the temperature that the strain gauges are exposed to is the conductivity of the rock. Table 3.2 shows the peak and cool down temperatures (1800 s (30 min) after overcoring stopped) at the position of the strain gauges for different conductivities of the rock. As seen, the conductivity influences the peak temperature less than the cool down temperature.

**Table 3.2 Peak and cool down temperatures (1800 s (30 min) after overcoring stopped) at the position of the strain gauges for different conductivities of the rock.**

| Conductivity [W/(m·K)] | Peak temperature, simulation with continuous heat flow from the drill bit [ºC] | Peak temperature, simulation with fixed temperature boundary condition on the drill bit [ºC] | Cool down temperature, simulation with continuous heat flow from the drill bit [ºC] |
|---|---|---|---|
| **1** | 138 | 26 | 70 |
| **3** | 154 | 28 | 35 |
| **5** | 149 | 29 | 25 |

# 4 Laboratory experiments

To determine which of the parameters logger, glue, strain gauges and material type that is most sensitive to temperature effects during overcoring, laboratory experiments were performed. The different cases tested were (i) logger, (ii) glue, (iii) strain gauges, (iv) glue + strain gauges, (v) material type and (vi) the system logger + glue + strain gauges + rock. The temperature sensitivity was determined by measuring the strains recorded by the *Borre* cell when heating the parameter(s) included in each test. Each experiment was performed by placing the object(s) of interest in a bucket filled with water. At first, the water was cooled by placing ice in it, thereafter heated and in some tests again cooled with ice. The equipment not being tested was held outside the bucket at constant room temperature to minimize the number of influencing factors.

## 4.1 Heating the *Borre* cell

### 4.1.1 Aim, material, method

The aim of this test was to determine the magnitude of the temperature dependence of the *Borre* cell strain readings when the printed circuit board in the logger unit was subjected to temperature change. This was done by heating the cell in water while the strain gauges and the surroundings were kept at constant temperature. The equipment and laboratory set-up is shown in Figure 4.1 below. To eliminate the effect of the strain gauges one out of three strain gauge rosettes was replaced by resistors of equal resistance (120 Ω) in some tests.

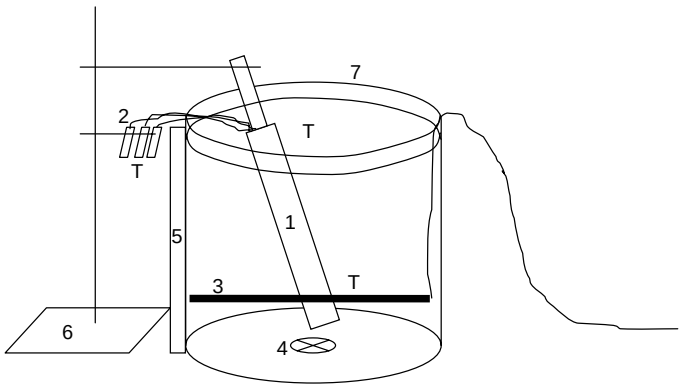


1) The *Borre* cell
2) 3 strain gauges connected to the *Borre* cell
3) Heater
4) Magnetic stirrer
5) Sheat of styrofoam for insulating purposes
6) Tripod
7) Plastic bucket with approximately 30 l of water
T) Thermometer. Two measuring the water temperature, a few centimeters above the bottom of the bucket and below the water level surface respectively, and one measuring the air temperatrue around the strain gauges.

**Figure 4.1 Laboratory equipment and set-up for testing the temperature dependence of the *Borre* cell strain readings.**

The following tests were performed:

Stepwise heating:
1) with three strain gauge rosettes
2) with resistors and two strain gauge rosettes

Continuous heating:
1) with three strain gauge rosettes
2) repeat of the first continuous heating test
3) with resistors and two strain gauge rosettes
4) with resistors and two strain gauge rosettes, including a cooling phase
5) repeat of the fourth continuous heating test, including a cooling phase

### 4.1.2 Results and analysis

#### Stepwise heating

In the first stepwise heating, three strain gauge rosettes were connected to the *Borre* cell. As seen in Figure 4.2 below, the initial temperature was 4 ºC and held constant for 30 minutes before heating started. The temperature was raised in intervals to 8, 10, 15, 20 and 28 ºC. The temperature was held constant at 8, 10, 15 and 20 ºC for 20 minutes before heating was continued. The response seemed somewhat delayed since the strain curve did not show stable, constant values at the same time as the water temperature and *Borre* temperature curves. The overall response was 3 microstrain/ºC. The mean strain showed in the figures below is the mean value of all strain gauges.

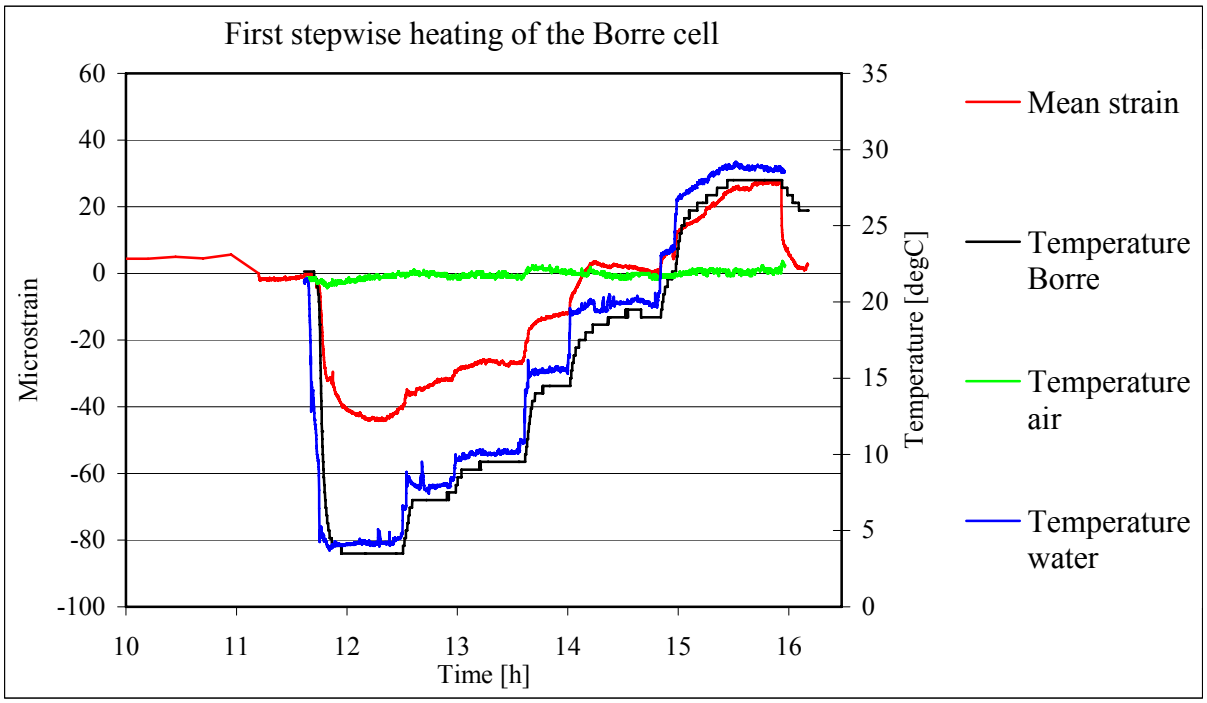


**Figure 4.2 Chart of recorded strains and temperatures during the first stepwise heating of the *Borre* cell.**

In the second stepwise heating one of the three rosettes (strain gauges number 1, 2 and 3) was replaced by resistors of equal resistance (120 Ω). As seen in Figure 4.3 below, the initial temperature was again 4 ºC and held constant for 30 minutes before heating started. The temperature was in intervals raised to 10, 20 and 27 ºC. The temperature was held constant at 10 and 20 ºC for 30 minutes before heating was continued. The response of the strain gauge rosettes as well as the resistors seemed immediate. Strain gauge number 6 showed divergent values and hence was excluded from the mean value calculation in this test. The resistors generally showed less response to temperature change than the strain gauges. The resistors indicated a response corresponding to a little more than 1 microstrain/ºC and the strain gauges just over 3 microstrain/ºC.

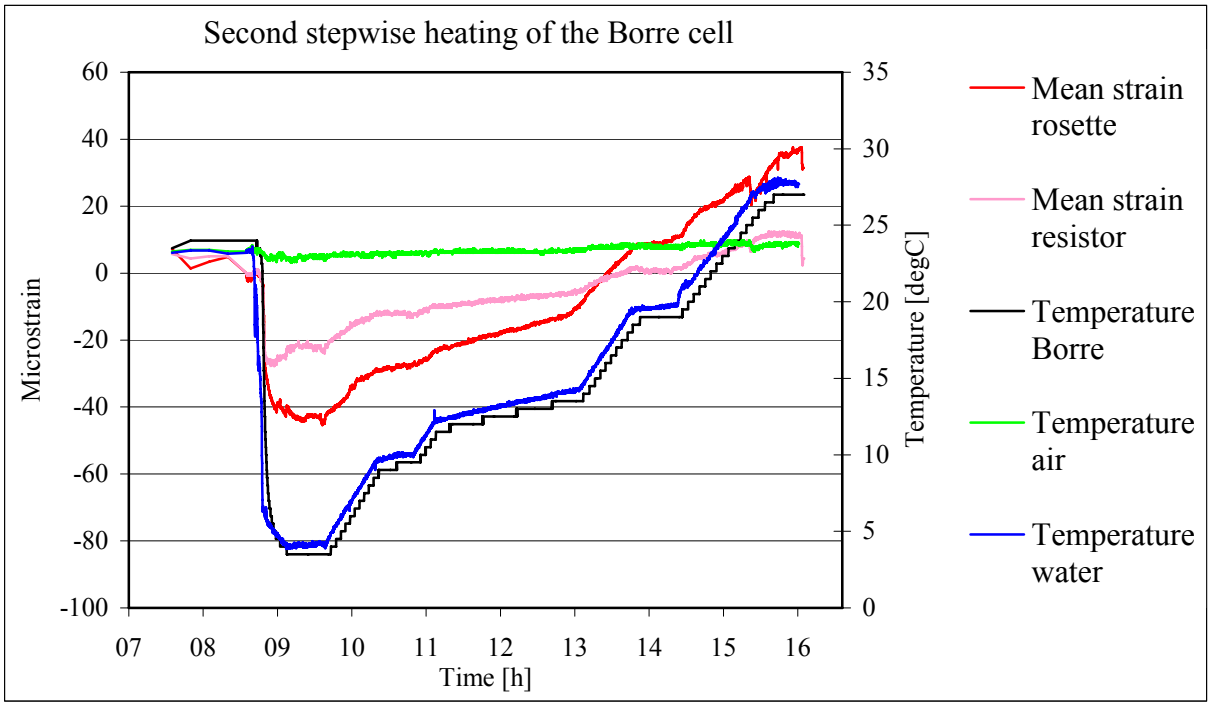


**Figure 4.3 Chart of recorded strains and temperatures during the second heating of the *Borre* cell.**

## Continuous heating

In the first continuous heating, three strain gauge rosettes were connected to the *Borre* cell. As seen in Figure 4.4 below, the initial temperature was 4ºC and held constant for 5 minutes before heating to 28ºC. The *Borre* cell now showed a linear response of 2 microstrain/ºC.

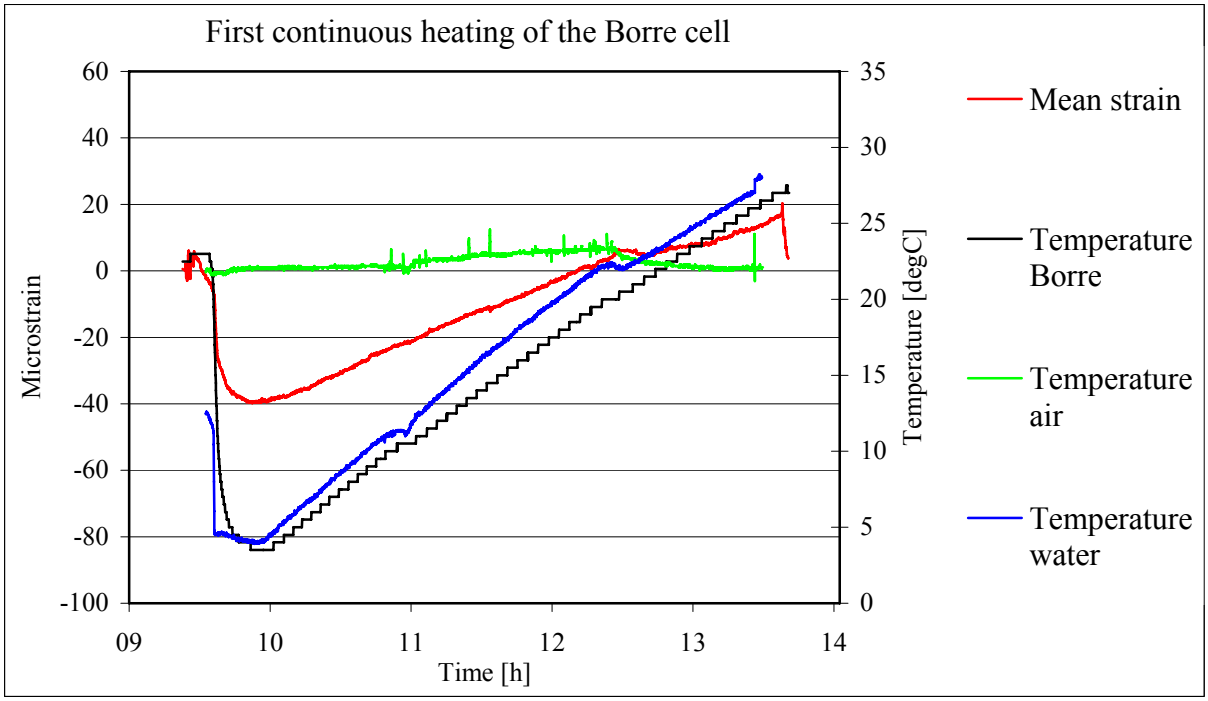


**Figure 4.4 Chart of recorded strains and temperatures during the first continuous heating of the *Borre* cell.**

Also in the second continuous heating three strain gauge rosettes were connected to the *Borre* cell. After 30 minutes at constant temperature the logger was heated from 4 to 29 ºC as seen in Figure 4.5 below. The abnormality in the strain readings around 4 ºC was probably due to a large amount of ice in the bucket. The water was cooled by placing ice in the water filled bucket and when the water temperature had reached 4 ºC the remaining ice was removed. The ice had probably cooled the *Borre* cell down to below 4 ºC and when it was removed the *Borre* cell adapted to the warmer temperature (4 ºC) and so after 20 minutes recorded constant strain values. The response seemed almost immediate since the inclination of the strain curves changed at the same time as the heating ratio changed. The *Borre* cell showed a response of 3 microstrain/ºC independent of heating ratio.

In the third continuous heating one of the three strain gauge rosettes (strain gauges number 1, 2 and 3) was replaced by resistors of equal magnitude. Just as previous the logger was heated from 4 to 31 ºC after 30 minutes at constant temperature which can be seen in Figure 4.6. The abnormality in the strain readings around 4 ºC can again, like above, be explained by ice in the bucket. Also the response seemed almost immediate since the inclination of the strain curves changed at the same time as the heating ratio changed. Strain gauge number 6 showed divergent values and hence was excluded from the mean value calculation. The resistors showed, overall, less response to temperature change than the strain gauges. The resistors indicated a linear response of a little less than 2 microstrain/ºC and the strain gauges 3 microstrain/ºC, both independent of heating ratio.

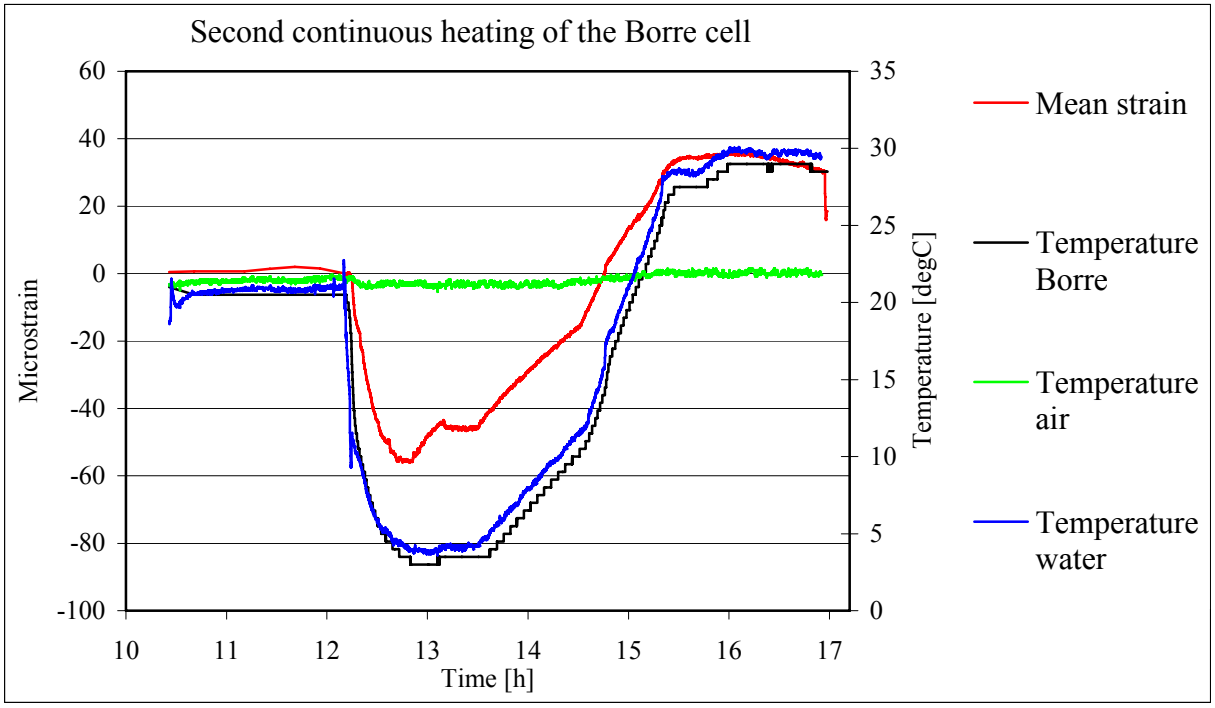


**Figure 4.5 Chart of recorded strains and temperatures during the second continuous heating of the *Borre* cell.**

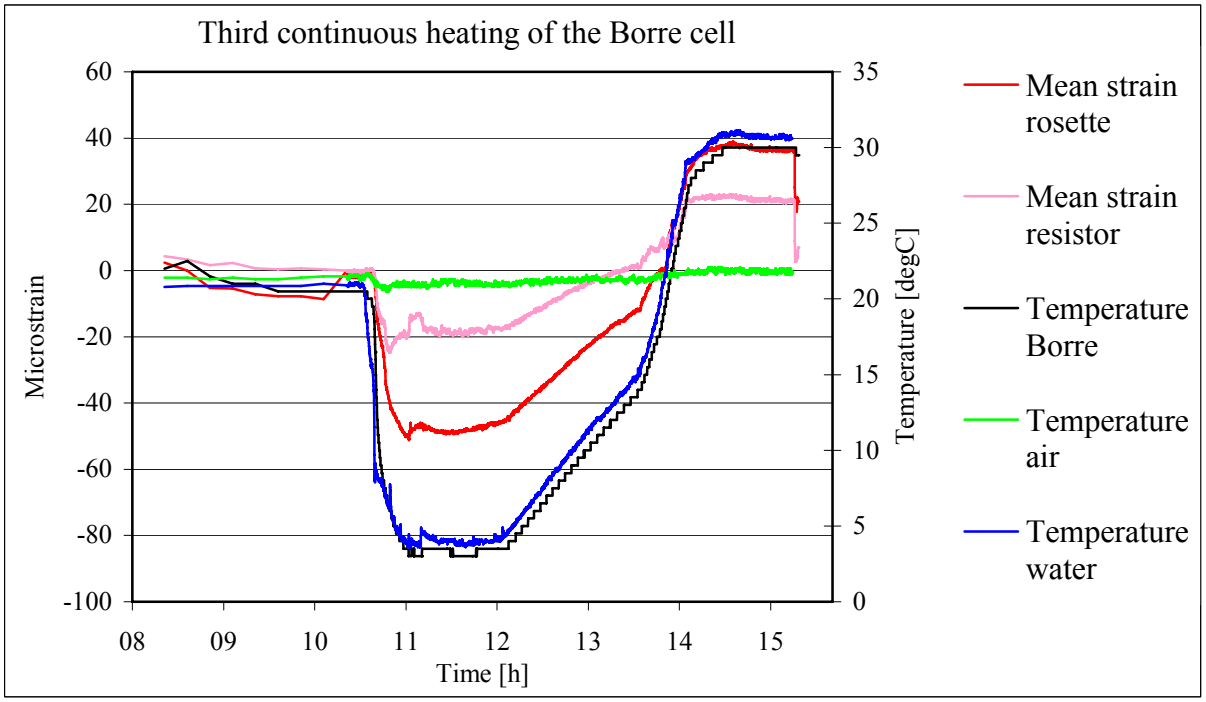


**Figure 4.6 Chart of recorded strains and temperatures during the third continuous heating of the *Borre* cell.**

Also in the fourth continuous heating, one of the three rosettes (strain gauges number 1, 2 and 3) was replaced by resistors of equal resistance. As seen in Figure 4.7 below, the initial water temperature was 4 ºC and held constant for 10 minutes. Worth noticing here is the fluctuation in the water temperature and strain readings right before the 4 ºC temperature is reached. Even though all ice was removed from the bucket the last 10 minutes before heating, the *Borre* cell did not register the same fluctuation in the temperature response. Furthermore the registered temperature difference between the water temperature and the *Borre* temperature was larger than seen before. Then the cell was heated to 50 ºC and thereafter allowed to cool down to 6 ºC. Around 27 ºC the resistors diverted from a linear response corresponding to a little more than 2 microstrain/ºC to an almost constant response or a possible linear response of maximum 0.4 microstrain/ºC. The strain gauge rosettes now showed a response of 2 microstrain/ºC in the heating phase. The strain readings corresponding to the same temperature in the heating and cooling phase were not of equal magnitude. In the cooling phase the resistors gave a response corresponding to 1 microstrain/ºC in the interval 50-25 ºC, 4 microstrain/ºC in the interval 25-15 ºC and 0.4 microstrain/ºC in the interval 15-4 ºC. The strain gauge rosettes gave the response 2 microstrain/ºC in the interval 50-40 ºC, 0.3 microstrain/ºC in the interval 40-25 ºC and 4 microstrain between 25 and 4 ºC. As this non-linear behaviour in the cooling phase was not seen in forthcoming heating, the test was considered unsuccessful.

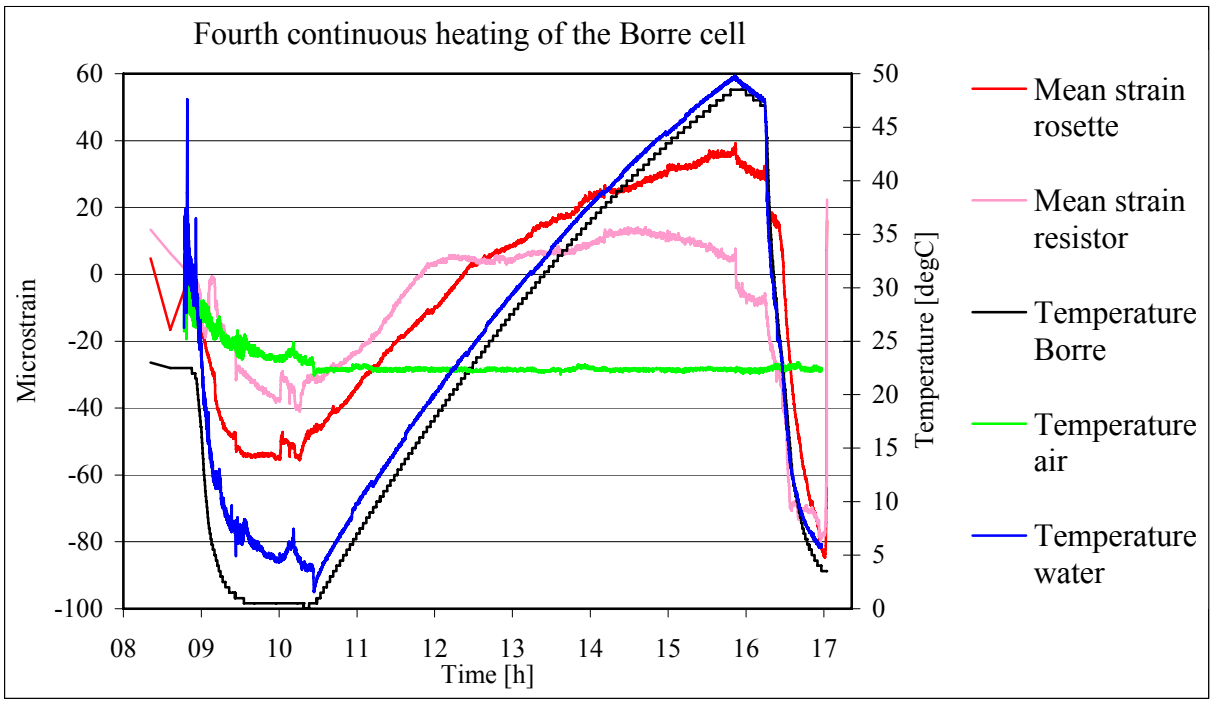


**Figure 4.7 Chart of recorded strains and temperatures during the fourth continuous heating of the *Borre* cell.**

To confirm the validity of the above results a repeat test was performed. The logger was heated from 5 ºC to 45 ºC and then cooled down again. As seen in Figure 4.8 below the result was the same as above only concerning the response behaviour of the resistors in the heating phase. Around 27 ºC the resistors diverted from the linear response of a little more than 1 microstrain/ºC to an almost constant response which in the cooling phase turned to 2 microstrain/ºC. The strain gauge rosettes on the other hand showed a non-elastic behaviour with a linear response of 2 microstrain/ºC in the heating phase and 3 microstrain/ºC in the cooling phase.

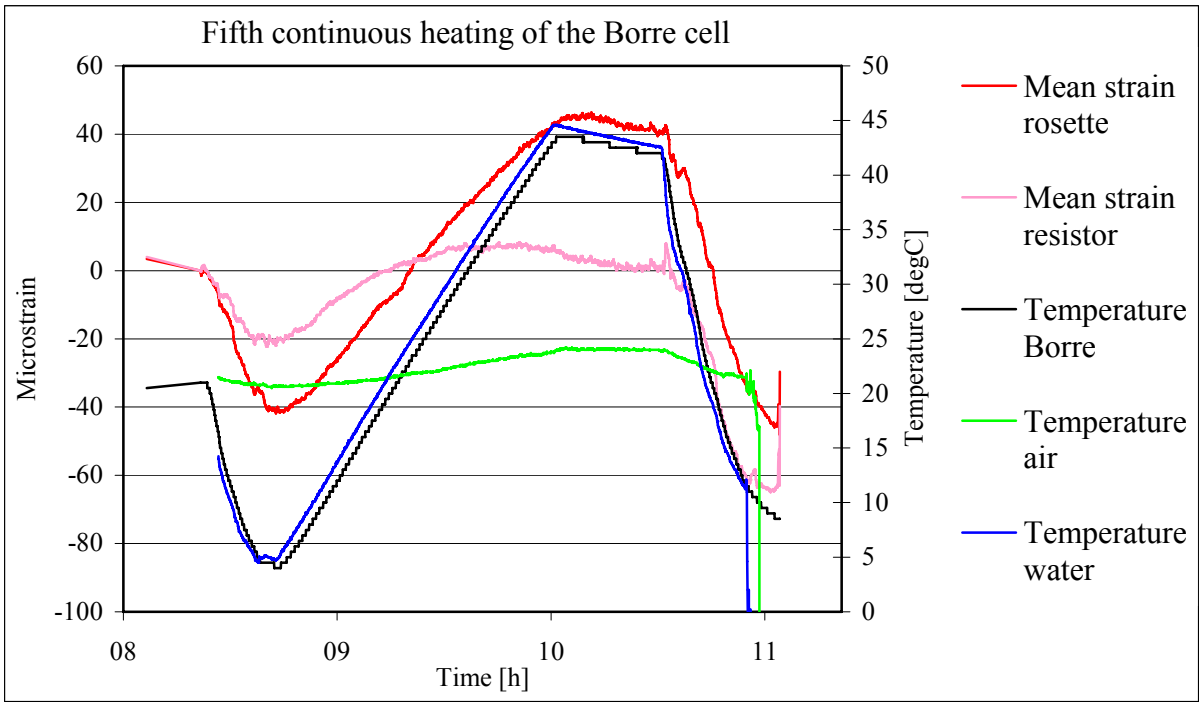


**Figure 4.8 Chart of recorded strains and temperatures during the fifth continuous heating of the *Borre* cell.**

The full raw data charts for all strain readings corresponding to the diagrams above are presented in Appendix B.

### 4.1.3 Discussion

These experiments showed that when subjected to temperature change, the strain reading response of the *Borre* cell was close to immediate (without time delay). They also showed that the response due to temperature change was quite small both for resistors and strain gauge rosettes. The response for the resistors corresponded to between 1 and 2 microstrain/ºC, and the response for the strain gauges was 3 microstrain/ºC.

The response was linear, but not elastic. This type of hysteresis is quite common in printed circuit boards and almost seen as normal (Carlson, 2007). Since the strains are less in the cooling phase, it might suggest that if the logger is subjected to temperature increase during overcoring, stresses are calculated from too low strain values even if strain readings are taken at the same temperature as the overcoring started with. This effect might be neglectable though since the response and hysteresis are very small in magnitude compared to strains typically recorded in overcoring measurements (cf. Figure 1.1 and Figure 1.2).

Assuming that the change in electronic properties in the logger affect all strain gauges with an absolute error of equal magnitude, Table 4.1 shows how much the calculated principal stresses from Forsmark, borehole KFM07C: test no. 2:9:1 were affected if the corresponding strain values were registered at an elevated temperature. Values greater than zero mean that the calculated principal stress from Forsmark, borehole KFM07C: test no. 2:9:1 was an overestimation of the in situ value and indicate how much of the calculated stress that was induced by temperature increase of the *Borre* cell.

**Table 4.1 Example of the effect on magnitude on calculated principal stresses, from Forsmark, borehole KFM07C: test no. 2:9:1, caused by temperature increase in the Borre cell.**

| **Temperature increase [ºC]** | **Equivalent strain increase [microstrain]** | **Change in principal stress magnitude, $\sigma_1$ [MPa]** | **Change in principal stress magnitude, $\sigma_2$ [MPa]** | **Change in principal stress magnitude, $\sigma_3$ [MPa]** |
|---|---|---|---|---|
| **3** | **9** | 1 | 1 | 1 |
| **5** | **15** | 1 | 1 | 2 |
| **10** | **30** | 2 | 2 | 4 |
| **20** | **60** | 4 | 4 | 8 |
| **Calculated principal stresses from Forsmark, borehole KFM07C: test no. 2:9:1** | | **$\sigma_1$ [MPa]** | **$\sigma_2$ [MPa]** | **$\sigma_3$ [MPa]** |
| | | **24** | **9** | **4** |

## 4.2 Heating strain gauges

### 4.2.1 Aim, material, method

The aim of this test was to determine the magnitude of the temperature dependence of the strain gauges (RY91) used together with the *Borre* cell. This was done by heating the strain gauges in water while the *Borre* cell and the surroundings were kept at constant temperature. The equipment and laboratory set up can be seen in Figure 4.9 below.

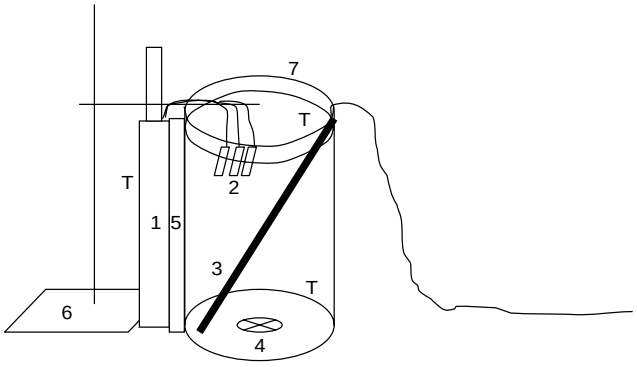


1) The *Borre* cell
2) 3 strain gauges connected to the *Borre* cell
3) Heater
4) Magnetic stirrer
5) Sheat of styrofoam for insulating purposes
6) Tripod
7) Plastic bucket with approximately 5 l of water

T) Thermometer. Two measuring the water temperature, a few centimeters above the bottom of the bucket and below the water level surface respectively, and one measuring the air temperatrue around the strain gauges.

**Figure 4.9 Laboratory equipment and set up for testing the temperature dependence of the strain gauges.**

### 4.2.2 Result

In Figure 4.10 below a heating of strain gauges is showed. The initial temperature was 4 ºC and held constant for 30 minutes before heating started. The temperature was raised in intervals to 8, 12, 16, 20, 24 and 28 ºC. It was held constant at 8, 12, 16, 20 and 24 ºC for 30 minutes before heating was continued, but even tough the temperature was held constant, the strains did not tend to approach stable values.

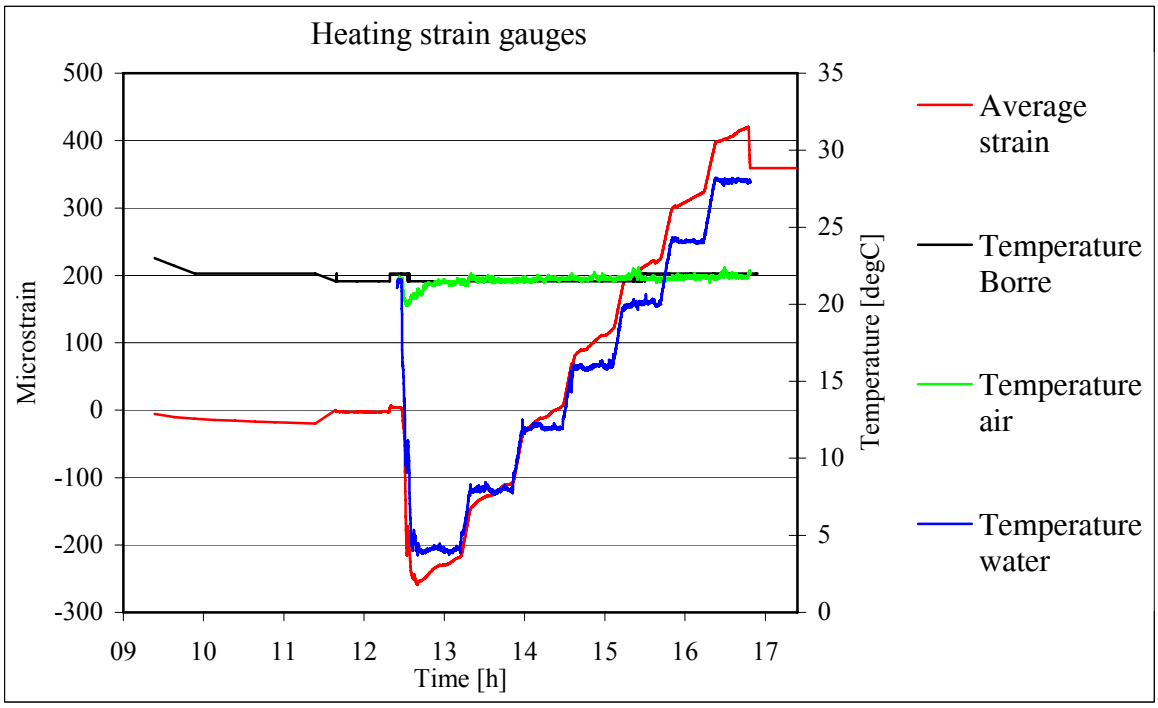


**Figure 4.10 Chart of recorded strains and temperatures during heating strain gauges.**

### 4.2.3 Discussion

After consulting the manufacturer of the strain gauges it was explained that the heat generated in the strain gauges, due to electric current, is supposed to be diverted by the material the gauge is mounted on (steel, aluminium, plastic etc.), otherwise it will be overheated and give misguiding values (Sandberg, 2007). This testing procedure is thus incorrect and further on rejected. The results achieved are not relevant and the strain gauges will instead be tested together with the glue, mounted on the reference material aluminium, see section 5.4.

## 4.3 Glue response

### 4.3.1 Aim, method

The aim of this test was to determine the magnitude of the temperature dependence of the glue that bonds the strain gauges to the rock. This was firstly attempted by placing strain gauges in a small cup of glue that after curing was heated and secondly by heating a lump of cured glue on which a strain gauge rosette had been mounted. Both the glue pot and the glue lump were allowed to cure under water, in room temperature (20-24 ºC) for three weeks before heating. Photos of the glue pot and glue lump are shown in Figure 4.11. The glue pot and glue lump were heated in a way similar to the strain gauges as shown in Figure 4.9.

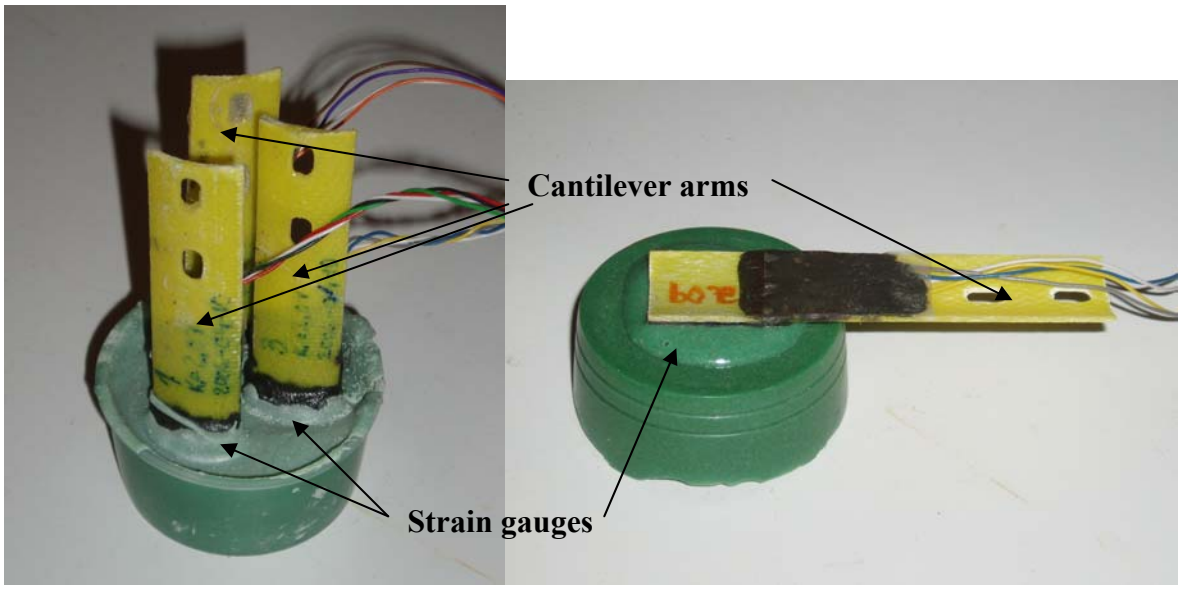


**Figure 4.11 Glue pot with three strain gauge rosettes to the left and glue lump with one strain gauge rosette to the right.**

### 4.3.2 Result and analysis

In the first heating the glue pot was tested. As seen in Figure 4.12 below, the initial temperature was 3 ºC and held constant for 10 minutes. Then it was heated to 75 ºC and thereafter was allowed cool down again. Strain gauge rosette number three (strain gauges number 7, 8 and 9) showed divergent values and hence were excluded from the mean value calculation. The glue pot showed an almost linear response of 40 microstrain/ºC in the initial heating phase before the abnormality in the strain readings around water temperature 35ºC compared to 10 microstrain/ºC after the abnormality. The glue cures from outside and in during heat release. The bump might therefore be due to the possibility that the strain gauges were exposed to a higher temperature than the ambient water temperature. Another explanation to it might be residual stresses or some visco-elastic phenomenon (Joffe, 2007). In the cooling phase the response was a little more than 10 microstrain/ºC in the interval 75-35 ºC and 50 microstrain/ºC in the interval 35-3 ºC. The final temperature in the cooling phase was the same as what the heating phase started with (3 ºC), but the corresponding strain values were not the same and hence the response was not elastic nor linear. Since the final strains were less than the initial, the difference cannot be explained as remaining thermal strains but rather as an indication of not fully cured glue. As the glue sample was heated above curing temperature (room temperature) the chemical reactions were resumed and new cross-links formed. As cross-links were formed, the polymer chains bonded tighter together and the material shrank.

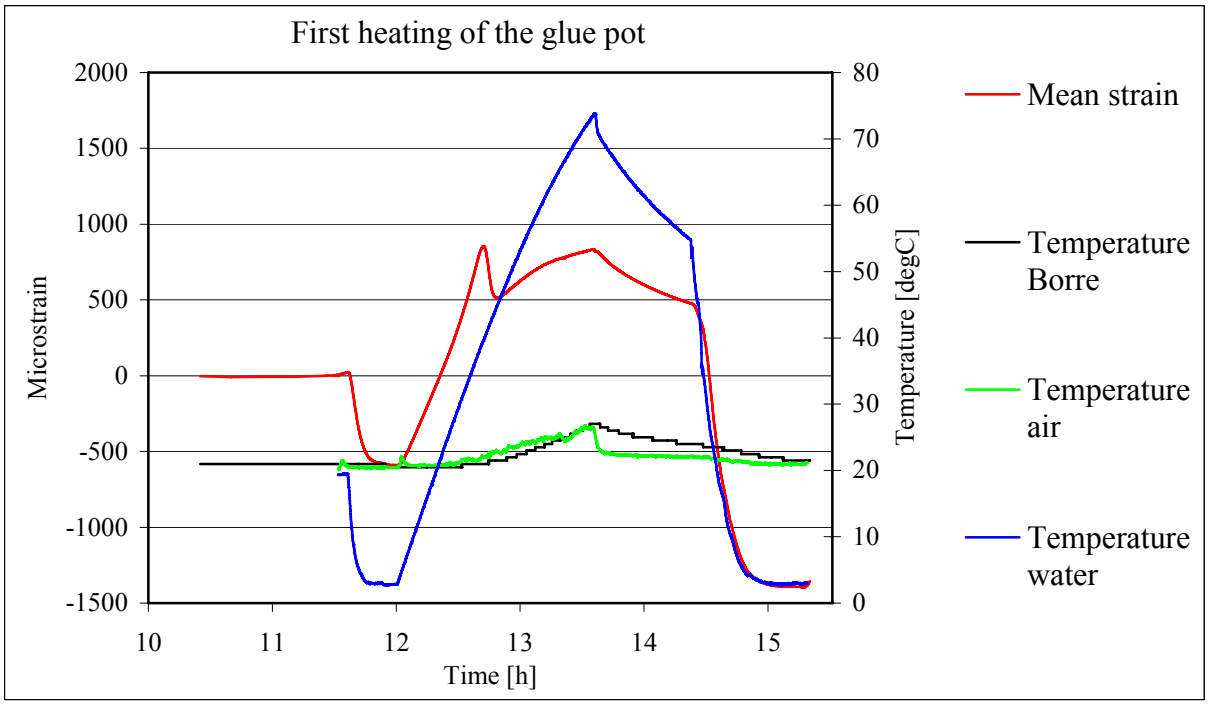


**Figure 4.12 Chart of recorded strains and temperatures during heating the glue pot 1.**

In the second heating the same glue pot as in the first heating was used. As seen in Figure 4.13 below, the pot was heated from 4ºC after 10 minutes at constant temperature to just above 70ºC before it was allowed to cool down again. The same "bump" in the strain readings as in the previous heating occurred around water temperature 40º. Strain gauge rosette number three (strain gauges number 7, 8 and 9) no longer showed divergent values and hence was included in the mean value calculation. The glue pot showed a response of 30 microstrain/ºC in the initial heating phase before the abnormality compared to 20 microstrain/ºC after it. In the cooling phase the response was 10 microstrain/ºC in the interval 70-30 ºC and 70 microstrain/ºC in the interval 30-4 ºC. The strain values at corresponding temperature values in the heating and cooling phase were neither in this heating the same, indicating that the glue had not yet fully cured.

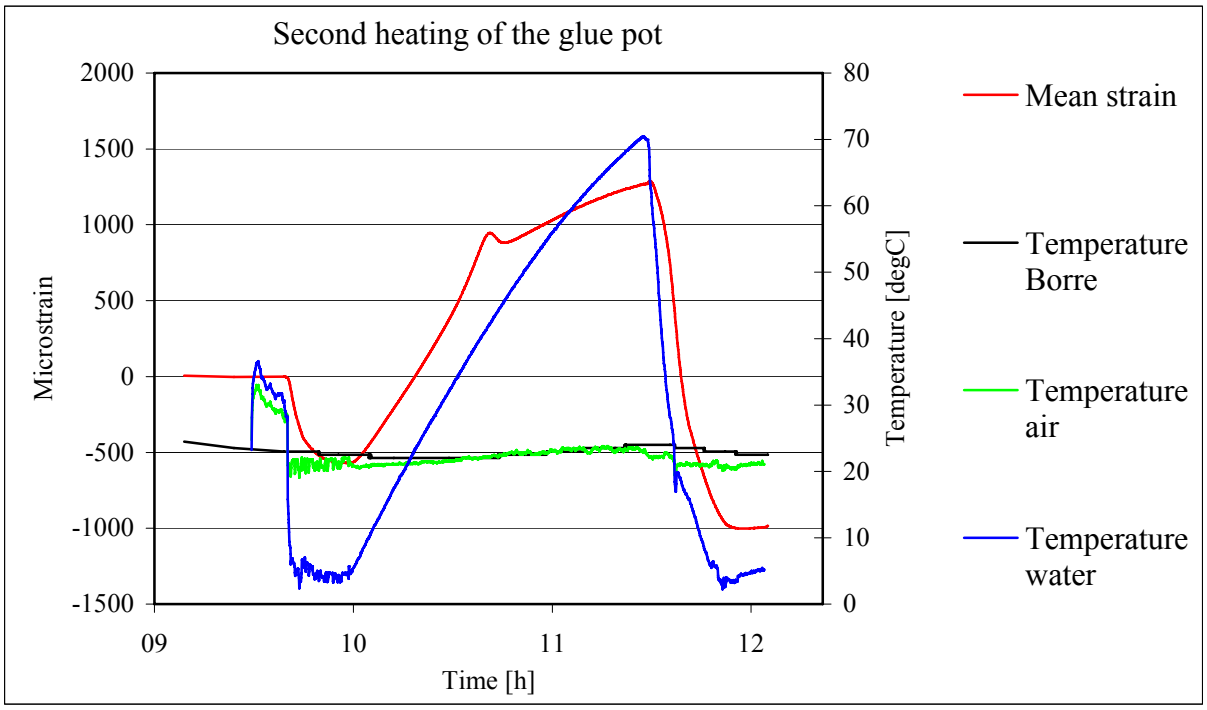


**Figure 4.13 Chart of recorded strains and temperatures during the second heating of the glue pot.**

In the third heating, the glue lump with one strain gauge rosette was tested. As seen in Figure 4.14, the lump was heated from 4 to 70 ºC and was then again cooled down to 4ºC. In the heating phase the response was 50 microstrain/ºC between 4 and 40 ºC and 20 microstrain/ºC in the interval 40-70 ºC. In the cooling phase the response was 20 microstrain/ºC in the interval 70-30 ºC and 90 microstrain/ºC between 30 and 4 ºC. Similar to heating the glue pot, the strain values at corresponding temperature values in the heating and cooling phase were not the same indicating that the glue had not fully cured.

Also in the second heating the glue lump was heated from 4 to 70 ºC and again cooled down to 4 ºC as seen in Figure 4.15. In the heating phase the response was 50 microstrain/ºC up to 40 ºC where it changed to 30 microstrain/ºC. In the cooling phase the response was 100 microstrain/ºC in the interval 70-30 ºC and 20 microstrain/ºC between 30 and 4 ºC. Once more, the strain values at corresponding temperature values in the heating and cooling phase were not the same indicating that the clue had not yet fully cured.

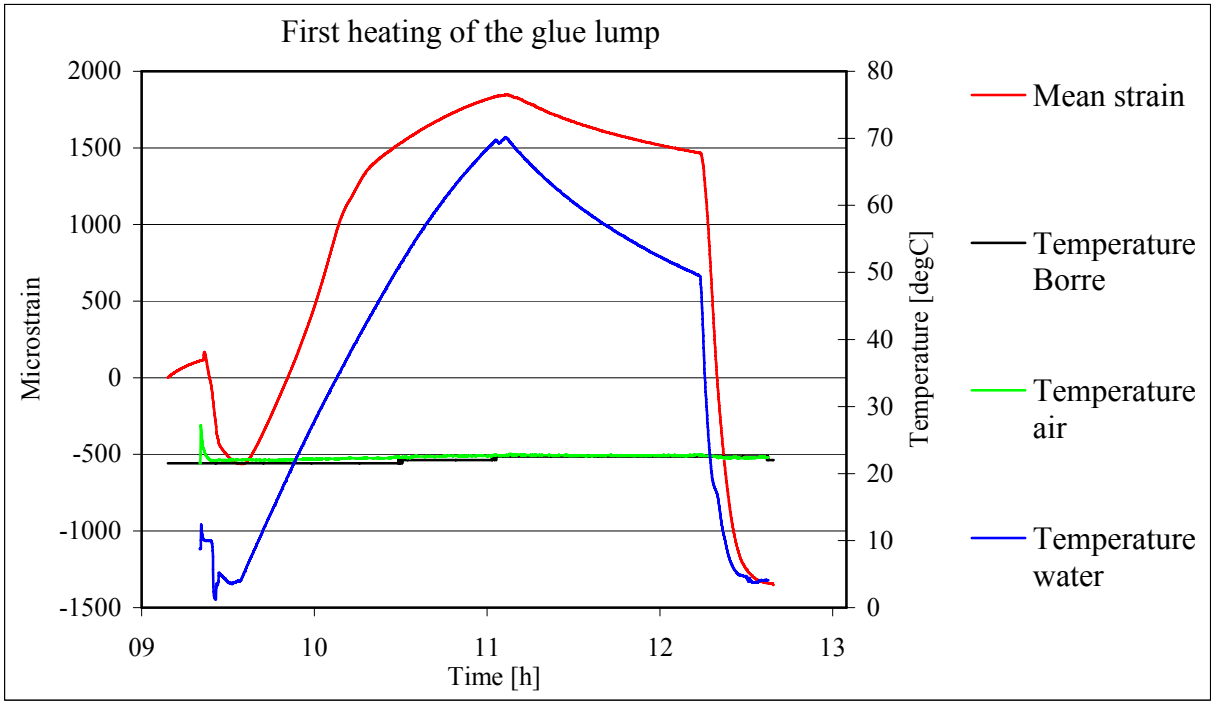


**Figure 4.14 Chart of recorded strains and temperatures during the first heating of the glue lump.**

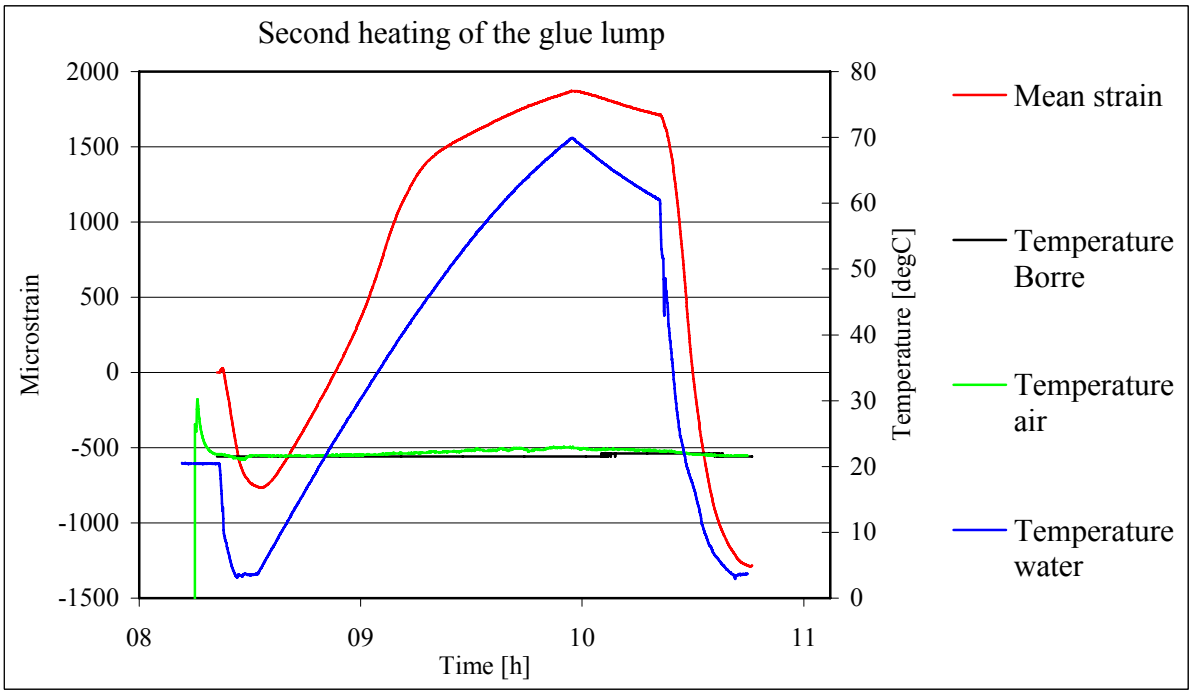


**Figure 4.15 Chart of recorded strains and temperatures during the second heating of the glue lump.**

After advise from Lennart Wallström (2007) the glue lump and glue pot were heated in approximately 70 ºC water for five hours. Thereafter yet another heating was performed in the same way and in the same temperature range as before. Now the response was elastic, as seen in Figure 4.16 below which indicate that a high degree of cure was achieved.

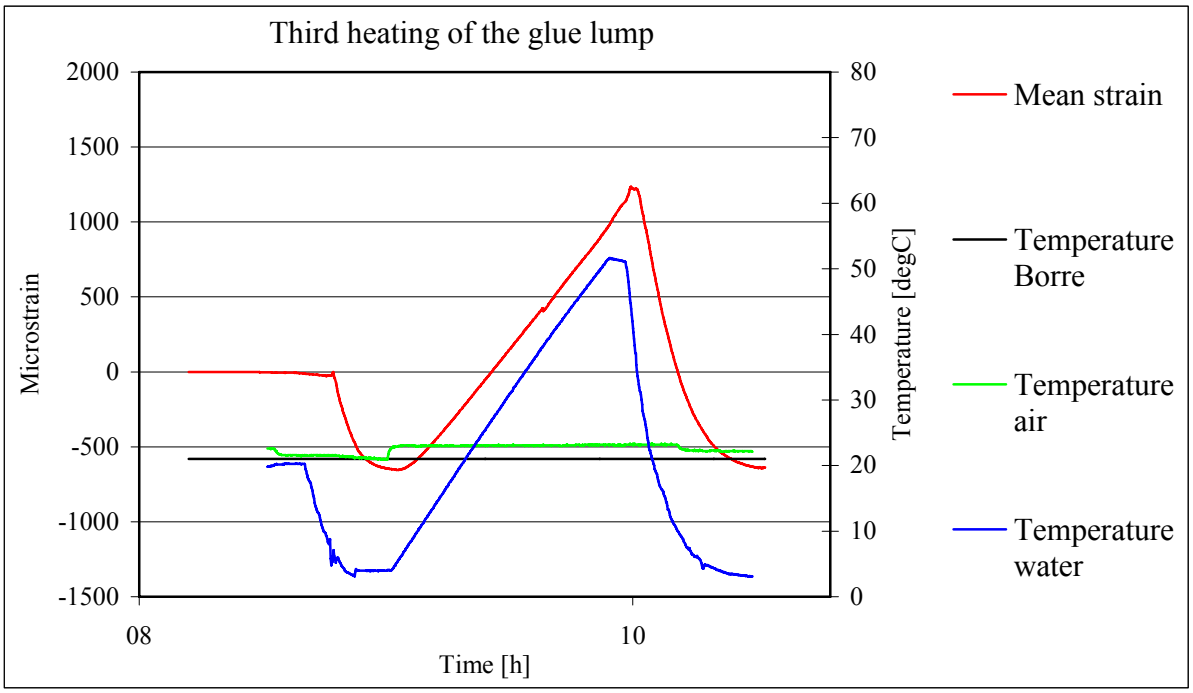


**Figure 4.16 Chart of recorded strains and temperatures during the third heating of the glue lump.**

The full raw data charts for all strain readings corresponding to the diagrams above are presented in Appendix C.

### 4.3.3 Discussion

The tests above showed that when working with an amount of glue as large as used in the glue pot and glue lump, the clue could not fully cure at room temperature in three weeks. However it seemed like the specimen could be heated up to 30-40 ºC before the forming of new cross-links were detectable in the strain readings.

If the response shown in above mentioned tests, also would occur when heating a smaller amount of glue, i.e. when used as adhesive for strain gauges, it would indicate that the glue is not fully cured when used during field conditions. This could thus affect strain readings if heated during overcoring.

## 4.4 Heating strain gauges and glue mounted on aluminium

### 4.4.1 Aim, method

The aim of this test was to determine the combined magnitude of the temperature dependence of the strain gauges and the glue. This was done by heating strain gauges glued into an aluminium cylinder of the same dimensions as an overcored rock sample and heating strain gauges glued onto a flat slab of aluminium. The tests with aluminium cylinders were preceded and concluded with biaxial pressure testing. Two different aluminium cylinders were used, one old with an already existing strain gauge installation and one new where the installation of the strain gauges were carried out before testing. The curing and test conditions for the different aluminium bodies are presented in Table 4.2.

**Table 4.2 Curing and test conditions for the aluminium bodies.**

| | New aluminium cylinder – installation A | New aluminium cylinder – installation B | New aluminium cylinder – installation C | Old aluminium cylinder | Aluminium slab |
|---|---|---|---|---|---|
| **Curing time** | 15-20 h | 15-20 h | 4 weeks | Several years | 15-20 h |
| **Curing temperature [ºC]** | 18-22 | 18-22 | 18-22 | 18-22 | 18-22 |
| **Curing environment** | under water | under water | under water | air | under water |
| **Temperature interval the aluminium bodies were tested in** | | | | | |
| **First heating [ºC]** | 4-29 | 4-61-4 | 5-62-5 | 4-42 | 4-35 |
| **Second heating [ºC]** | 4-35 | - | 5-51-5 | 4-42 | 4-45 |
| **Third heating [ºC]** | - | - | - | 4-61-4 | 4-68-4 |

A photo of one of the cylinders and the slab is shown in Figure 4.17 below. The cylinders and the slab were heated in a way similar to the logger as shown in Figure 4.1.

**Figure 4.17 Aluminium cylinder with attached strain gauge rosettes to the left and aluminium slab with strain gauge rosettes to the right.**

### 4.4.2 Temperature compensation

According to the manufacturer of the strain gauges, the thermal induced strain is given by

$$\varepsilon_a = \varepsilon_m + \varepsilon_s + (\alpha_m - \alpha_{SG})\cdot\Delta T, \quad (5.1)$$

where
$\varepsilon_a$ [$10^{-6}$] = the strain indicated by the amplifier,
$\varepsilon_m$ [$10^{-6}$] = the strain triggered by mechanical load,
$\varepsilon_s$ [$10^{-6}$] = the apparent strain as per the strain gauge pack,
$\alpha_m$ [$10^{-6}$/ºC] = thermal coefficient of linear expansion of the workpiece,
$\alpha_{SG}$ [$10^{-6}$/ºC] = thermal coefficient of linear expansion of the strain gauges,
T [ºC] = temperature.

(http://www.hbm.com/uploads/faqs/FAQ03_037_en.pdf)

The apparent strain for the RY91 strain gauge rosette is specified on the strain gauge pack and given by

$$\varepsilon_s = -25 + 2.06T - 4.8\cdot10^{-2}T^2 + 2.19\cdot10^{-4}T^3 \quad (5.2)$$

In addition to the thermal induced strain there is the temperature response of the *Borre* cell that also should be added to the right hand side of equation 5.1.

If compensated for correctly and solving for the mechanical load, the strain value should be zero. The mechanical load is given by

$$\varepsilon_m = \varepsilon_a - \varepsilon_s - (\alpha_m - \alpha_{SG})\cdot\Delta T - br = 0, \quad (5.3)$$

where

br [$10^{-6}$] = the apparent strain registered by the *Borre* cell.

### 4.4.3 Result and analysis of the new aluminium cylinder

#### Installation A

Prior to the first heating a biaxial pressure test was performed, see Figure 4.18 below. In the strain-time plot, the lines corresponding to gauges in the same direction (vertical, tangential, 45º) did not respond in the exact same way. This could be an indication of insufficient bonding between the gauges and cylinder. In the strain-load plot the paths of the loading and unloading curves did not coincide totally, which is an indication of an inelastic behaviour that is not expected for aluminium. This together with the calculated values of Young's modulus and Poisson's ratio not being particularly close to those specified for the material (E = 70 GPa, ν = 0.35) made the quality of the installation questionable.

a)

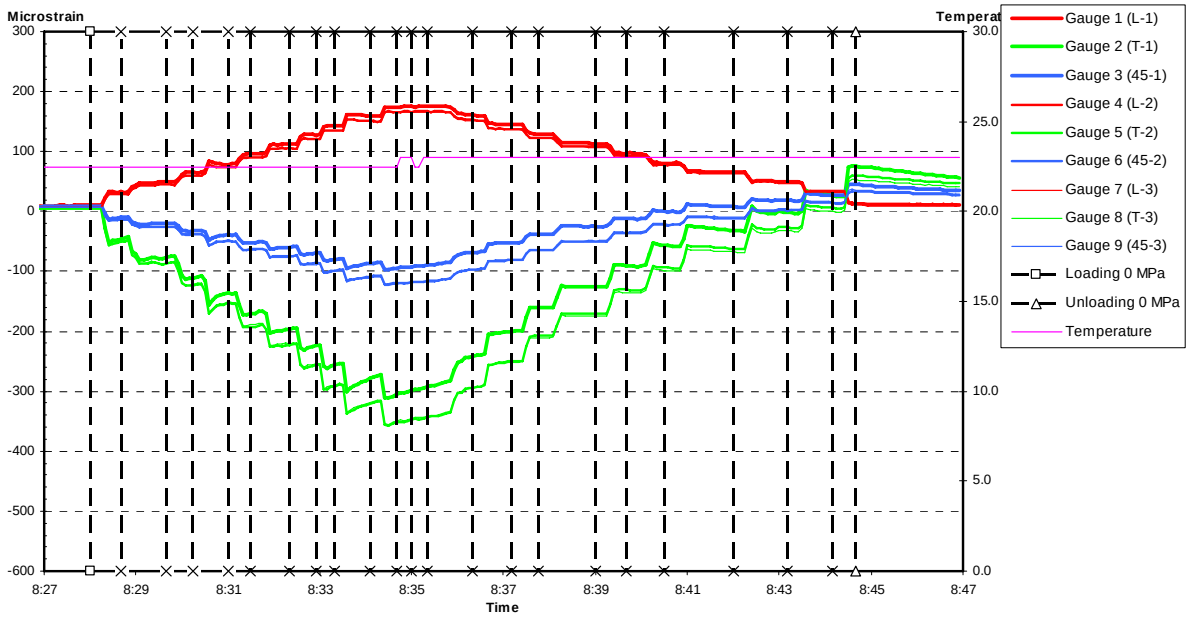


b)

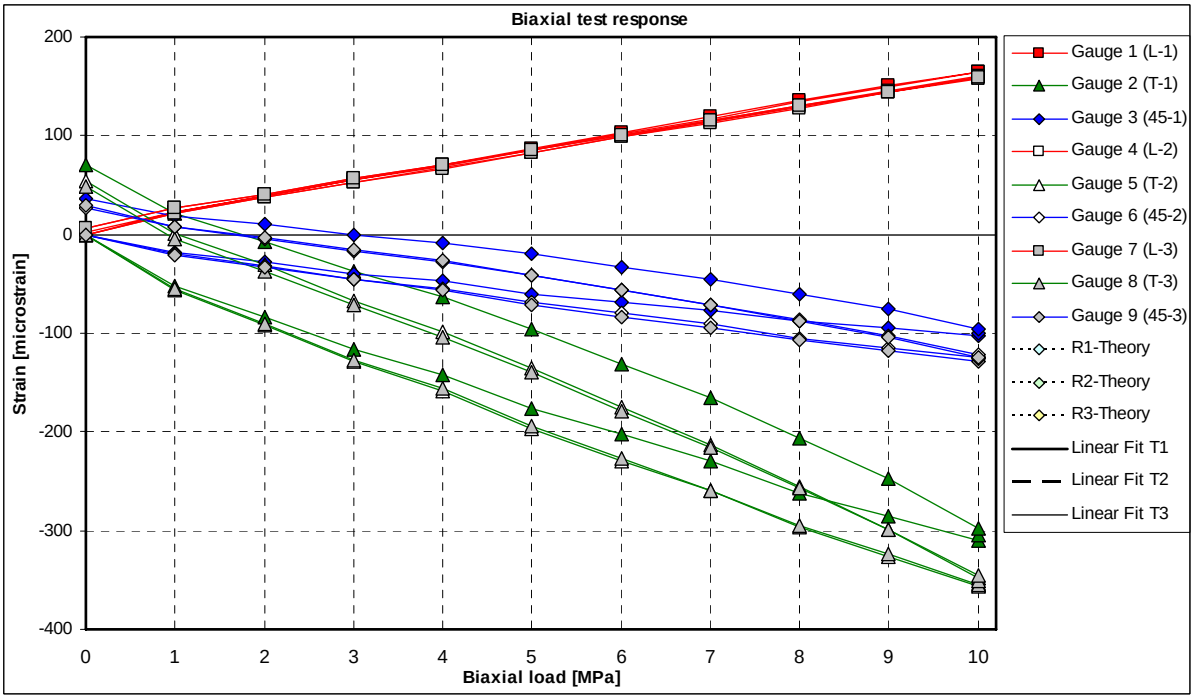


c)

**Mean values for unloading curve**

**Pressure range [MPa]**

Loading

Unloading

$P_{max}$ 8

$P_{min}$ 3

**Include/exclude gauges**

| Tangential | Inclined |
|---|---|
| ☑ Rosette 1 | ☐ Rosette 1 |
| ☑ Rosette 2 | ☐ Rosette 2 |
| ☑ Rosette 3 | ☐ Rosette 3 |

| Secant value mean | | Linear fit (10-0) mean | |
|---|---|---|---|
| $E$ = | 83.3 | $E$ = | 82.3 |
| $\nu$ = | 0.45 | $\nu$ = | 0.41 |

**Figure 4.18 First biaxial pressure test prior to the first heating of the new aluminium cylinder, installation A. a) Strain-time plot. b) Strain-load plot. c) Calculated values of Young's modulus and Poisson's ratio.**

To make sure the above result was not due to imprecise testing performance, another test was done right after the first one, but the results were of the same quality as the first test.

After the biaxial pressure tests, the aluminium cylinder was heated. As seen in Figure 4.19 below, the cylinder was heated from 4 ºC to 29 ºC. The aluminium cylinder showed a linear temperature response of a little more than 10 microstrain/ºC. The temperature-induced strains were almost completely compensated for according to the guidelines from HBM. The calibrated strain curve gave a slightly negative linear response which could be an indication of the glue not being fully cured.

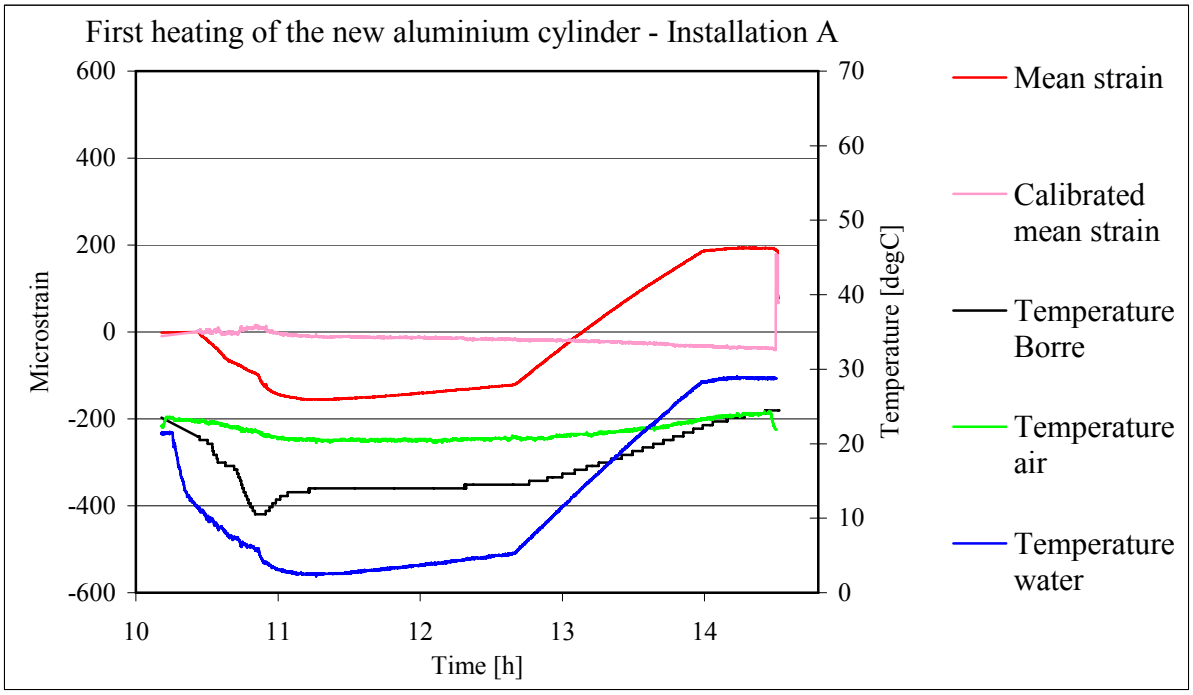


**Figure 4.19 Chart of recorded strains and temperatures during the first heating of the new aluminium cylinder, installation A.**

In the raw data chart of the above diagram, all strain gauges responded in the same way and no indication of insufficient bonding could be detected. In the following biaxial pressure test though, clear indications of debonding could be seen in the strain-time plot as well as in the strain-load plot, see Figure 4.20. Several gauges, and in particular the 45º-gauges, showed divergent and drifting values.

a)

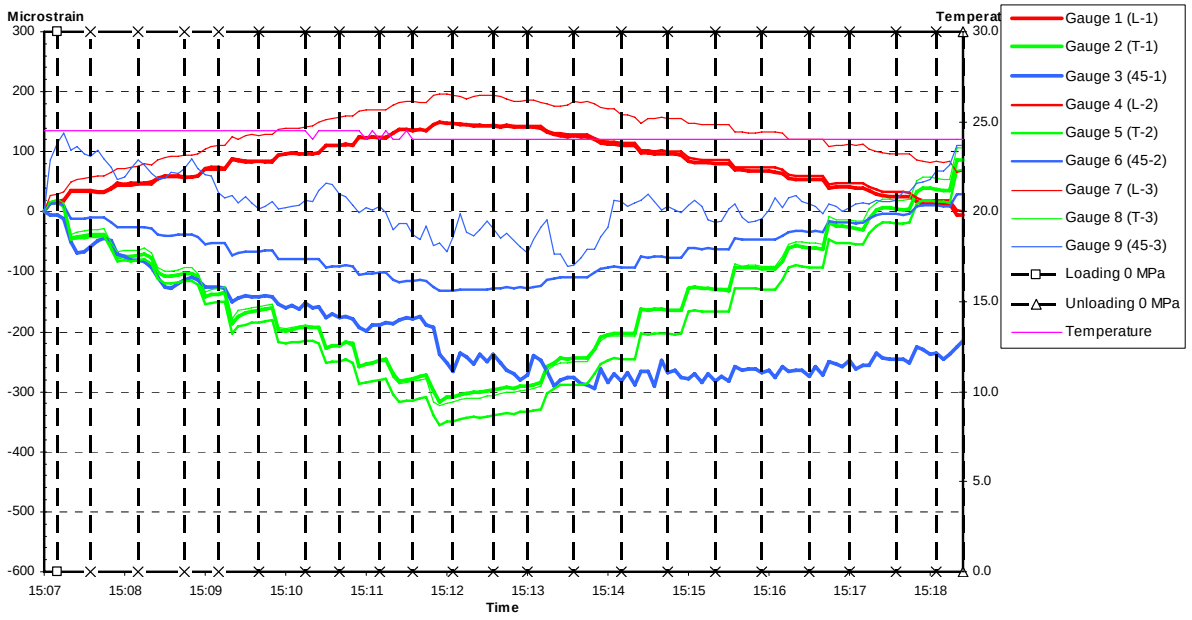


b)

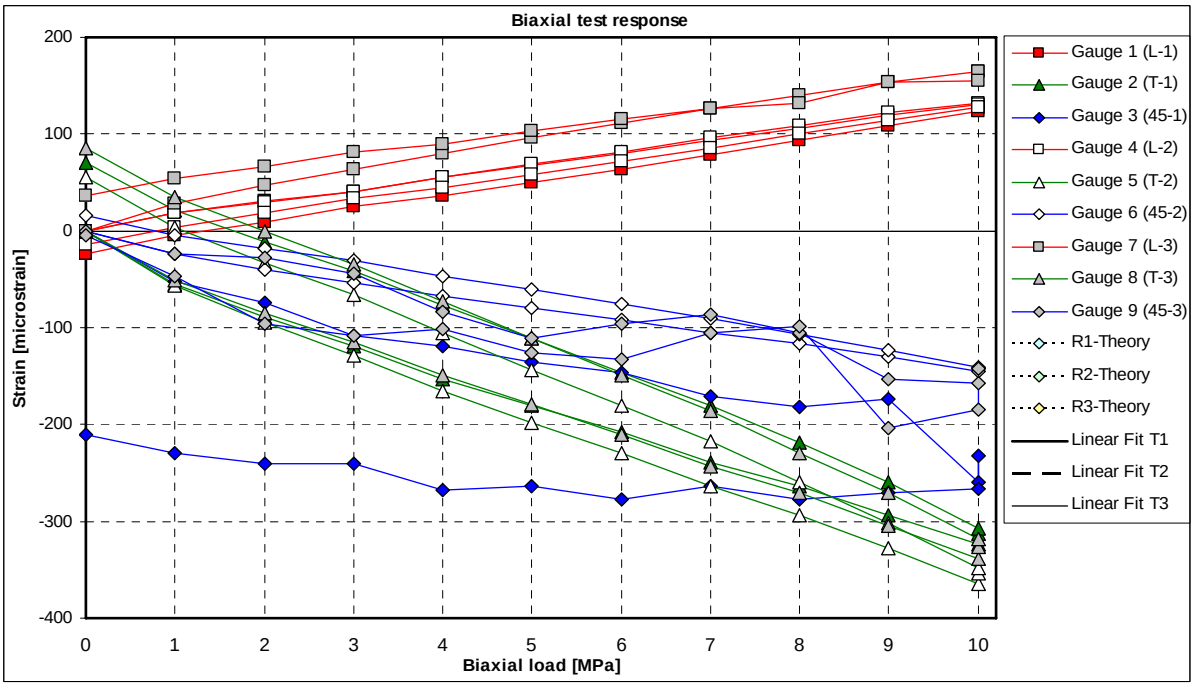


c)

**Mean values for unloading curve**

**Pressure range [MPa]**

Loading / Unloading

$P_{max}$ 8

$P_{min}$ 3

**Include/exclude gauges**

| Tangential | Inclined |
|---|---|
| ☑ Rosette 1 | ☐ Rosette 1 |
| ☑ Rosette 2 | ☐ Rosette 2 |
| ☑ Rosette 3 | ☐ Rosette 3 |

| Secant value mean | | Linear fit (10-0) mean | |
|---|---|---|---|
| $E$ = | 79.0 | $E$ = | 79.8 |
| $\nu$ = | 0.37 | $\nu$ = | 0.35 |

**Figure 4.20 Biaxial pressure test after the first heating of the new aluminium cylinder and prior to the second heating, installation A. a) Strain-time plot. b) Strain-load plot. c) Calculated values of Young's modulus and Poisson's ratio.**

After this second biaxial pressure test yet another heating was conducted. As seen in Figure 4.21 below, the initial temperature was 4 ºC and held constant for 40 minutes before heating started. The temperature was raised in intervals to 10, 15, 20, 25, 30 and 35 ºC. It was held constant at 10, 15, 25 and 30 ºC for 20 minutes and at 20 ºC for 45 minutes before heating was continued. Strain gauges 2, 3, 6, 7, 9 showed divergent and drifting values and hence were excluded in the mean value calculation. The aluminium cylinder showed a linear temperature response of a little more than 10 microstrain/ºC. The temperature-induced strains were completely compensated for according to the guidelines from HBM as the calibrated strain curve oscillated randomly around zero. This probably means that the glue now had reached a high degree of cure.

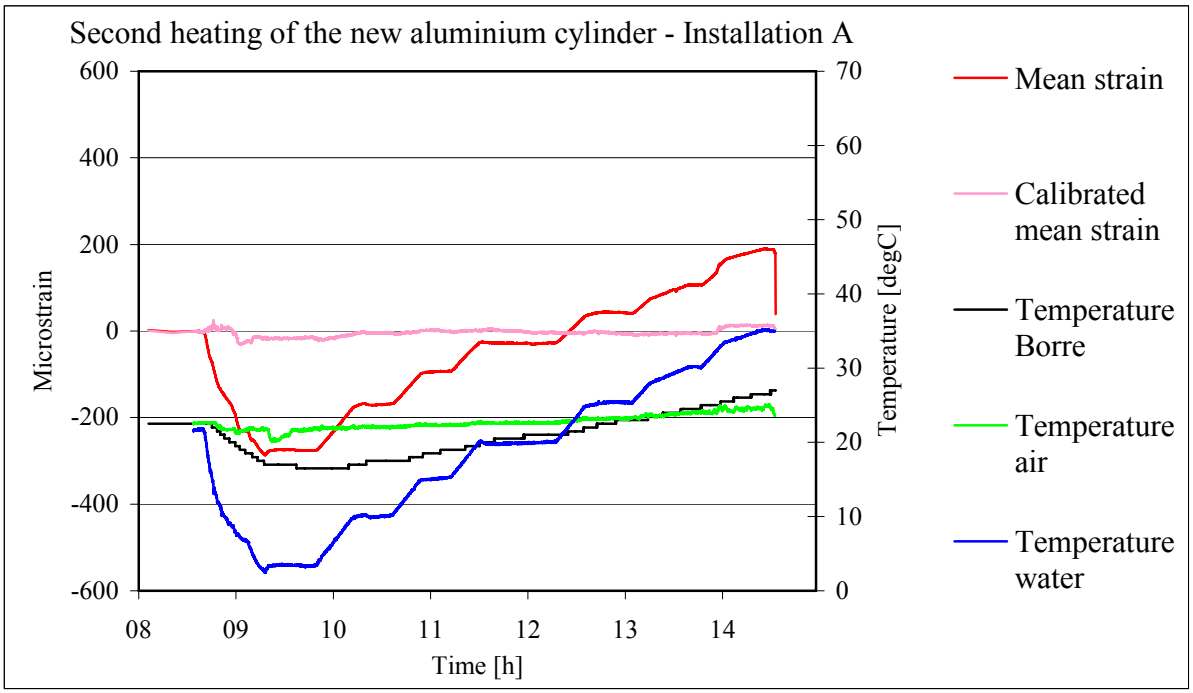


**Figure 4.21 Chart of recorded strains and temperatures during the second heating of the new aluminium cylinder, installation A.**

The biaxial pressure test after the second heating showed nearly perfect values as seen in Figure 4.22 below, but it was still decided to make a new installation of the strain gauges in the aluminium cylinder to ensure that the gauges were sufficiently bonded.

a)

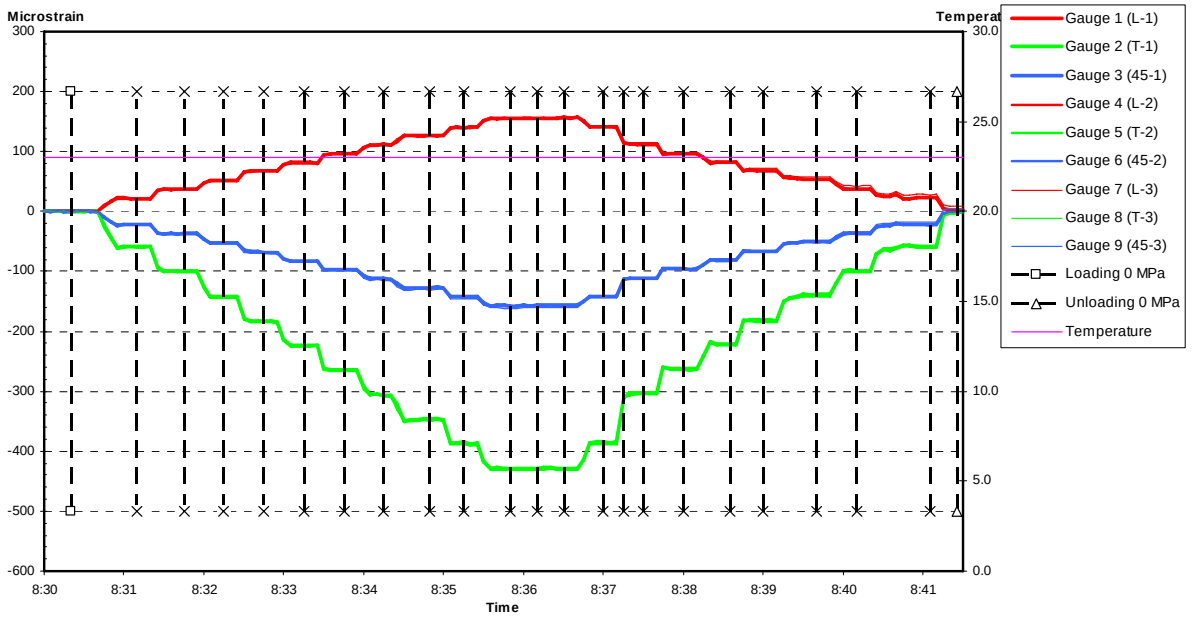


b)

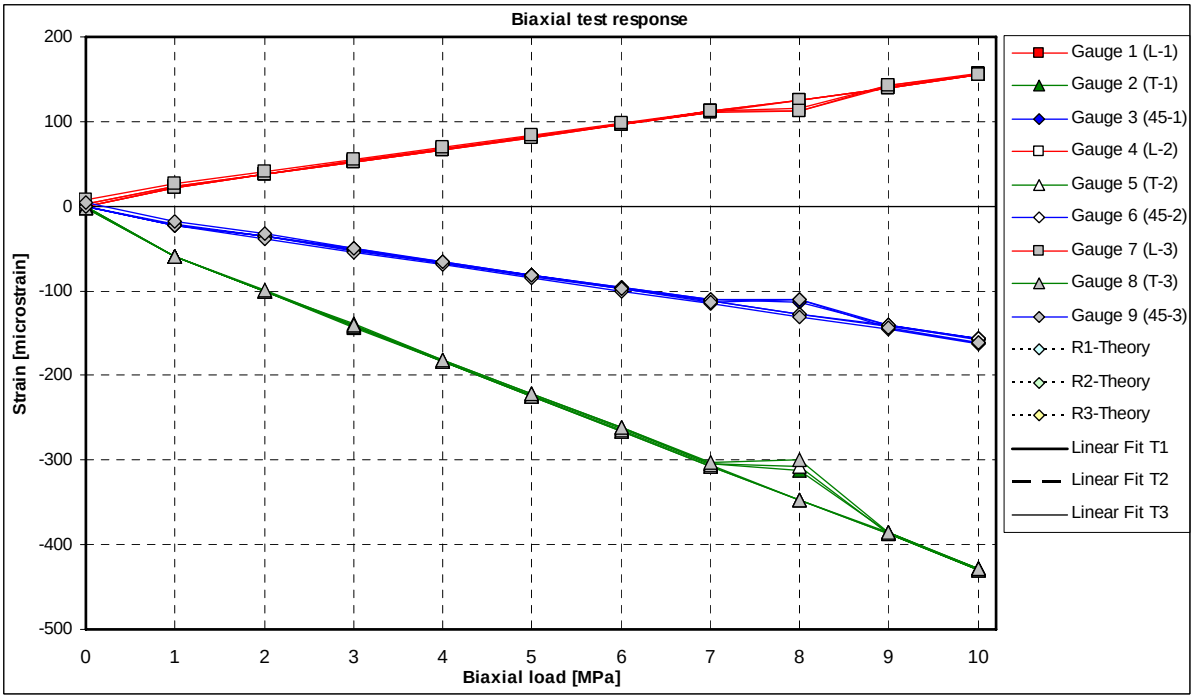


c)

**Mean values for unloading curve**

**Pressure range [MPa]**

Loading

Unloading

$P_{max}$ 8

$P_{min}$ 3

**Include/exclude gauges**

| Tangential | Inclined |
|---|---|
| ☑ Rosette 1 | ☐ Rosette 1 |
| ☑ Rosette 2 | ☐ Rosette 2 |
| ☑ Rosette 3 | ☐ Rosette 3 |

| Secant value mean | | Linear fit (10-0) mean | |
|---|---|---|---|
| $E$ = | 71.0 | $E$ = | 74.7 |
| $\nu$ = | 0.36 | $\nu$ = | 0.36 |

**Figure 4.22 Biaxial pressure test after the second heating of the new aluminium cylinder, installation A. a) Strain-time plot. b) Strain-load plot. c) Calculated values of Young's modulus and Poisson's ratio.**

## Installation B

As seen in Figure 4.23 below, the biaxial pressure test prior to the first heating with the second installation showed moderately good values, similar to those prior to the first heating with the first installation.

a)

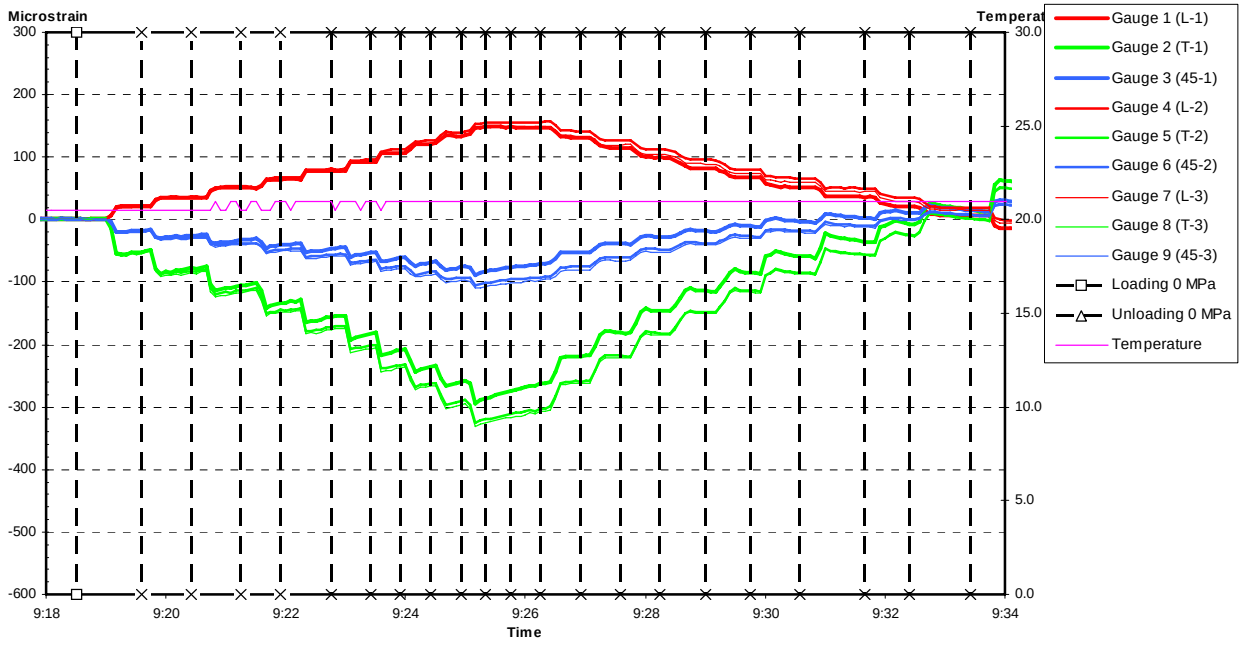


b)

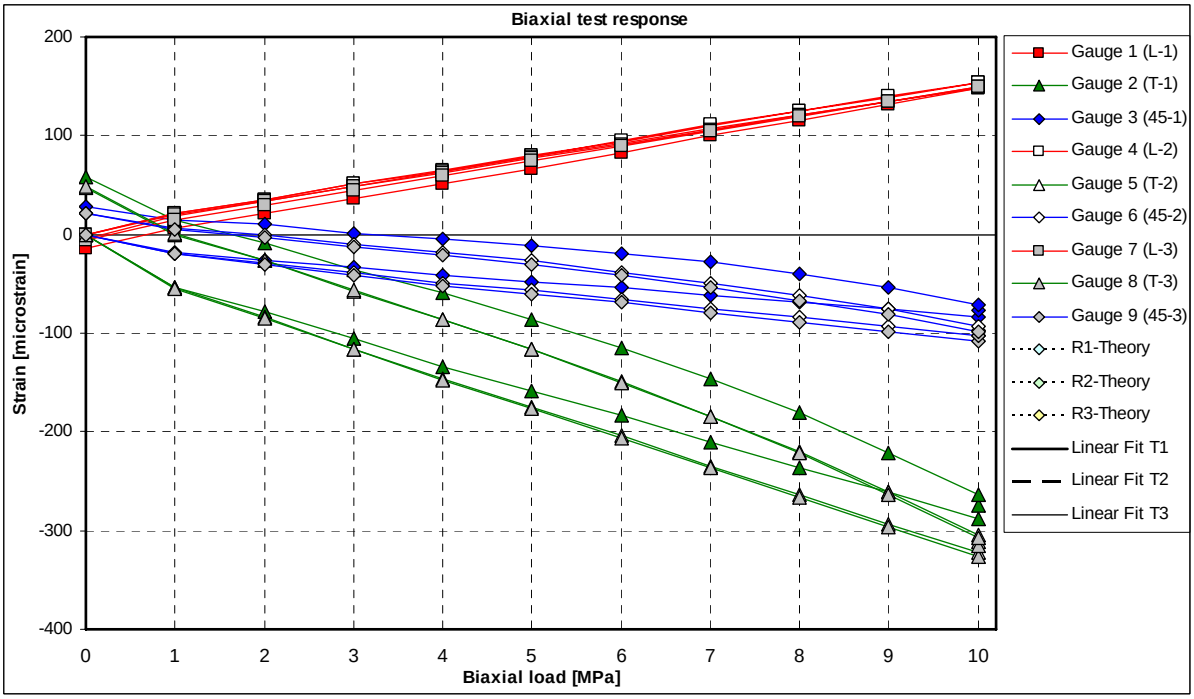


**Figure 4.23 Biaxial pressure test prior to the first heating of the new aluminium, installation B. a) Strain-time plot. b) Strain-load plot. c) Calculated values of Young's modulus and Poisson's ratio.**

c)

| Mean values for unloading curve | | | | |
|---|---|---|---|---|
| Pressure range [MPa] | | | Include/exclude gauges | |
| | | | Tangential | Inclined |
| Loading | $P_{max}$ | 8 | ☑ Rosette 1 | ☐ Rosette 1 |
| Unloading | $P_{min}$ | 3 | ☑ Rosette 2 | ☐ Rosette 2 |
| | | | ☑ Rosette 3 | ☐ Rosette 3 |

| Secant value mean | | Linear fit (10-0) mean | |
|---|---|---|---|
| $E$ = | 95.1 | $E$ = | 92.9 |
| $\nu$ = | 0.51 | $\nu$ = | 0.47 |

**Figure 4.23 (Continued)**

The heating following the biaxial pressure test can be seen in Figure 4.24 below. The initial temperature was again 4 ºC and held constant for 15 minutes before heating to 61 ºC started. Strain gauges 1, 2 3, 4 and 5 showed divergent values and hence were excluded in the mean value calculation. The aluminium cylinder now showed a linear temperature response of 10 microstrain/ºC in the heating phase and 20 microstrain/ºC in the cooling phase. The final temperature in the cooling phase was the same as the heating phase started with (4 ºC), but the corresponding strain values were not the same. Hence the response was not elastic. Since the final strains were less than the initial, the difference cannot be explained as remaining temperature-induced strains but rather as an effect of uncured glue. Therefore, the temperature-induced strains could not be compensated for according to the guidelines from HBM either.

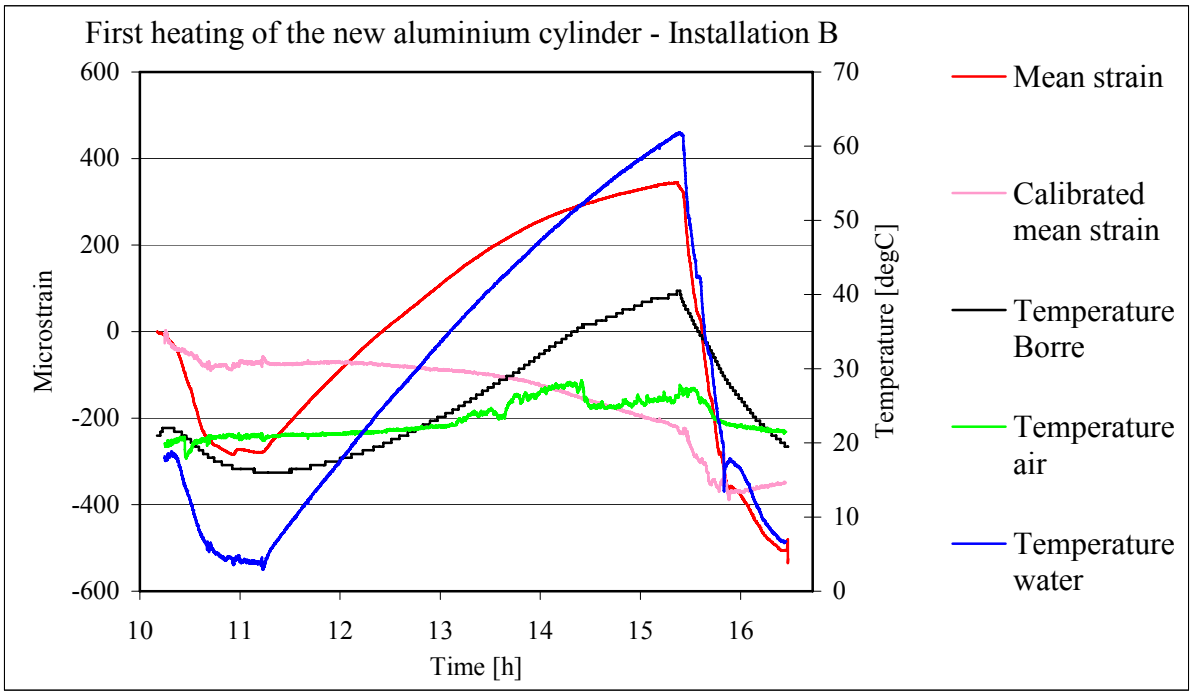


**Figure 4.24 Chart of recorded strains and temperatures during the first heating of the new aluminium cylinder, installation B.**

During the heating, several gauges showed divergent and drifting values indicating debonding. But similar to the first installation, the following biaxial pressure test again showed nearly perfect values, as seen in Figure 4.25 below, indicating good bonding. But as the logger was detached from the cylinder one strain gauge rosette easily fell off as if it had not been bonded at all. Hence, one more installation was decided upon.

a)

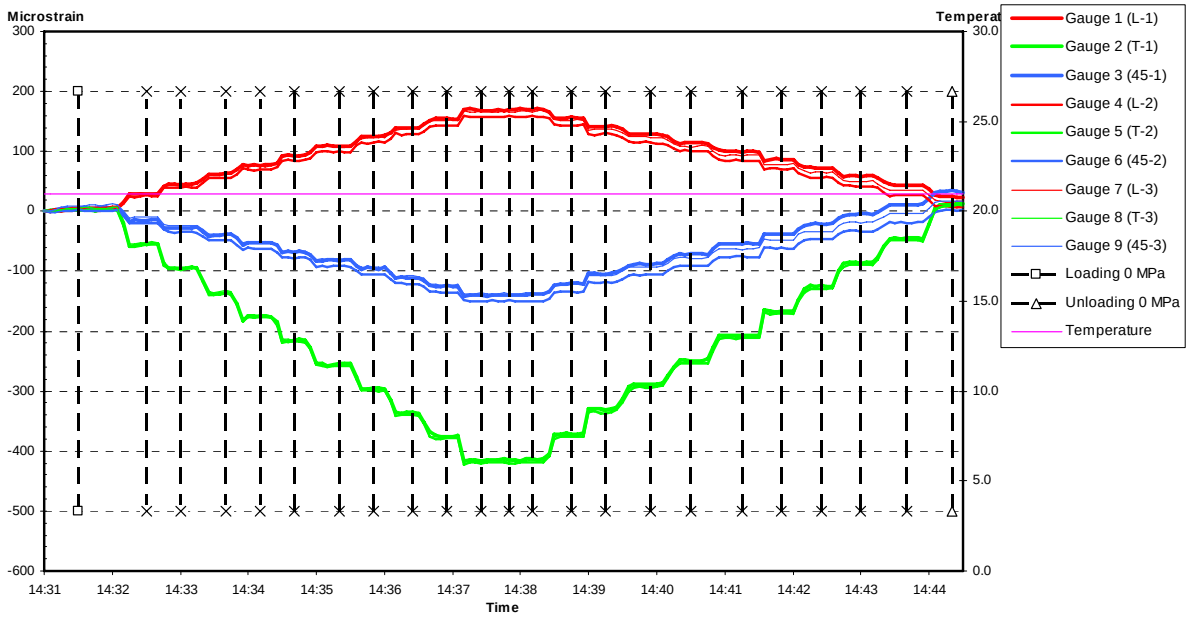


b)

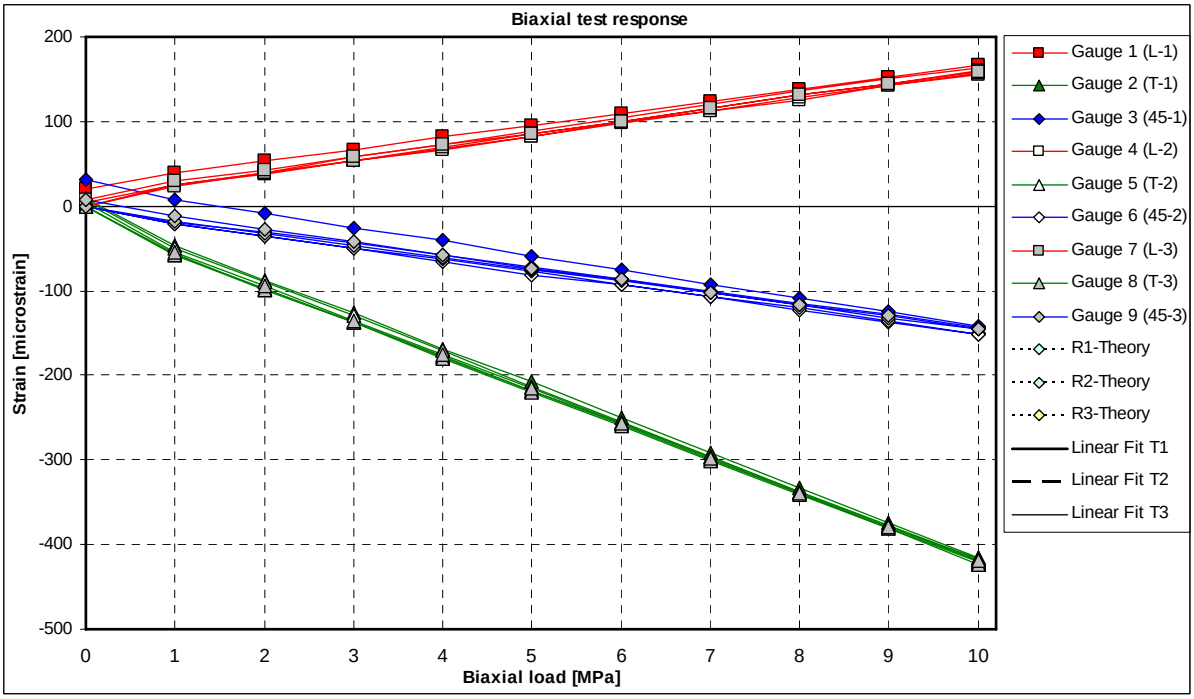


**Figure 4.25 Biaxial pressure testing after the first heating of the new aluminium cylinder, installation B. a) Strain-time plot. b) Strain-load plot. c) Calculated values of Young's modulus and Poisson's ratio.**

c)

| Mean values for unloading curve | | | | |
|---|---|---|---|---|
| Pressure range [MPa] | | | Include/exclude gauges | |
| | | | Tangential | Inclined |
| Loading | $P_{max}$ | 8 | ☑ Rosette 1 | ☐ Rosette 1 |
| Unloading | $P_{min}$ | 3 | ☑ Rosette 2 | ☐ Rosette 2 |
| | | | ☑ Rosette 3 | ☐ Rosette 3 |
| Secant value mean | | | Linear fit (10-0) mean | |
| $E$ = | 69.3 | | $E$ = | 73.1 |
| $\nu$ = | 0.35 | | $\nu$ = | 0.35 |

**Figure 4.25 (Continued)**

## Installation C

As seen in Figure 4.26 below, the biaxial pressure test prior to the first heating with the third installation showed much better values than the two previous installations. All strain gauges in respective direction (vertical, tangential, 45º) responded in a similar way in the strain-time plot and the strain-time plot showed very good linear elasticity.

a)

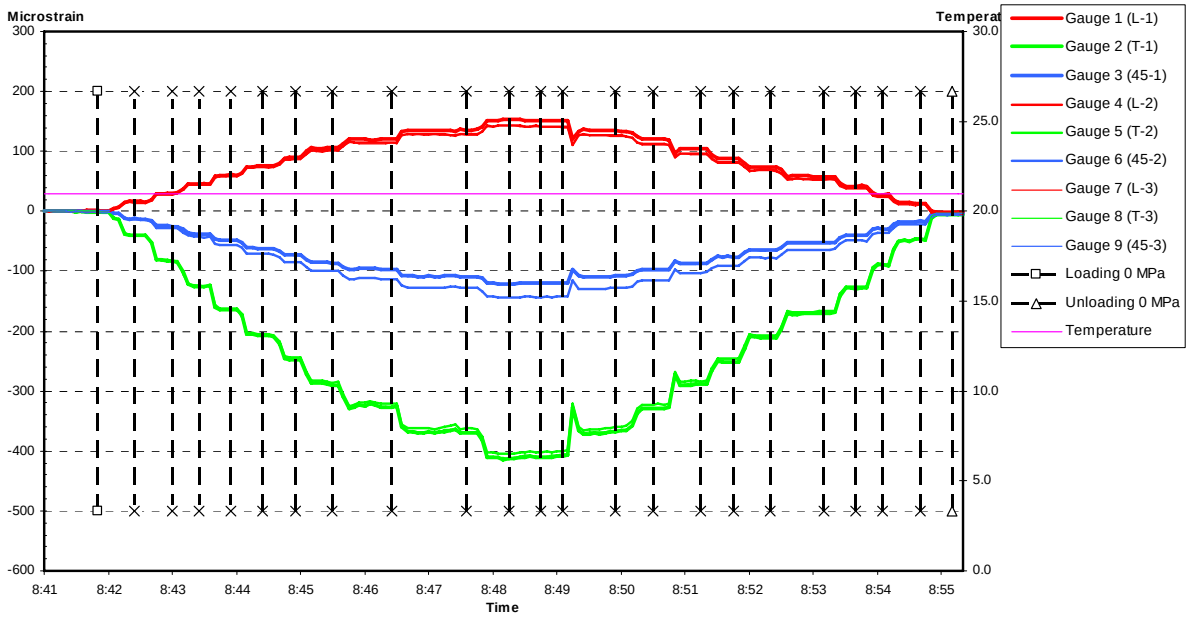


**Figure 4.26 Biaxial pressure test prior to the first heating of the new aluminium cylinder, installation C. a) Strain-time plot. b) Strain-load plot. c) Calculated values of Young's modulus and Poisson's ratio.**

b)

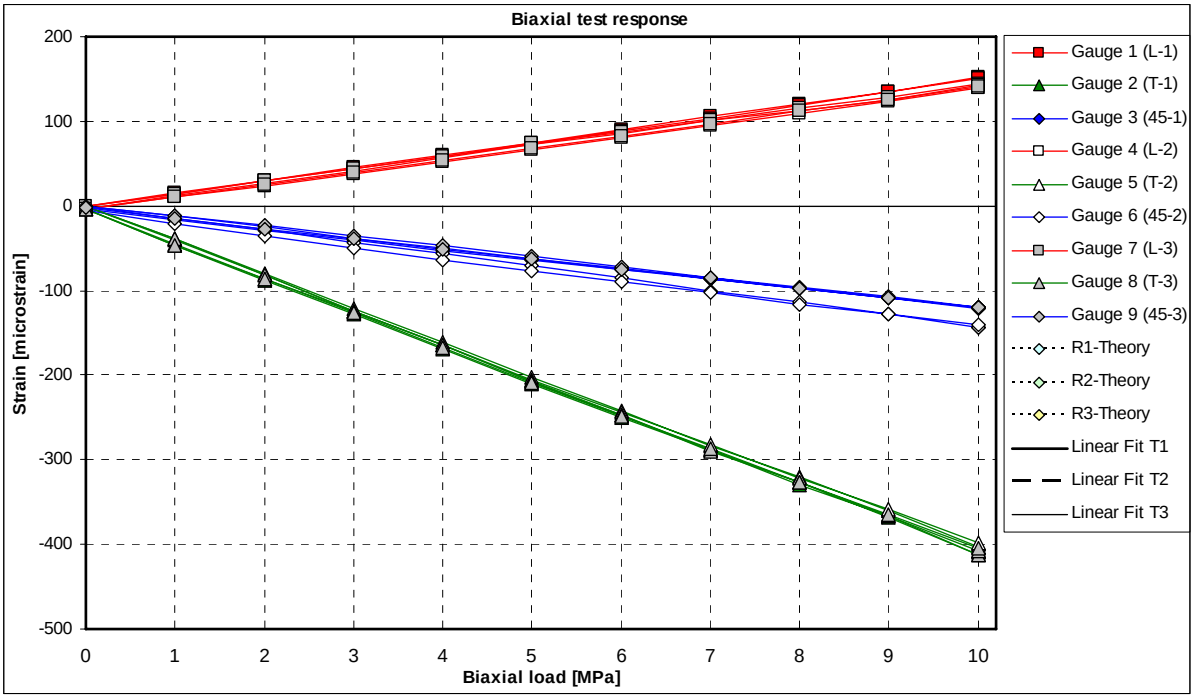


c)

| Mean values for unloading curve | | | | |
|---|---|---|---|---|
| Pressure range [MPa] | | Include/exclude gauges | | |
| Loading | $P_{max}$ 8 | Tangential | | Inclined |
| Unloading | $P_{min}$ 3 | ☑ Rosette 1 | | ☐ Rosette 1 |
| | | ☑ Rosette 2 | | ☐ Rosette 2 |
| | | ☑ Rosette 3 | | ☐ Rosette 3 |
| Secant value mean | | Linear fit (10-0) mean | | |
| $E$ = | 74.9 | $E$ = | 76.4 | |
| $\nu$ = | 0.35 | $\nu$ = | 0.37 | |

**Figure 4.26 (Continued)**

Following the biaxial pressure test was the heating shown in Figure 4.27 below. The aluminium cylinder was heated from 5 to 62 ºC before it was allowed to cool down to 5 ºC again. In the heating phase a linear response of a little more than 10 microstrain/ºC was indicated compared to a little less than 20 microstrain/ºC in the cooling phase. The fact that the strain values at corresponding temperatures in the heating and cooling phase were not the same, was as previously explained, probably due to not fully cured glue.

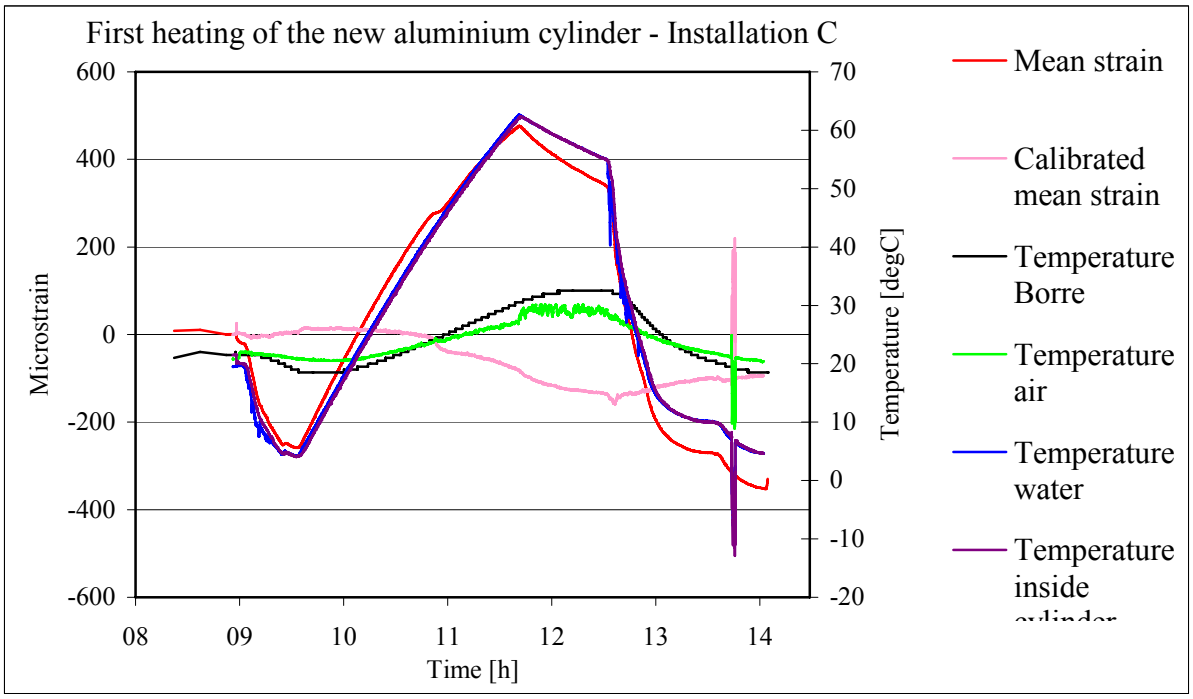


**Figure 4.27 Chart of recorded strains and temperatures during the first heating of the new aluminium cylinder, installation C.**

The biaxial pressure test after the heating showed values similar to those in the test before. All strain gauges seemed to have bonded well and the installation was judged successful.

a)

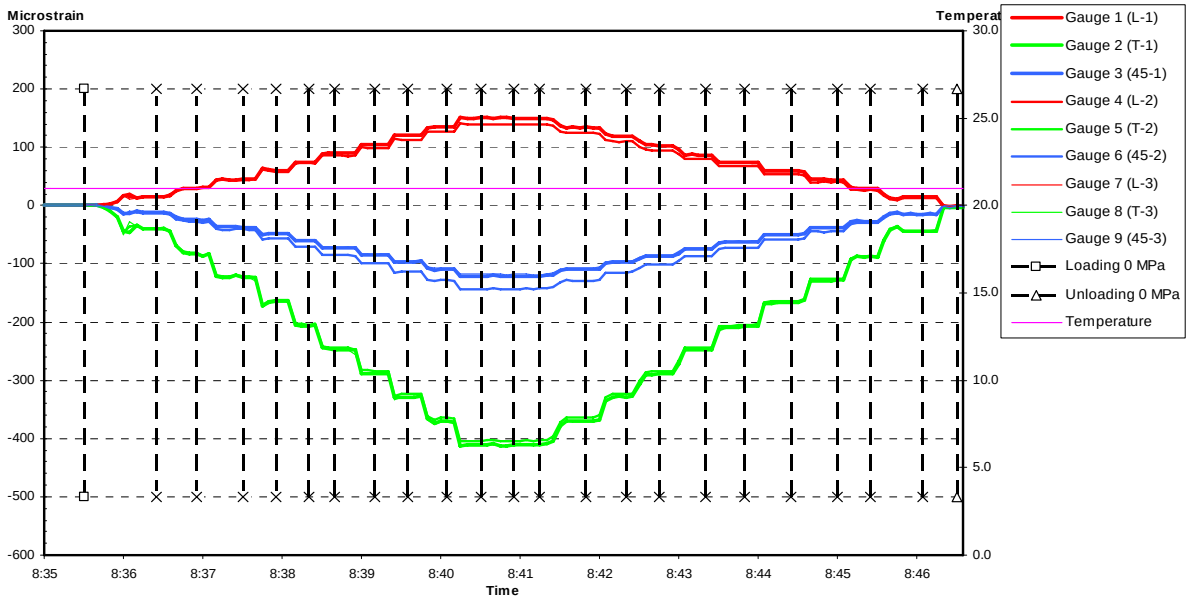


b)

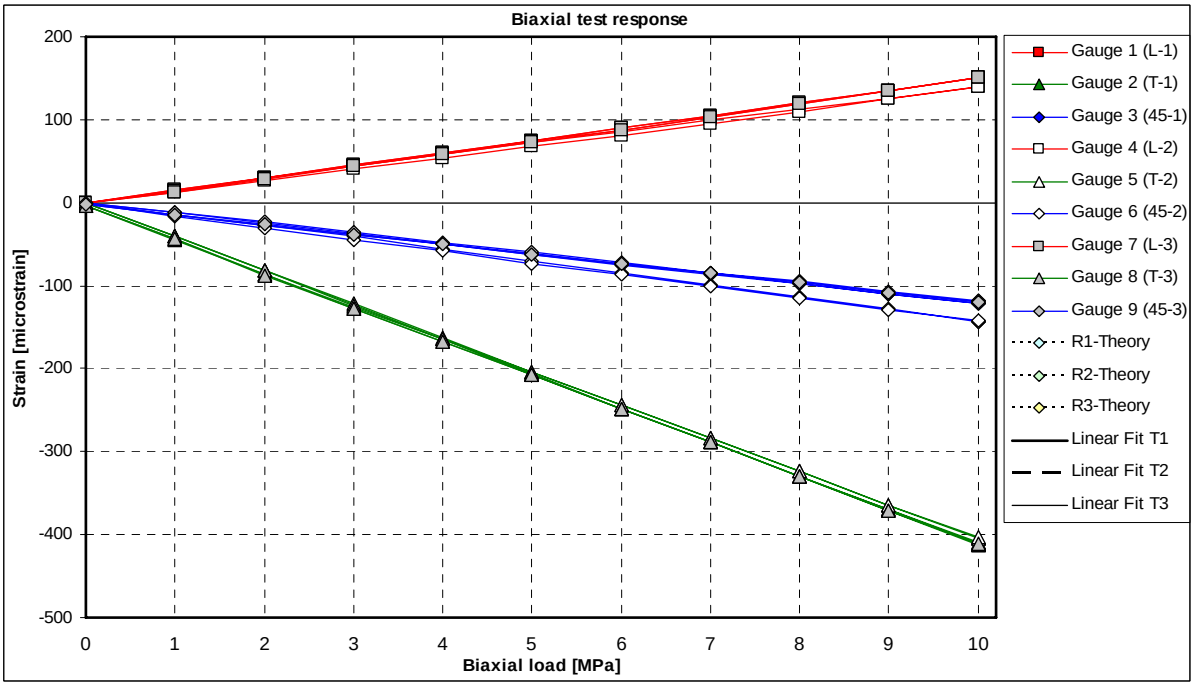


c)

**Mean values for unloading curve**

**Pressure range [MPa]**

Loading

Unloading

$P_{max}$ 8

$P_{min}$ 3

**Include/exclude gauges**

| Tangential | Inclined |
|---|---|
| ☑ Rosette 1 | ☐ Rosette 1 |
| ☑ Rosette 2 | ☐ Rosette 2 |
| ☑ Rosette 3 | ☐ Rosette 3 |

| Secant value mean | | Linear fit (10-0) mean | |
|---|---|---|---|
| $E$ = | 75.1 | $E$ = | 75.5 |
| $\nu$ = | 0.36 | $\nu$ = | 0.36 |

**Figure 4.28 Biaxial pressure test after the first heating of the new aluminium cylinder and prior to the second heating of the new aluminium cylinder, installation C. a) Strain-time plot. b) Strain-load plot. c) Calculated values of Young's modulus and Poisson's ratio.**

Before the following heating was performed, the cylinder was immersed in 65 ºC water for two hours to ensure a high degree of cure. As expected, the cylinder thereafter showed an elastic behaviour with a linear response of a little more than 10 microstrain/ºC both in the heating and cooling phase as seen in Figure 4.29 below. The slight temperature dependence remaining in the calibrated value could be better compensated for by adding a term of the form $-k \cdot \Delta T$ to equation 4.3. No linear regression has been made, but the estimated value $k = 1.5$ seemed to be a relatively good approximation. Assuming that the apparent strain triggered by the strain gauges, $\varepsilon_s$, and the coefficient of thermal expansion for the aluminium cylinder as well as for the strain gauges, $\alpha_m$ respectively $\alpha_{SG}$, were correctly specified, this term would then imply that the glue as a material affected the strain readings by this amount and that k would be equivalent to $\alpha_{glue}$.

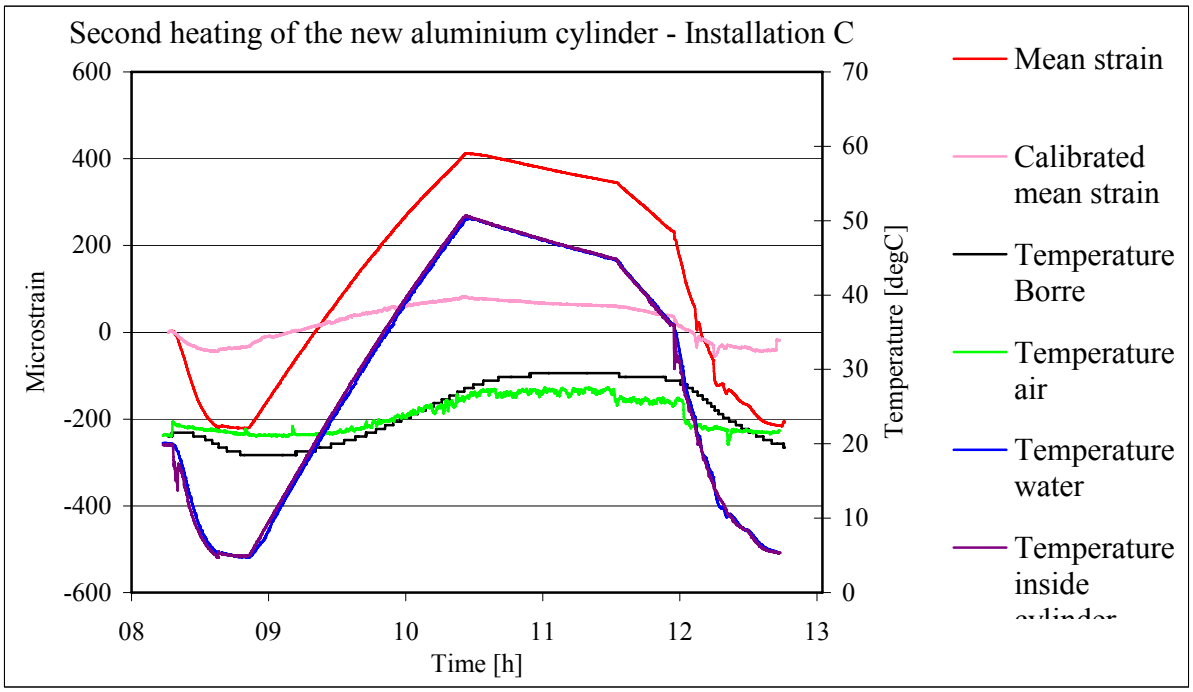


**Figure 4.29 Chart of recorded strains and temperatures during the second heating of the new aluminium cylinder, installation C.**

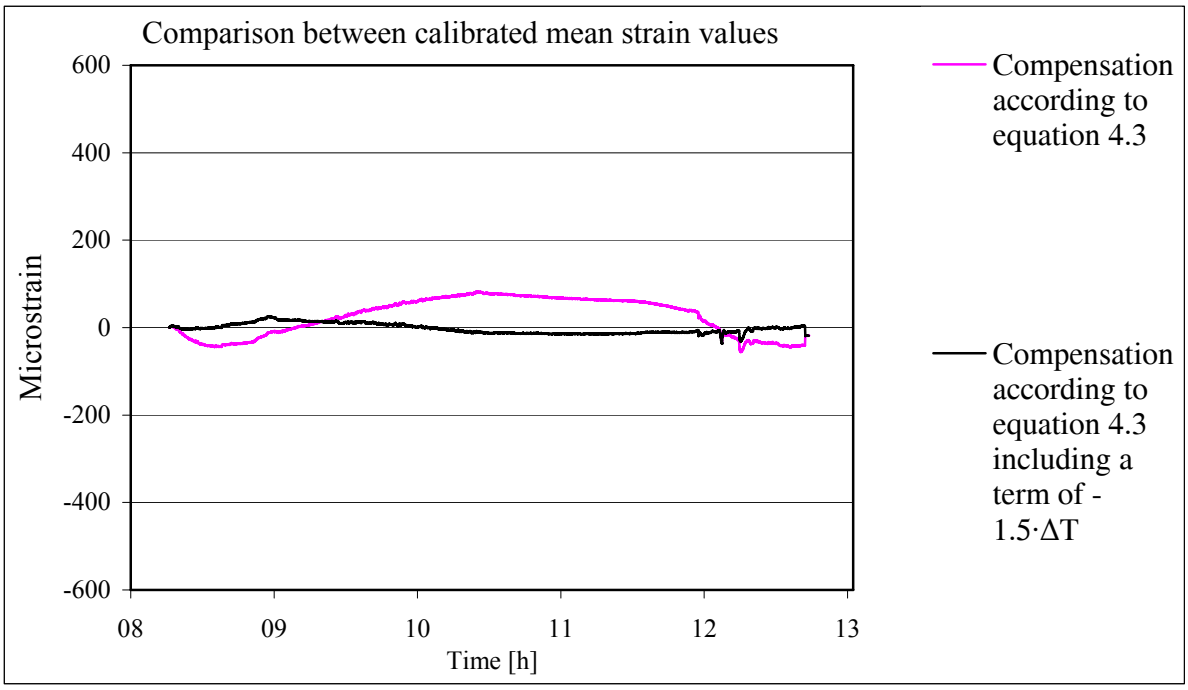


**Figure 4.30 Comparison between the calibrated mean strain compensated according to equation 4.3 and compensated according to equation 4.3 with the addition of the term -1.5·ΔT.**

Except for the drifting values of strain gauge number 6, the biaxial pressure test concluding the test series showed nothing but expected values in all plots as seen in Figure 4.31.

a)

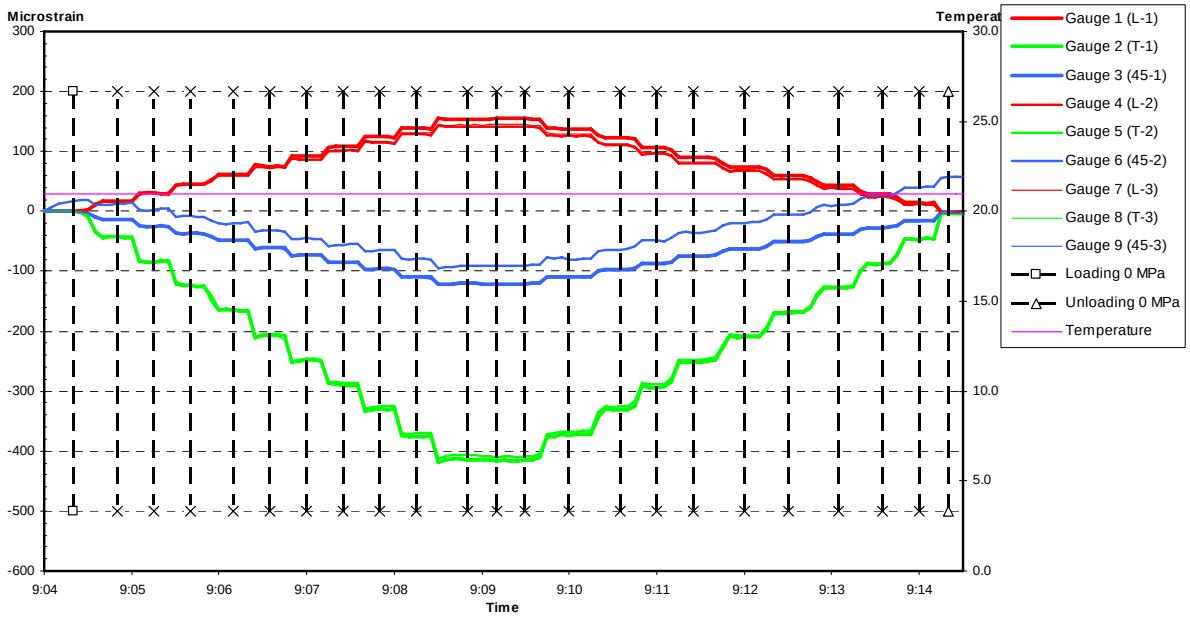


**Figure 4.31 Biaxial pressure test after the second heating of the new aluminium cylinder, installation C. a) Strain-time plot. b) Strain-load plot. c) Calculated values of Young's modulus and Poisson's ratio.**

b)

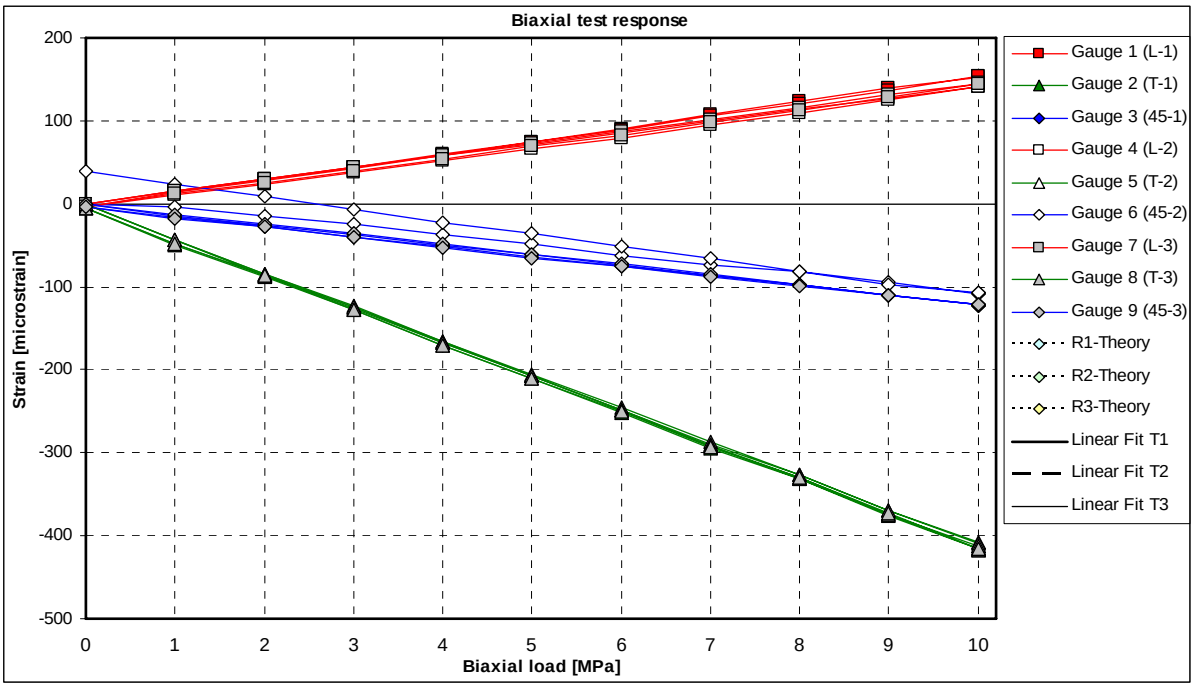


c)

**Mean values for unloading curve**

**Pressure range [MPa]**

Loading

Unloading

$P_{max}$ 8

$P_{min}$ 3

**Include/exclude gauges**

| Tangential | Inclined |
|---|---|
| ☑ Rosette 1 | ☐ Rosette 1 |
| ☑ Rosette 2 | ☐ Rosette 2 |
| ☑ Rosette 3 | ☐ Rosette 3 |

| Secant value mean | | Linear fit (10-0) mean | |
|---|---|---|---|
| $E$ = | 74.5 | $E$ = | 74.8 |
| $\nu$ = | 0.36 | $\nu$ = | 0.37 |

**Figure 4.31 (Continued)**

The full raw data charts for all strain readings corresponding to the diagrams above can be viewed in Appendix D.

### 4.4.4 Result and analysis of the old aluminium cylinder

The result from the biaxial pressure test prior to the first heating was as expected, as seen in Figure 4.32. All strain gauges in respective direction responded in a similar way in the strain-time plot, the behaviour in the strain-load plot was liner elastic and the calculated values of Young's modulus and Poisson's ratio were within the expected range.

a)

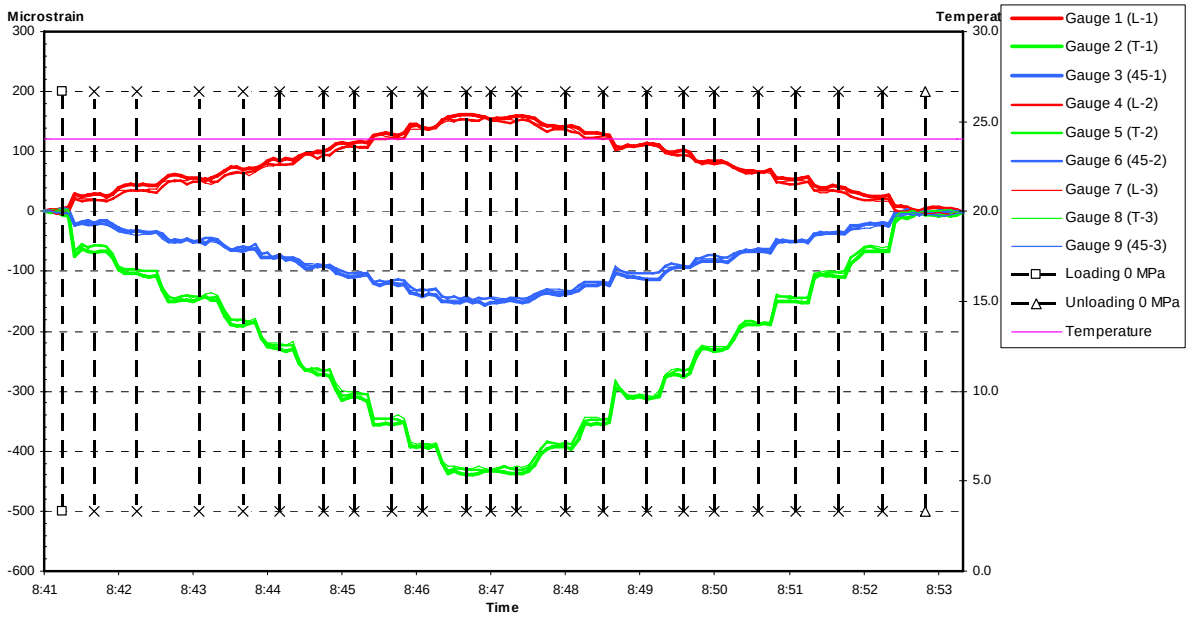


b)

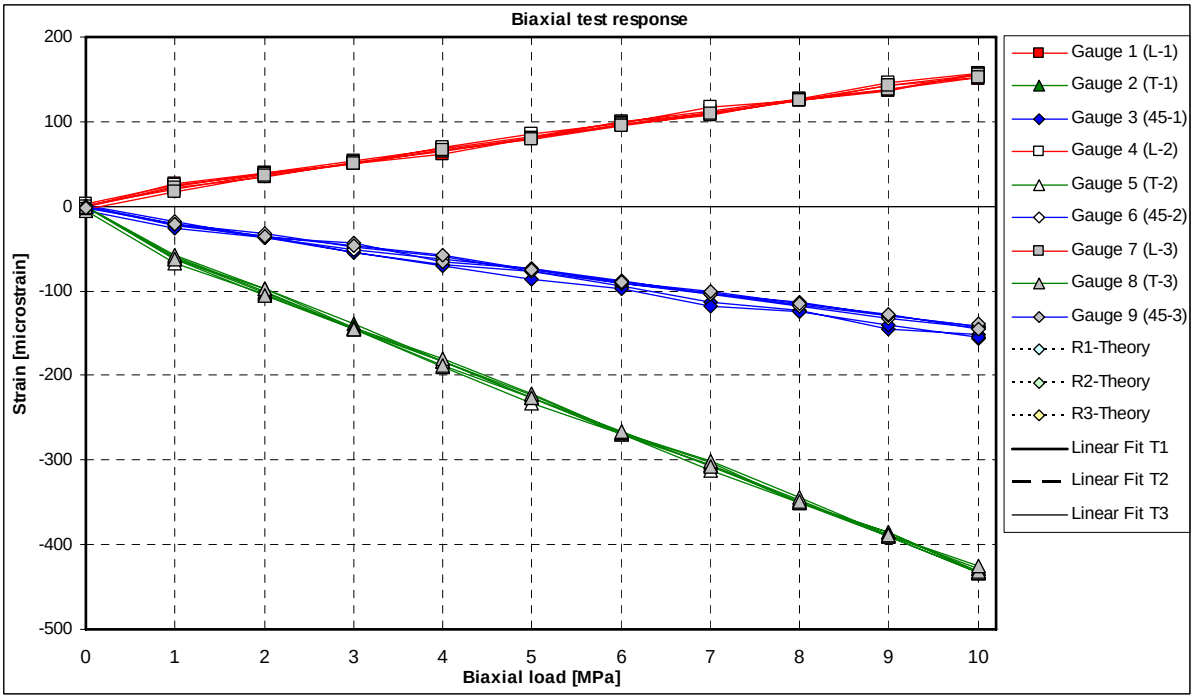


c)

**Mean values for unloading curve**

**Pressure range [MPa]**

Loading

Unloading

$P_{max}$ 8

$P_{min}$ 3

**Include/exclude gauges**

| Tangential | Inclined |
|---|---|
| ☑ Rosette 1 | ☐ Rosette 1 |
| ☑ Rosette 2 | ☐ Rosette 2 |
| ☑ Rosette 3 | ☐ Rosette 3 |

| Secant value mean | | Linear fit (10-0) mean | |
|---|---|---|---|
| $E$ = | 67.6 | $E$ = | 72.9 |
| $\nu$ = | 0.36 | $\nu$ = | 0.36 |

**Figure 4.32 Biaxial pressure testing prior to the first heating of the old aluminium cylinder. a) Strain-time plot. b) Strain-load plot. c) Calculated values of Young's modulus and Poisson's ratio.**

The heating following the biaxial pressure test can be seen in Figure 4.33 below. The initial temperature was again 4 ºC and held constant for 30 minutes before heating to 42 ºC started. The aluminium cylinder showed a linear temperature response of a little more than 10 microstrain/ºC. The temperature-induced strains were again almost completely compensated for according to the guidelines from HBM. Similar to the third heating of the new aluminium cylinder, installation C, a slight temperature dependence remained in the calibrated value, indicating that the strains might not have been compensated enough in the temperature dependent terms. This temperature dependence was again eliminated by adding the -1.5·ΔT-term to equation 4.3.

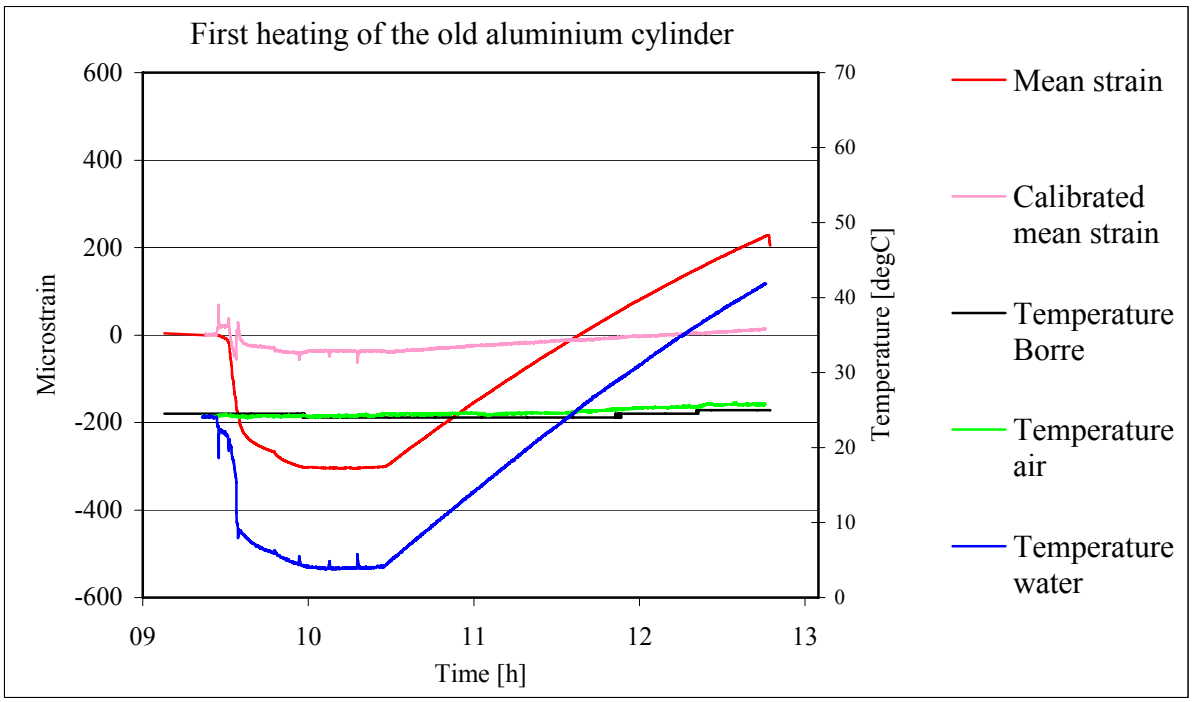


**Figure 4.33 Chart of recorded strains and temperatures during the first heating of the old aluminium cylinder .**

Right after the heating a biaxial pressure test was conducted. Now the response in the strain-load plot was no longer completely linear elastic in addition to somewhat higher values of Young's modulus and Poisson's ratio as seen in Figure 4.34.

a)

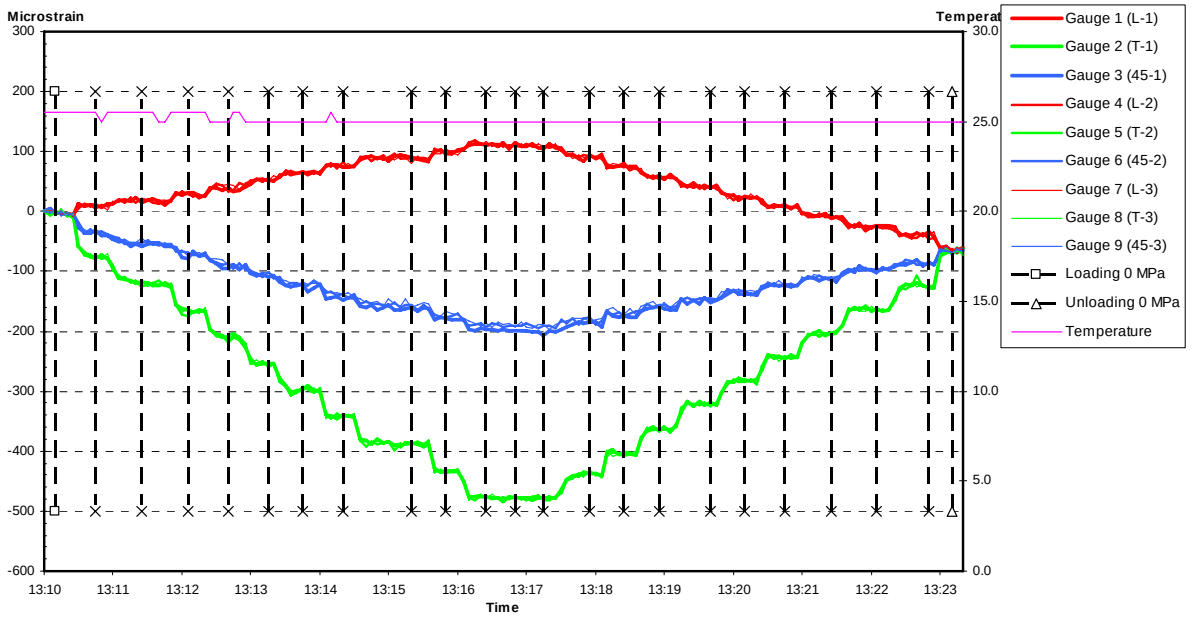


b)

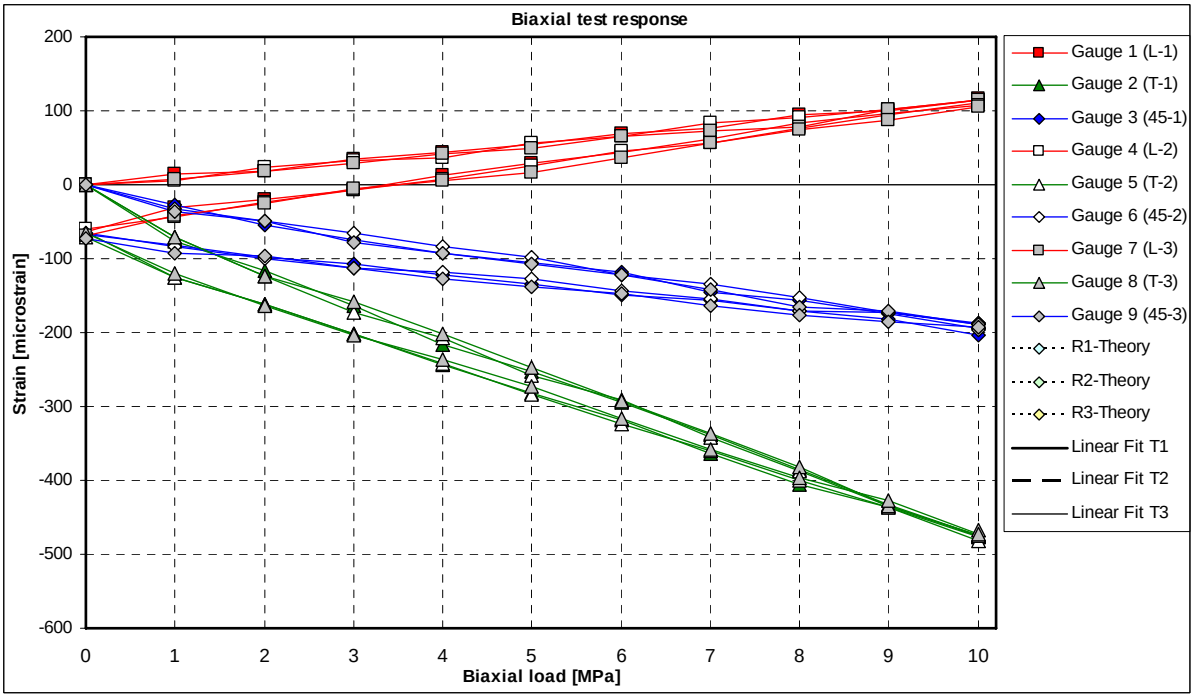


c)

**Mean values for unloading curve**

**Pressure range [MPa]**

Loading

Unloading

$P_{max}$ 8

$P_{min}$ 3

**Include/exclude gauges**

| Tangential | Inclined |
|---|---|
| Rosette 1 | Rosette 1 |
| Rosette 2 | Rosette 2 |
| Rosette 3 | Rosette 3 |

| Secant value mean | | Linear fit (10-0) mean | |
|---|---|---|---|
| $E$ = | 71.1 | $E$ = | 76.0 |
| $\nu$ = | 0.42 | $\nu$ = | 0.42 |

**Figure 4.34 First biaxial pressure test after the first heating of the old aluminium cylinder and prior to the second heating of the old aluminium cylinder.**

The day after a new biaxial pressure test was conducted. As seen in Figure 4.35 below, the response now was as expected with coinciding loading and unloading curves in the strain-load plot. The non-linear elastic behaviour from the previous test can hence probably be explained as remaining thermal strains in the aluminium cylinder.

a)

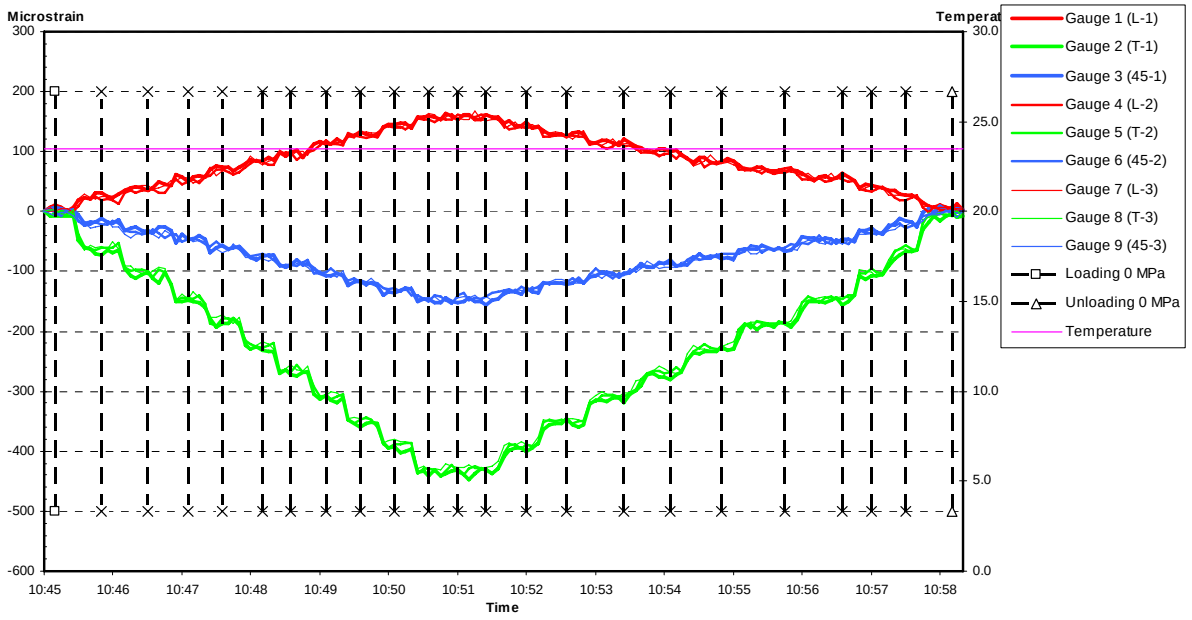


b)

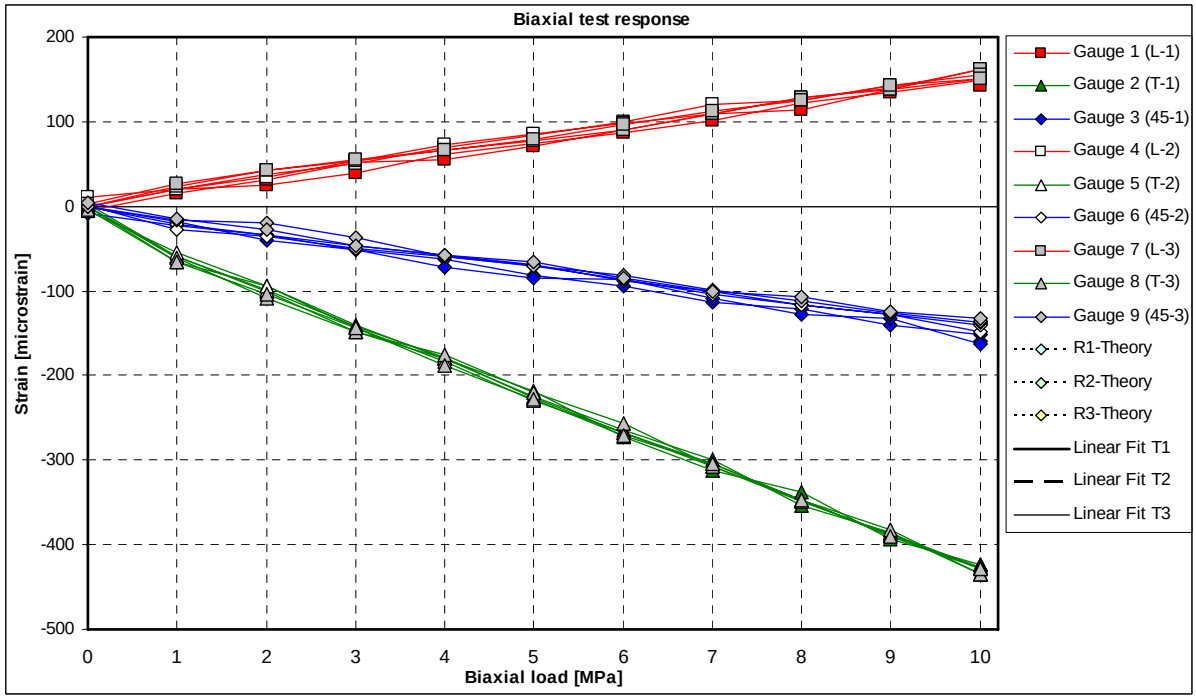


**Figure 4.35 Second biaxial pressure test after the first heating of the old aluminium cylinder and prior to the second heating of the old aluminium cylinder.**

c)

**Mean values for unloading curve**

**Pressure range [MPa]**

Loading
Unloading

$P_{max}$ 8
$P_{min}$ 3

**Include/exclude gauges**

| Tangential | Inclined |
|---|---|
| ☑ Rosette 1 | ☐ Rosette 1 |
| ☑ Rosette 2 | ☐ Rosette 2 |
| ☑ Rosette 3 | ☐ Rosette 3 |

| Secant value mean | | Linear fit (10-0) mean | |
|---|---|---|---|
| $E$ = | 68.1 | $E$ = | 72.9 |
| $\nu$ = | 0.35 | $\nu$ = | 0.36 |

**Figure 4.35 (Continued)**

Following the biaxial pressure test a new stepwise heating was conducted. As seen in Figure 4.36 below, the initial temperature was 4 ºC. The temperature was raised in intervals to 15, 25 and 35 ºC and held constant at each level for 20 minutes before heating continued. Finally the temperature was raised to 42 ºC. The aluminium cylinder again showed a linear response of a little more than 10 microstrain/ºC, independent of heating ratio. Again a slight remaining temperature dependence in the calibrated strain values was almost eliminated by adding the -1.5·ΔT-term to equation 4.3.

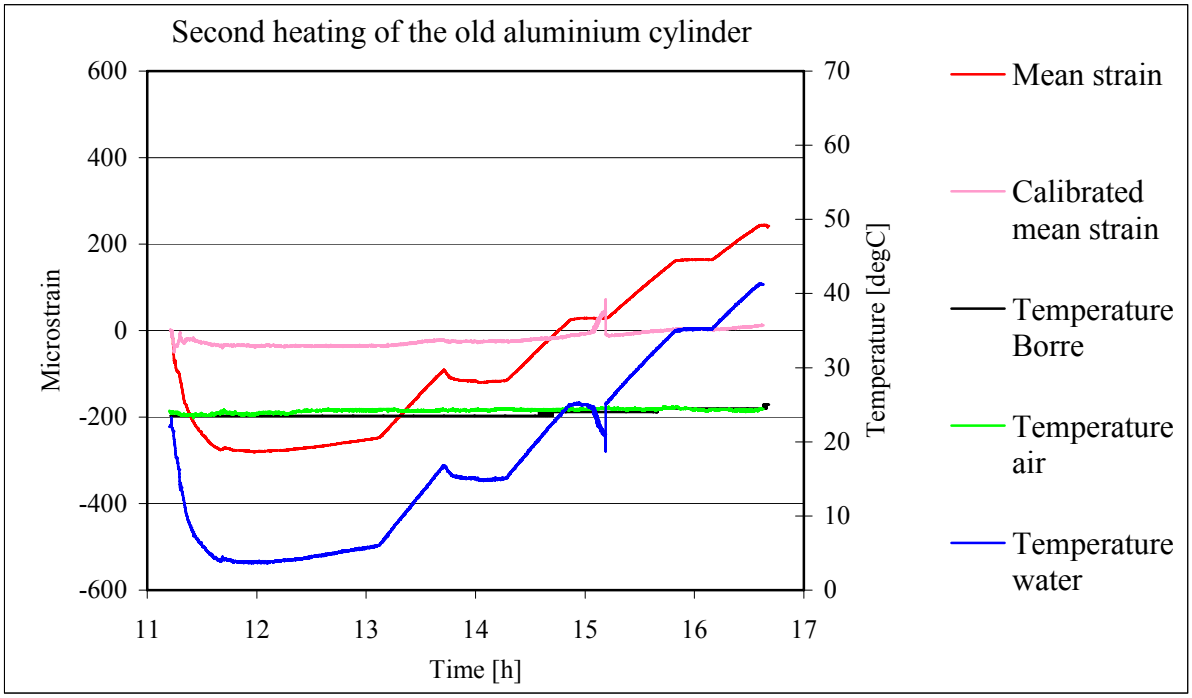


**Figure 4.36 Chart of recorded strains and temperatures during heating the old aluminium cylinder 2.**

Next a continuous heating was performed. The initial temperature was 4 ºC and held constant for 15 minutes before heating to 61 ºC. Thereafter the aluminium cylinder was allowed cool down, once again to 4ºC as seen in Figure 4.37 below. The aluminium cylinder again gave a linear temperature response of a little more than 10 microstrain/ºC both in the heating phase and the cooling phase. The strain values corresponding to the same temperature values in the heating and cooling phase were the same which mean that no deformation has occurred, i.e., no residual strains exist, the glue has reached a high degree of cure and the behaviour of the

aluminium cylinder is linear elastic. The temperature dependence of the calibrated strain values was more pronounced now due to heating to higher temperatures, but as in previous heatings the addition of the -1.5·ΔT-term to equation 4.3 made the strain values better calibrated.

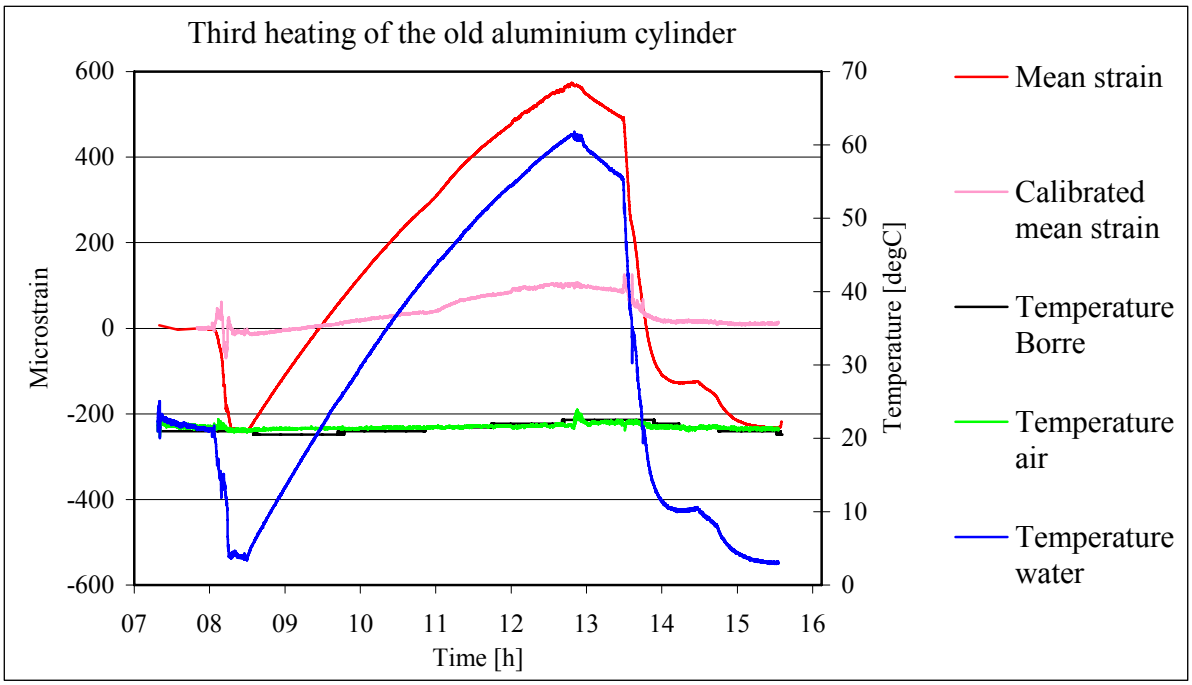


**Figure 4.37 Chart of recorded strains and temperatures during heating the old aluminium cylinder 3.**

**The biaxial pressure test concluding the test series confirmed this linear elastic behaviour by showing nothing but expected values in all plots as seen in**

Figure 4.38.

**a)**

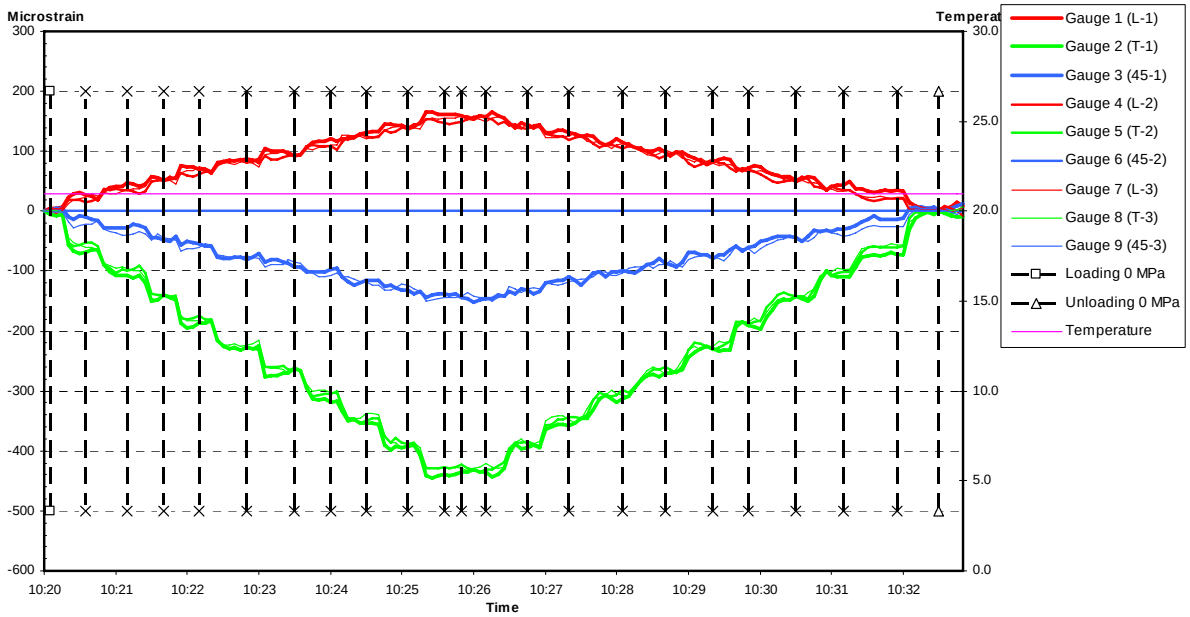

**Figure 4.38 Biaxial pressure test after the third heating of the old aluminium cylinder. a) Strain-time plot. b) Strain-load plot. c) Calculated values of Young's modulus and Poisson's ratio.**

b)

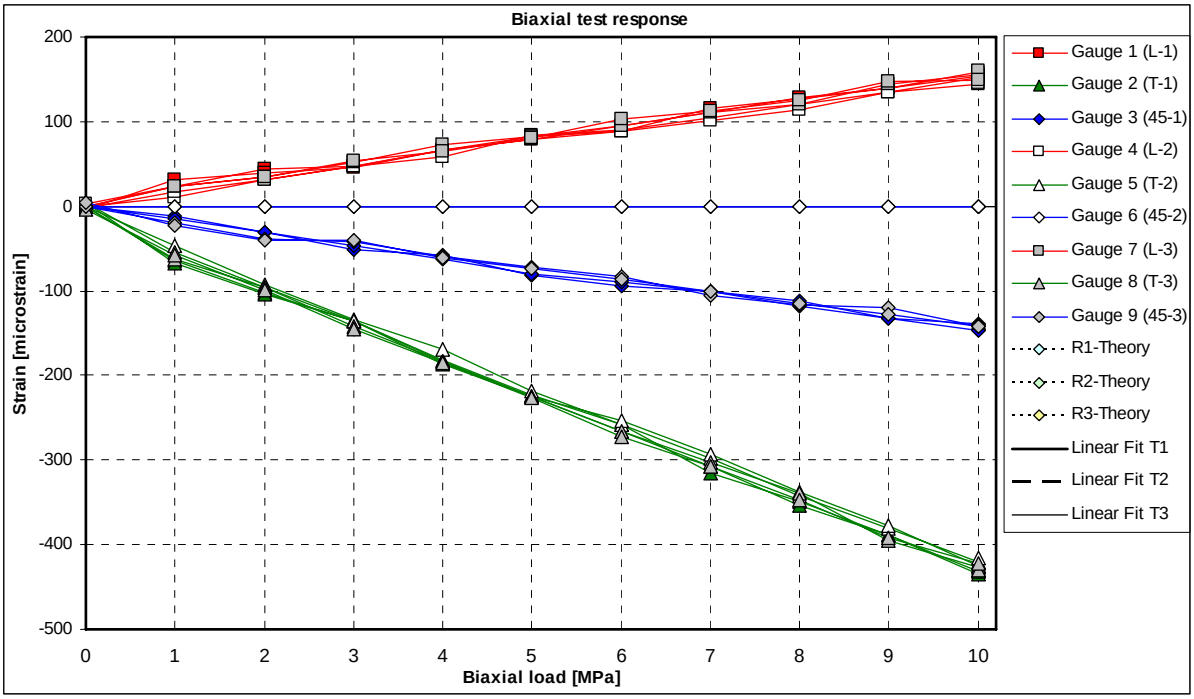


c)

| Mean values for unloading curve | | | | |
|---|---|---|---|---|
| Pressure range [MPa] | | Include/exclude gauges | | |
| Loading | $P_{max}$ 8 | Tangential | | Inclined |
| Unloading | $P_{min}$ 3 | Rosette 1 | | Rosette 1 |
| | | Rosette 2 | | Rosette 2 |
| | | Rosette 3 | | Rosette 3 |
| Secant value mean | | | Linear fit (10-0) mean | |
| $E$ = | 67.7 | | $E$ = | 72.8 |
| $\nu$ = | 0.36 | | $\nu$ = | 0.36 |

**Figure 4.38 (Continued)**

The full raw data charts for all strain readings corresponding to the diagrams above can be viewed in Appendix E.

### 4.4.5 Result and analysis of the aluminium slab

Analogous to previously conducted heatings, the initial temperature was 4 ºC also when heating the aluminium slab as seen in Figure 4.39. The temperature was held constant for 30 minutes before heating to 35 ºC. The aluminium slab showed a linear temperature response of a little less than 20 microstrain/ºC. The temperature-induced strains were also with this aluminium body almost completely compensated for according to the guidelines from HBM but just as before they showed a slight temperature dependence that was better compensated for when adding the term $-1.5 \cdot \Delta T$ to equation 4.3.

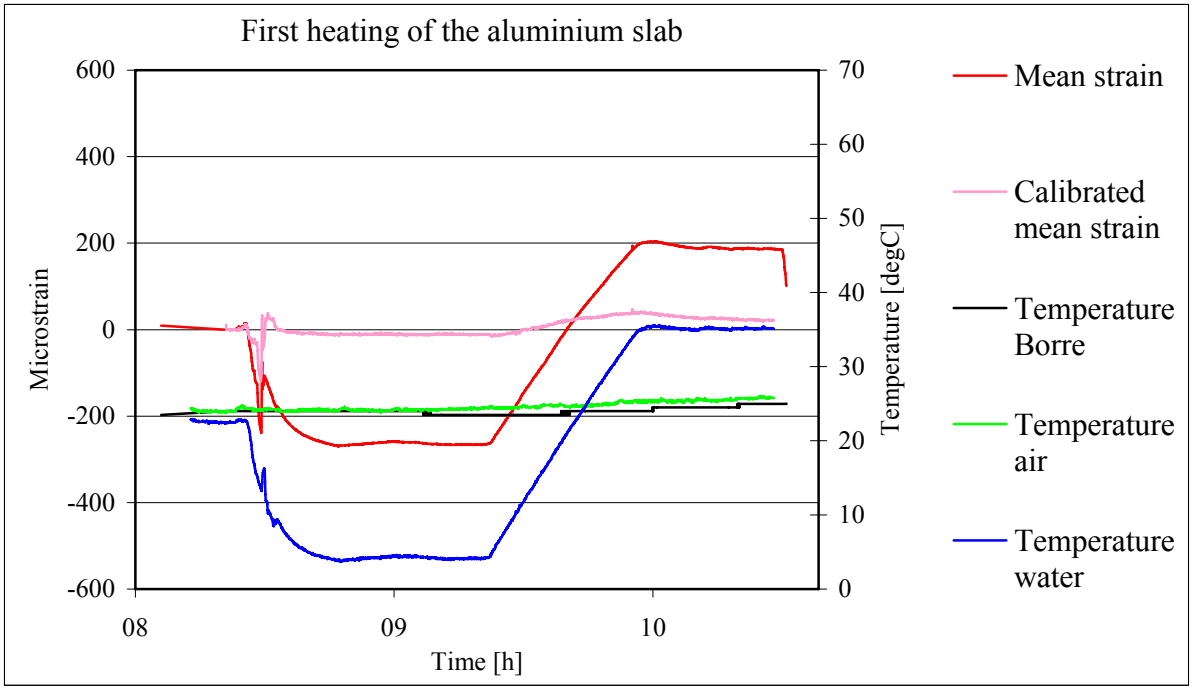


**Figure 4.39 Chart of recorded strains and temperatures during heating the aluminium slab 1.**

Also in the second heating the initial temperature was 4 ºC and held constant for 50 minutes. The temperature was in intervals raised to 15, 25, 35 and 45 ºC. At each level the temperature was held constant for 20 minutes, see Figure 4.40. The aluminium slab again showed a linear response of a little less than 20 ºC. As before the temperature-induced strains were better compensated for when adding the term -1.5·ΔT to equation 4.3.

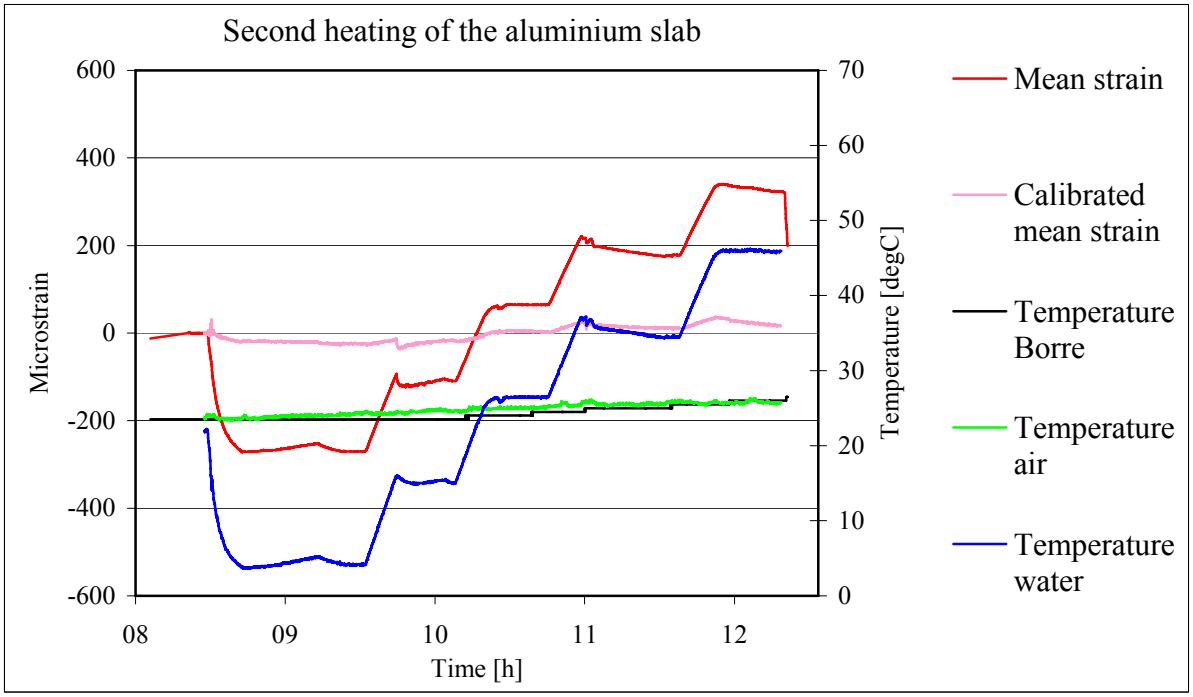


**Figure 4.40 Chart of recorded strains and temperatures during the second heating of the aluminium slab.**

The procedure in the third heating was similar to the two preceding, as seen in Figure 4.41 below. The initial temperature was 4 ºC and held constant for 20 minutes before heating to 68 ºC started. After the heating the slab was allowed to cool down to 4 ºC again. The aluminium slab showed a linear response of a little more than 10 microstrain/ºC in the heating phase and a little less than 20 microstrain/ºC in the cooling phase. The final temperature in the cooling phase was the same as the heating phase started with (4 ºC), but the corresponding strain values were not the same. Since the final strains were less than the initial, the difference could not be explained as remaining strains or deformation but rather as an effect of not fully cured glue. Therefore, similar to the first heating of the new cylinder, installation B (Chapter 4.4.3), the temperature-induced strains could not be compensated for according to the guidelines from HBM.

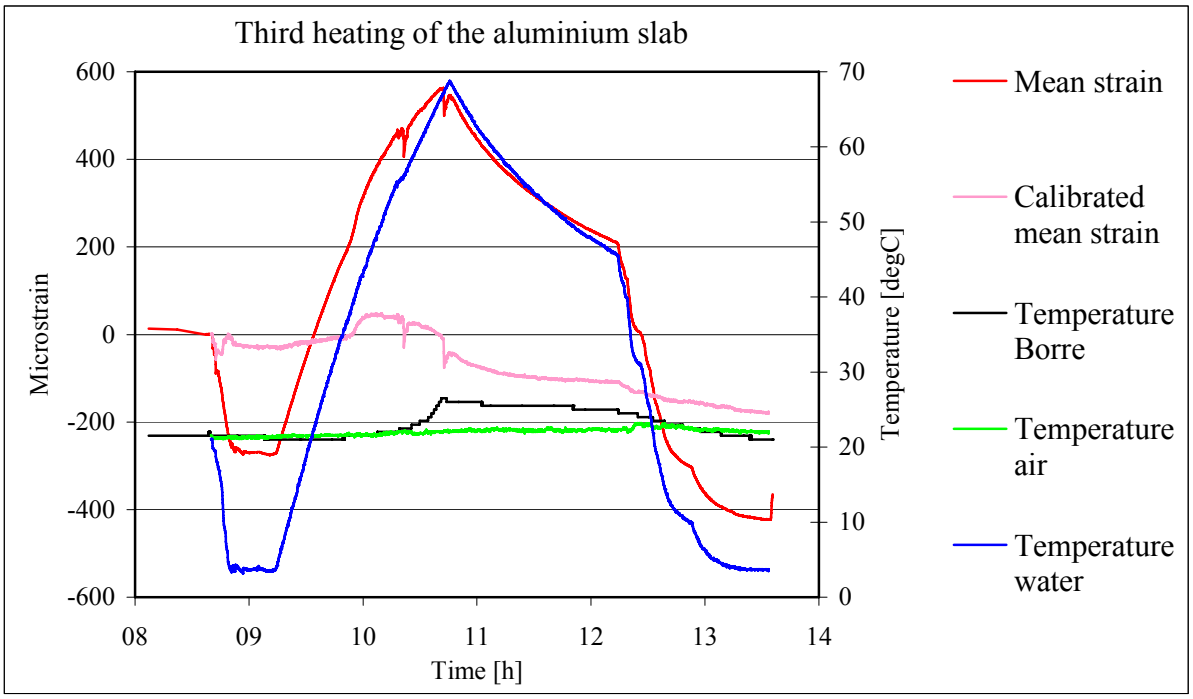


**Figure 4.41 Chart of recorded strains and temperatures during the third heating of the aluminium slab.**

Discussion When removing the gauges from the slab it was discovered that the strain gauge rosette number 1 was best mounted. The glue thickness on the other two was a little more than desired. Valid for all three rosette was that the glue thickness on the sides was too thick due to the fact that the rosette is arched and the slab is flat.

The full raw data charts for all strain readings corresponding to the diagrams above are presented in Appendix F.

### 4.4.6 Discussion

All bodies showed a linear response of a little more than 10 microstrain/°C. Compensation for this response according to the guidelines from HBM did not seem totally applicable. It was indicated that he strain values could be better compensated for by adding the term $-1.5 \cdot \Delta T$ to equation 4.3.

Comparing the results from the old and the new cylinders indicated that it takes very long for the glue to reach a high degree of cure at room temperature. Four weeks, as was the case for

the installation C, were obviously not enough for the glue to fully cure. This indicates that the glue is not fully cured when used during field conditions, which could affect strain readings if heated during overcoring.

If the response from heating the not fully cured glue was averaged, the response was -4 microstrain/ºC in installation B and -2 microstrain/ºC in installation C. That is, if the glue was subjected to 1 ºC temperature increase and then cooled down to its original temperature again, the *Borre* cell would indicate a value of 4 respectively 2 microstrain lower than it should have. However, when uncured glue is subjected to a temperature higher than its curing temperature, it is very possible that the rate, at which the forming of new cross-links takes place, is higher the higher temperature increase it is subjected to. A relatively small temperature increase above curing temperature might hence not be detectable in the strain readings.

Assuming that the not fully cured glue affects all strain gauges with an absolute error of equal magnitude, Table 4.3 shows how much the calculated principal stresses from Forsmark, borehole KFM07C: test no. 2:9:1 were affected if the glue was subjected to an elevated temperature before the strains were recorded. Values less than zero mean that the calculated principal stress was an underestimation of the true in situ value.

**Table 4.3 Example of the effect on magnitude on calculated principal stresses, from Forsmark, borehole KFM07C: test no. 2:9:1, caused by temperature increase of not fully cured glue.**

| **Temperature increase [ºC]** | **Equivalent strain decrease [microstrain]** | **Change in principal stress magnitude, $\sigma_1$ [MPa]** | **Change in principal stress magnitude, $\sigma_2$ [MPa]** | **Change in principal stress magnitude, $\sigma_3$ [MPa]** |
|---|---|---|---|---|
| **10** | **40** | -3 | -3 | -5 |
| **20** | **80** | -5 | -5 | -10 |
| **30** | **120** | -8 | -10 | -12 |
| **40** | **160** | -10 | -15 | -15 |
| **Calculated principal stresses from Forsmark, borehole KFM07C: test no. 2:9:1** | | **$\sigma_1$ [MPa]** | **$\sigma_2$ [MPa]** | **$\sigma_3$ [MPa]** |
| | | **24** | **9** | 4 |

## 4.5 Heating strain gauges and glue mounted on rock.

### 4.5.1 Aim, method

The aim of this test was to determine the combined magnitude of the temperature dependence of the strain gauges and the glue when mounted on rock. This was done by heating strain gauges glued into an overcored rock sample. Two cores from Forsmark were tested. In the first installation the sample from borehole KFM07C: test no. 2:9:1, that had shown severe temperature response during overcoring, was tested and in the second installation the sample from borehole KFM07C: test no. 1:1:5, that had not shown any significant temperature response, was tested. The tests were not preceded and concluded with biaxial pressure testing on basis of the risk of inducing additional microcracks in the core. The rock samples were heated in a way similar to the logger as shown in Figure 4.1, with the addition that the temperature inside the rock cores also was recorded.

### 4.5.2 Result and analysis

#### Installation in core with temperature effects

As in previous laboratory heating tests the rock core from test no. 2:9:1 was heated from 5 to 55 ºC and again cooled down to 5 ºC. The response was though, not as expected. As the sample was cooled from room temperature down to 5 ºC it expanded and as it was heated from 5 to 30 ºC it contracted as seen in Figure 4.42 below. The behaviour was thus the opposite to that expected for a material subjected to temperature change. As the heating continued from 30 to 55 ºC the rock core started to expand like most materials do and as it was cooled from 55 to 40 ºC it contracted. When the cooling phase proceeded from 40 to 5 ºC the core changed behaviour and again started to expand. The strains levelled out as the temperature did at the end of the cooling phase.

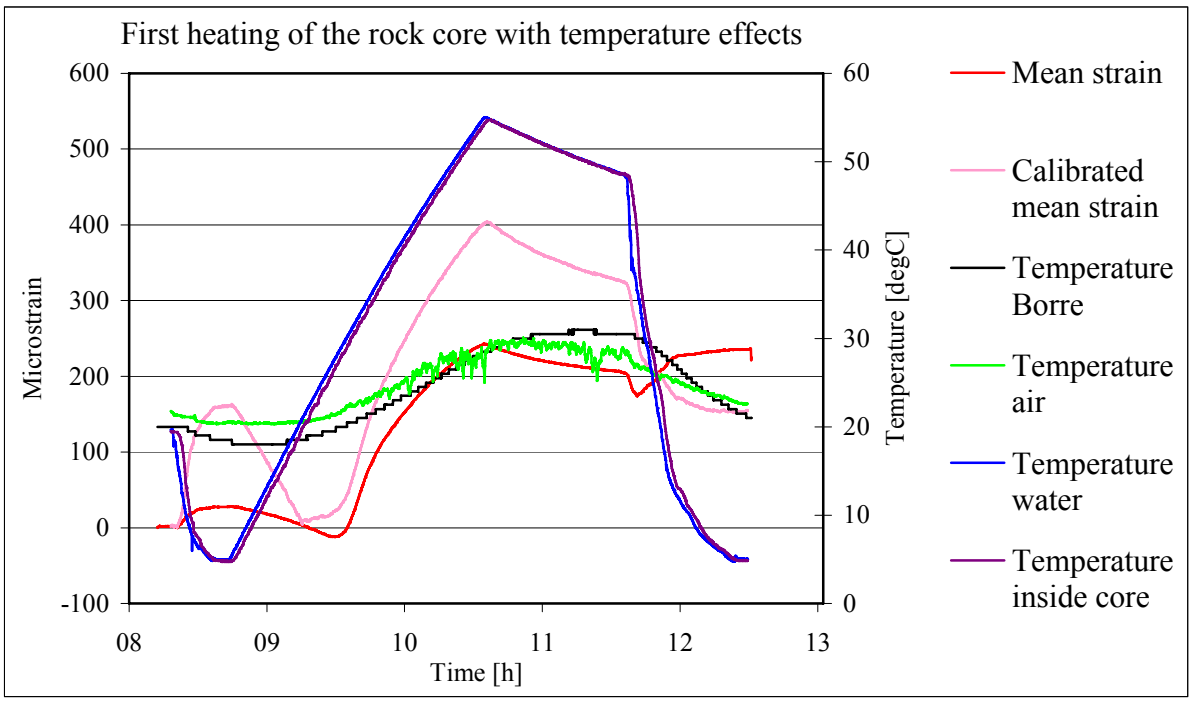


**Figure 4.42 Chart of recorded strains and temperatures during the first heating of the rock core with temperature effects.**

As this response was very peculiar a repeat heating was performed to determine the validity of the above described test. In Figure 4.43 below it can be seen that the response in the repeat test was similar to that in the first heating.

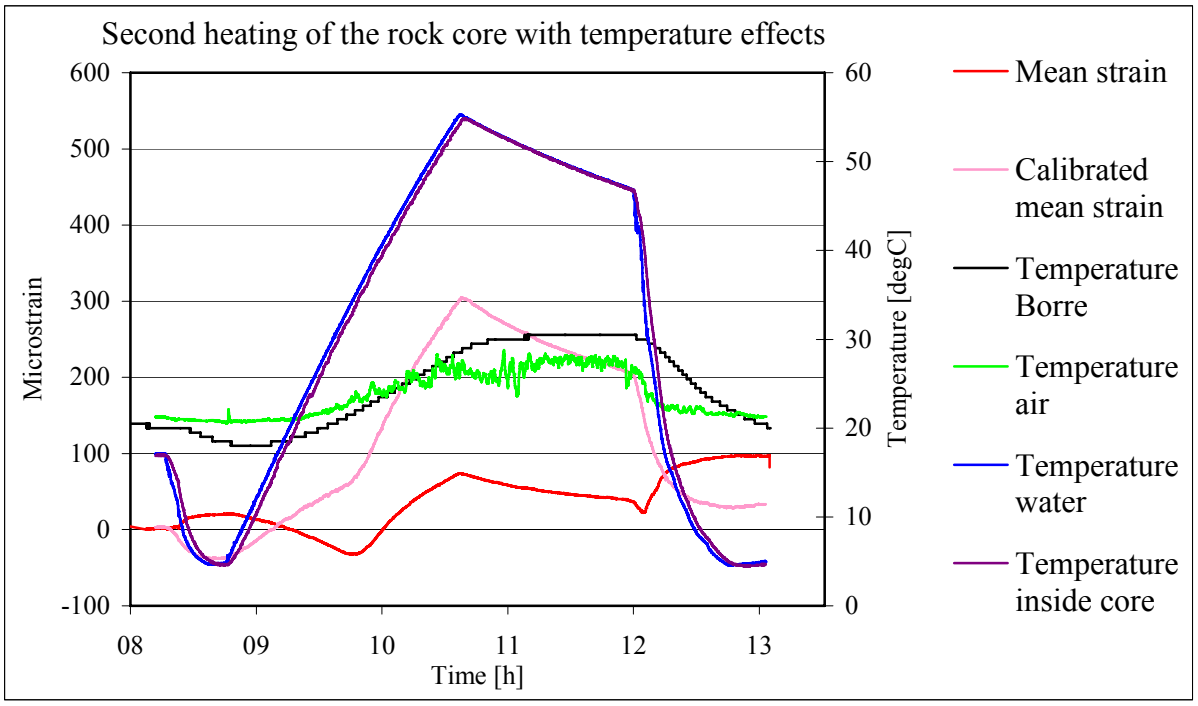


**Figure 4.43 Chart of recorded strains and temperatures during the second heating of the rock core with temperature effects.**

## Installation in core without temperature effects

When heating the second rock core from test no. 1:1:5, the test was performed by heating it from 5 to 55 ºC and then cooling back to 5 ºC. The response was similar to the that of the first core tested. As the sample was cooled from room temperature down to 5 ºC it expanded and as it was heated from 5 to 30 ºC the core contracted as seen in Figure 4.44 below. Then as the heating continued from 30 to 55 ºC the rock core started to expand and as it was cooled from 55 to 30 ºC it contracted. When the cooling phase proceeded from 30 to 5 ºC the core changed behaviour and again started to expand.

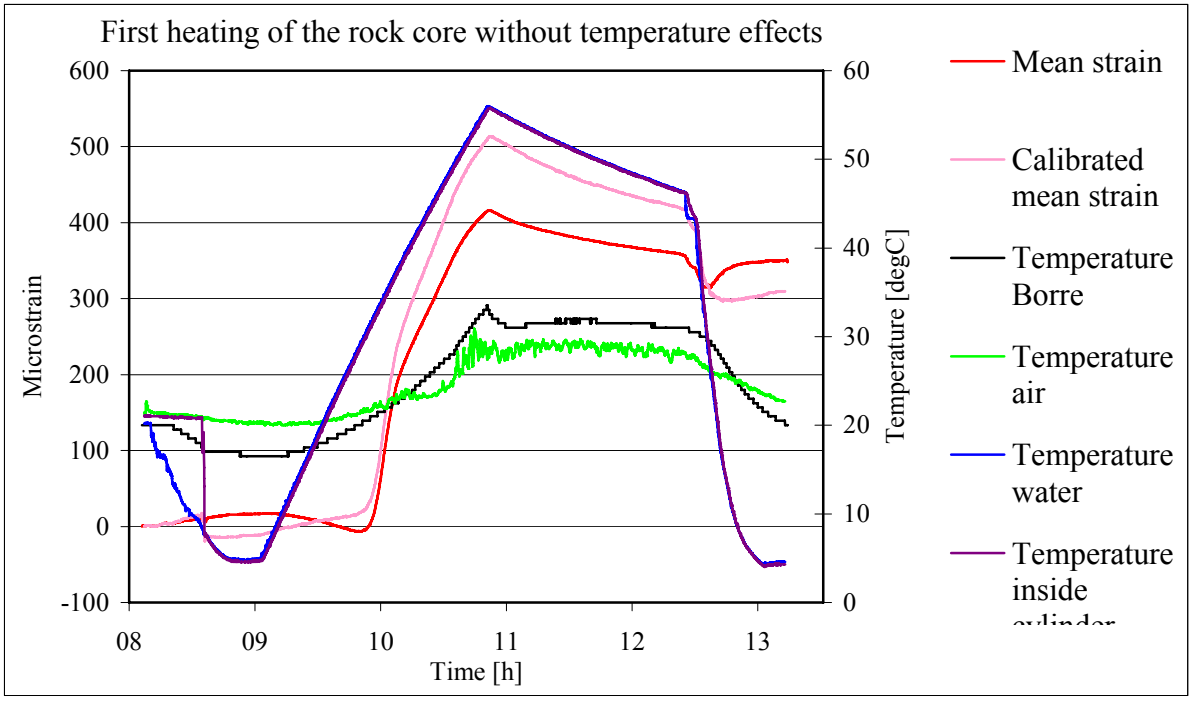


**Figure 4.44 Chart of recorded strains and temperatures during the first heating of the rock core without temperature effects.**

The full raw data charts for all strain readings corresponding to the diagrams above are presented in Appendix G

### 4.5.3 Discussion

The response did not differ in behaviour between the core that had shown temperature effects (test no. 2:9:1) during overcoring and the core that had not (test no. 1:1:5). Below 30 ºC the cores responded in the opposite way to that expected for a material subjected to temperature change and above 30 ºC they expanded and contracted as expected.

The rock hence showed a response to temperature change, but the response could not be quantified or explained based on the tests performed. However it was obvious that the rock did not behave as an ideal material. It is possible that this behaviour was caused by micro cracks induced by the thermal stresses during the test or by the preceding overcoring and/or biaxial testing. However this is simply one hypothesis which cannot be verified or discarded based on the present knowledge.

The guidelines from HBM did, in this case, not seem applicable at all. The strain values seemed rather aggravated than calibrated.

## 4.6 Heating the logger together with strain gauges and glue mounted on rock

### 4.6.1 Aim, method

The aim of this test was to determine the combined magnitude of the temperature dependence of the strain gauges and the glue when mounted on rock, heated as a system together with the logger.

### 4.6.2 Discussion

This test was not considered necessary to perform on basis of the small response of the logger. It was assumed that the response of this test would not differ much from those performed in section 5.5.

# 5 Conclusions and evaluation

## Numerical simulations

The simulation with continuous heat flow from the drill bit (in which the drill bit was set as heat generating domain with no compensation for the flushing water around the drill bit) seemed to be conceptually right when comparing to the strain curve registered by the *Borre* cell during overcoring, but quantitatively wrong.

The approach of the simulation with fixed temperature boundary condition on the drill bit (where the outgoing drill water was set as heat generating domain) was correct to the extent that the flushing water around the drill bit should even out the temperature.

Further work in calculating and simulating the energy distribution between fracturing the rock, the amount of heat absorbed by the flushing water contra the amount of heat dissipated by the rock, is needed to get a more accurate value, closer to field conditions. In addition, more data on actual temperatures during field work would be required to better calibrate the model to real conditions. The option to simulate a convective heat flow above the drill bit and continuous conductive heat flow below it would also be desirable to get results closer to field conditions.

The maximum temperature the connection sockets can be exposed to is 60 ºC as the Vaseline protecting them from short circuits melts at this temperature.

The temperature at the strain gauge positions 1800 s (30 min) after overcoring stops was more affected by the conductivity of the rock than of the temperature peak value experienced.

## The *Borre* logger

The experiments showed that the strain reading response due to temperature change for the *Borre* cell was quite small, both when connected to resistors and when connected to strain gauge rosettes. The response when connected to resistors was between 1 and 2 microstrain/ºC and 3 microstrain/ºC when connected to strain gauge rosettes.

One source of error is that the logger could not be tested completely isolated from other factors (strain gauges and resistors) and that the response differed from the cases when it was connected to strain gauges and when connected to resistors. The response might hence also be dependent on whether the strain gauges are mounted on a material or not, and therefore give a different response in an actual overcoring. Other factors that could have affected these results and caused errors should have been of systematic nature, like monitoring errors, since the results achieved seemed repeatable.

Considering that the logger unit probably does not register strain values at higher temperature than the temperature of the flushing water, the effect on registered strain values might be neglectable on basis of the small magnitude of the absolute error it causes. (for typical values on measured stresses)

Comparing the relative change in calculated principal stress magnitude that the *Borre* cell causes (based on the calculated principal stresses from Forsmark, borehole KFM07C: test no. 2:9:1) to the relative change in principal stress magnitude presented by Martin & Christiansson (1991) shows that the results are of comparable magnitude concerning $\sigma_1$ as

seen in Table 5.1. The calculated change in principal stress magnitudes for $\sigma_3$ differs though. Since the calculated value of $\sigma_3$ from Forsmark was of very small magnitude (4 MPa) even a small absolute error causes a big relative error.

**Table 5.1 Comparison between the affect on magnitude on calculated principal stresses caused by temperature increase presented by Martin & Christiansson (1991) and the *Borre* logger.**

| Temperature increase [ºC] | Change in principal stress magnitude, $\sigma_1$ [%] (Martin & Christiansson, 1991) | Change in principal stress magnitude, $\sigma_3$ [%](Martin & Christiansson, 1991) | Change in principal stress magnitude, $\sigma_1$ [%] | Change in principal stress magnitude, $\sigma_3$ [%] |
|---|---|---|---|---|
| **2** | No significant change | No significant change | 2 | 21 |
| **8** | 11 | 23 | 7 | 273 |
| **15** | 22 | 59 | 14 | 373 |

## Aluminium and glue

All bodies showed a linear response of a little more than 10 microstrain/°C. Compensation for this response according to the guidelines from HBM did not seem totally applicable. It was indicated that he strain values could be better compensated for by adding the term $-1.5 \cdot \Delta T$ to equation 4.3.

One factor that could have affected these results was the unknown curing behaviour and behaviour in general of the glue, and hence causing a misinterpretation of it. The difficulty in getting a successful installation of the strain gauges in the new aluminium cylinder complicated the desire to show repeatability in the tests.

The tests showed that the glue might not be fully cured when used during field conditions. It is very possible that the rate, at which the forming of new cross-links takes place, is higher the higher temperature increase the glue is subjected to. The longer time the glue is subjected to the temperature increase, the more new cross-links can be formed. If the glue only is subjected to a small temperature increase or if it is subjected to a higher temperature increase, but only for a short period of time, the fact that the chemical reactions are reactivated might therefore not be detectable in the strain readings. Also the amount of glue is important. In a thinner layer of glue the total number of cross-links that can be formed is less than for a thicker layer and hence the thinner layer can reach a higher degree of cure in less time than the thick layer.

Comparing the relative change in calculated principal stress magnitude that the glue causes (based on the calculated principal stresses from Forsmark, borehole KFM07C: test no. 2:9:1) to the relative change in principal stress magnitude presented by Martin & Christiansson (1991) shows that the results are of comparable magnitude concerning $\sigma_1$ as seen in

Figure 5.1. The calculated change in principal stress magnitudes for $\sigma_3$ differs though. Since the calculated value of $\sigma_3$ from Forsmark was of very small magnitude (4 MPa) even a small absolute error causes a big relative error.

**Figure 5.1 Comparison between the affect on magnitude on calculated principal stresses caused by temperature increase presented by Martin & Christiansson (1991) and the glue.**

| Temperature increase [ºC] | Change in principal stress magnitude, $\sigma_1$ [%] (Martin & Christiansson, 1991) | Change in principal stress magnitude, $\sigma_3$ [%](Martin & Christiansson, 1991) | Change in principal stress magnitude, $\sigma_1$ [%] | Change in principal stress magnitude, $\sigma_3$ [%] |
|---|---|---|---|---|
| **2** | No significant change | No significant change | 2 | 20 |
| **8** | 11 | 23 | 7 | 48 |
| **15** | 22 | 59 | 14 | 65 |

A DSC (Differential Scanning Calorimetry) test of the glue was also considered. This test would give the change in enthalpy of a cured clue sample being heated compared to an uncured sample being heated, i.e. it would give the degree of cure for a glue sample. The test was rejected on basis of the cost and the information achieved not answering the right question.

## Rock

The rock showed a peculiar response to temperature change. The response was of significant magnitude but could not be quantified or explained based on the tests performed. Below 30 ºC the cores responded in the opposite way to that expected for a material, that is, expanded when cooled and contracted when heated. Above 30 ºC however, they expanded and contracted as expected.

A source of error was that the material properties and the quality of the rock cores used in the tests not were representative for rock during overcoring as it is assumed that the rock then behaves as an ideal material. Other factors that could have affected these results should have been of systematic nature, like monitoring errors since the results achieved seemed repeatable

# 6 Recommendations

### Monitoring/estimating the temperature the strain gauges are exposed to

It is recommended that the *Borre* cell is modified in a way that enables temperature measurement at the position of the strain gauges. This would make it possible to determine if the strains readings are taken in stable temperatures and if not, how much the strain readings should be compensated for.

If it is not possible to connect one more channel to the logger, this would require wireless on-line logging of the temperature which today is impossible to perform during overcoring (Wiederholm, 2006).

A more thorough numerical simulation of the overcoring process is also suggested which would give a better estimation of the temperature that the strain gauges are exposed to.

### Minimizing the temperature effect

In the case when the strain gauges are exposed to great temperature differences it is proposed to try implementing a temperature controlled drill water system like the one used for the overcoring stress measurements in the AECL's stress measurement program at the URL. This would demand measurements of the ingoing and outgoing flushing water temperature.

It could also be of interest to investigate the temperature heating/cooling effect of different drill bits and different overcoring diameters as well as optimizing the penetration rate.

Numerical simulations with different overcoring diameter can be used to estimate the possible reduction of temperature increase at the position of the strain gauges. A larger overcoring diameter locates the heat source further away from the strain gauges and hence lowers the maximum temperature they are exposed to.

By numerical simulations investigating whether the strain gauges are more affected by a lower penetration rate compared to a higher, the penetration rate could be optimized to minimize the temperature effect on the strain gauges. A lower penetration rate is associated with a lower temperature for a longer time whereas a faster penetration rate results in a higher, but more rapid temperature pulse. The conceptual behaviour would be possible to simulate.

### Compensation of future measurements

The temperature-induced strain compensation according to the guidelines from HBM seemed applicable to the tests performed on aluminium within this study when adding the term $-1.5 \cdot \Delta T$ to equation 4.3. Knowing the temperature at the strain gauges and knowing the factor of thermal expansion of the rock (assuming that the rock normally behaves like an ideal material, i.e., expands when heated and contracts when cooled) would make it possible to eliminate the temperature-induced strains from the registered ones.

### Other

It should be investigated if it is possible to add a softener to the glue without changing its texture and other properties. A softener makes the molecule chains slip past each other more easily and would lower the glass transition temperature and hence make it possible for the

glue to reach a high degree of cure at a lower temperature. If this was achievable, a temperature increase would have less influence, if any, on the strain readings.

.

# References


Amadei B. & Stephansson O. (1997). *Rock stress and its measurement.* London, Chapman & Hall, pp. 211-212.

Berglund L.A. (1997). *Introduction to polymer engineering.* Course literature, Luleå tekniska universitet, Sweden, pp. 4-5, 11-15, 87-91.

Bergteknik (1985). *Bergteknik 1985.* Course literature, Högskolan i Luleå, Sweden.

Cai M. & Thomas L.J. (1993). Performance of overcoring stress measurement devices in various rock types and conditions. *Transactions of the Institution of Mining & Metallurgy, Section A: Mining Industry*, vol. 102, pp. 134-140.

Carlson J. (2007-09-17). Senior teacher in computer science and electrical engineering at Luleå University of Technology, Sweden. E-mail.

Drillcon, (2007-08-06); Protek Norr, (2007-08-06); Rockma (2007-08-06). Representatives from the core drilling companies. Phone call.

Garritty P., Irvin R.A. & Farmer I.W. (1985). Problems associated with near surface in-situ stress measurements by the overcoring method. *Proceedings-Symposium on Rock Mechanics,* vol. 2, pp. 1095-1102. Research & Engineering Applications in Rock Masses, Proceedings of the 26th US Symposium on Rock Mechanics: 26-28 June 1985; Rapid City, SD, USA.

Hakala M (2006). *Quality control for overcoring stress measurement data.* Posiva 2006-03. Posiva Oy, Olkiluoto, Finland.

Heinz W.F. (1989) *Diamond drilling handbook.* 2nd ed. Republic of South Africa, Halfway House, pp. 78-80.

Joffe R. (2007-09-18). Senior teacher in applied physics, mechanical and material engineering at Luleå University of Technology, Sweden. Personal communication.

Leijon B. (1988). *Rock stress measurements using the LUT-gauge overcoring method.* Doctoral thesis 1988:66. Tekniska högskolan i Luleå, Sweden.

Lindfors U. (2007-09-17). Vattenfall Power Consultant, Sweden. E-mail.

Lindfors U. et al. (2007). *Forsmark site investigation. Overcoring rock stress measurements in borehole KFM07C.* SKB P-report, in progress. Swedish Nuclear Waste and Management Company, Stockholm, Sweden.

Lummus J.L. & Azar J.J. (1986). *Drilling fluids optimization. A practical field approach.* Penn Well publishing company, Tulsa, Oklahoma, USA.

Martin C.D. & Christiansson R. (1991). Overcoring in highly stressed granite: Comparison of the USBM and modified CSIR devices. *Rock Mechanics and Rock engineering,* 24(4):207-235.

Martino J.B. et al. (1997). *The in situ stress program at AECL's underground research laboratory. 15 years of research (1982-1997).* Nuclear Waste Management. Report No: 06819-REP-01200-0053 R00. Atomic Energy of Canada Ltd. Whiteshell Laboratories, Toronto, Ontario, Canada.

Nilsson G. (2007-06-15, 2007-08-06). Drill expert at SKB, Sweden. Phone call.

Nordlund E., Rådberg G. & Sjöberg J. (1998) *Bergmekanikens grunder.* Course literature, Avdelningen för bergmekanik, Luleå tekniska universitet, Sweden, pp. 9, 67-69, 75.

Sandberg M. (2007-05-11). Metrolink Scandinavia, Sweden. E-mail.

Sjöberg J. (2007). Vattenfall Power Consultant, Sweden. Personal communication.

Sjöberg J. (2004) *Overcoring rock stress measurements in borehole KFM01B. Forsmark site investigation.* SKB P-report, 04-83. Swedish Nuclear Waste and Management Company, Stockholm, Sweden.

Sjöberg J. & Klasson H. (2003). Stress measurements in deep boreholes using the *Borre* (SSPB) probe. *International Journal of Rock Mechanics & Mining Sciences*, 40 (2003) 1205-1223.

Sjöberg J. & Perman F. (2006) *Overcoring rock stress measurements in borehole KLX04. Oskarshamn site investigation.* SKB P-report, 05-69. Swedish Nuclear Waste and Management Company, Stockholm, Sweden.

Thompson P.M., Lang P.A. & Sneider G.R. (1986). Recent improvements to in situ stress measurements using the overcoring method. *Canadian Geotechnical Conference,* pp. 143-150. Proceedings of the 39th Canadian Geotechnical Conference, 27-30 August 1986, Ottawa, Ontario, Canada.

Tuomas G. (2004). *Water powered percussive rock drilling: process analysis, modelling and numerical simulation.* Doctoral thesis 2004:58. Luleå tekniska universitet, Sweden.

Wallström L. (2007-08-29). Senior teacher in polymer materials at Luleå University of Technology, Sweden. Personal communication.

Wernersson H. (1994). *Fracture characterization of wood adhesive joints.* Doctoral thesis TVSM-1006. Lund University, Sweden.

Wiederholm I. (2006). *Investigation of on-line measurement for the Borre overcoring stress cell.* Master's thesis, Umeå universitet, Sweden.

URL

*Boart Longyear drilling products*
Available: <http://www.boartlongyear.com> (2007-08-06)
/Drilling products/Exploration/Core Barrels

*Homepage of COMSOL*
Available: <www.comsol.com> (2007-07-23)
/company/pressrelease/06-sep-05

*Correcting thermally induced strain during SG measurements.*
Available: <http://www.hbm.com/uploads/faqs/FAQ03_037_en.pdf> (2007-06-23)

*Strain gages and accessories.*
Available: <www.hbm.com/data/softdoc/hbm/data/s1265.pdf> (2007-06-23)

*Homepage of SKB*
Available <www.skb.se> (2007-06-23)
/
/in English/Final repository/Finding a site/Site investigation
/in English/Final repository/Finding a site/Site investigation/Investigations

*Methods of drilling*
Available: <http://toolboxes.flexiblelearning.net.au/demosites> (2007-08-06)
/series 7/706. Methods of drilling/conventional core
/series 7/706. Methods of drilling/wireline core

*Homepage of Geawelltech*
Available: <http://www.welltech.se> (2007-08-06)
/geoteknik/kärnborrning

# Appendix A

## Simulation with continuous heat flow from the drill bit

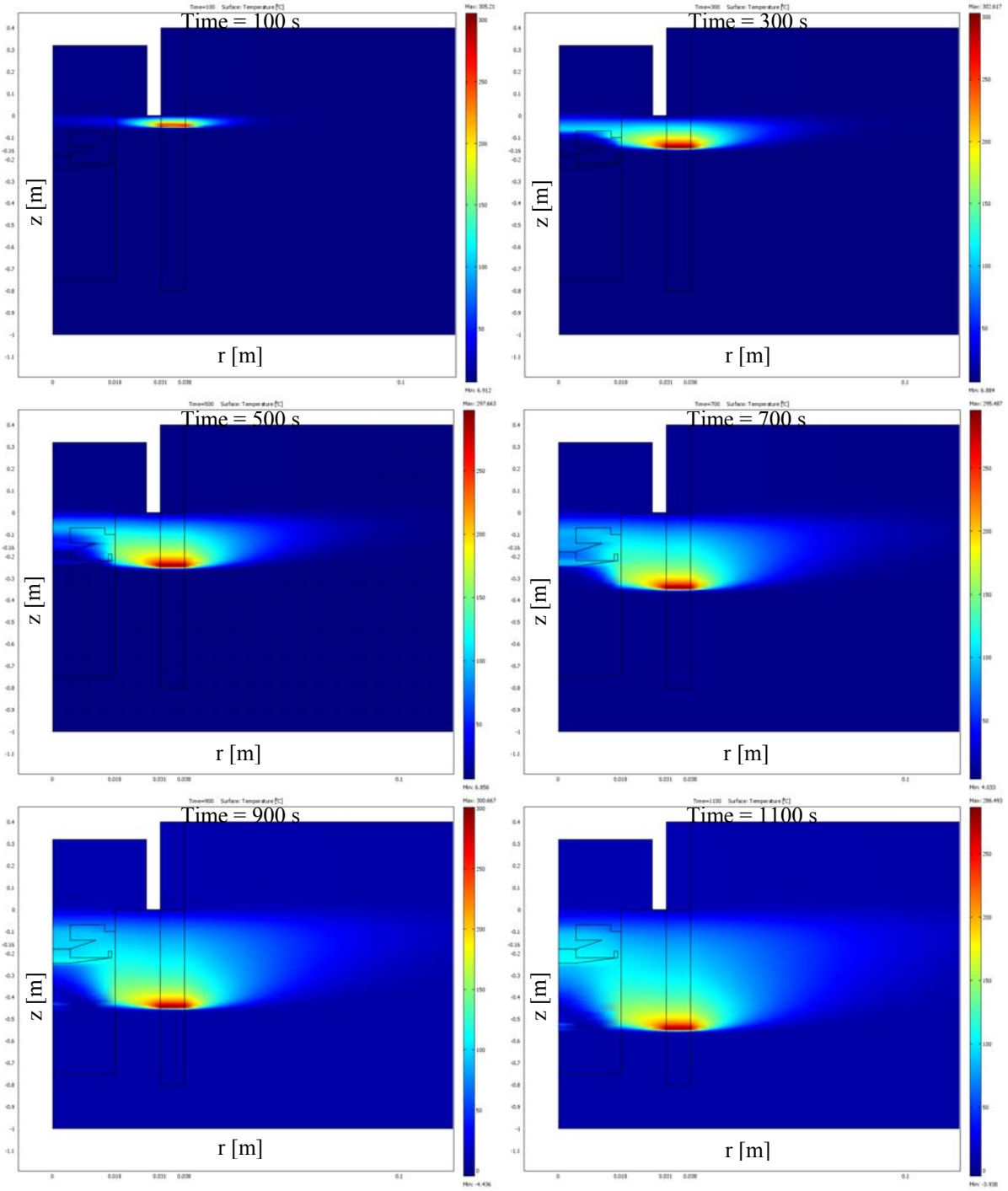


**Figure A. 1 Plots of temperature distributions for different time steps, Simulation with continuous heat flow from the drill bit.**

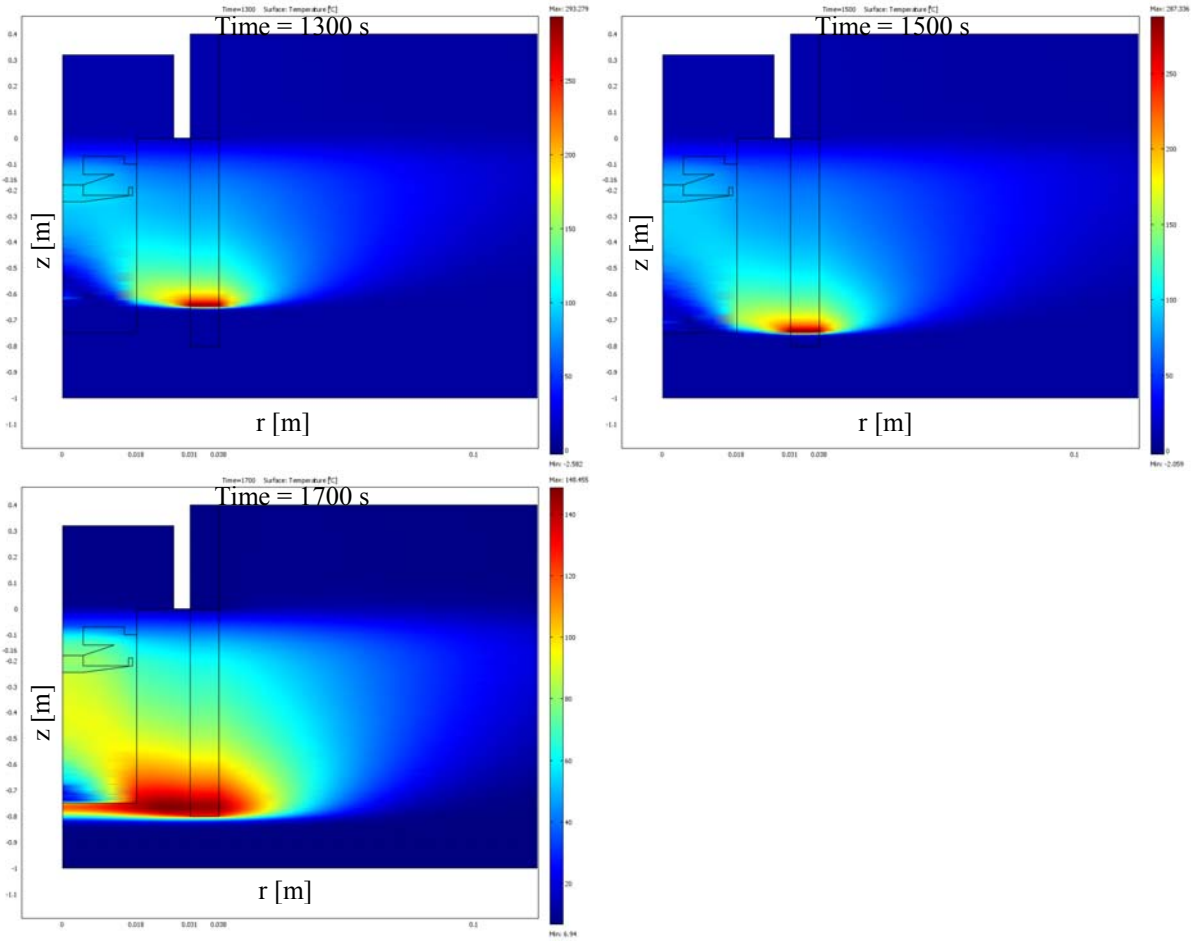


**Figure A. 1 (Continued).**

## Simulation with fixed temperature boundary condition on the drill bit

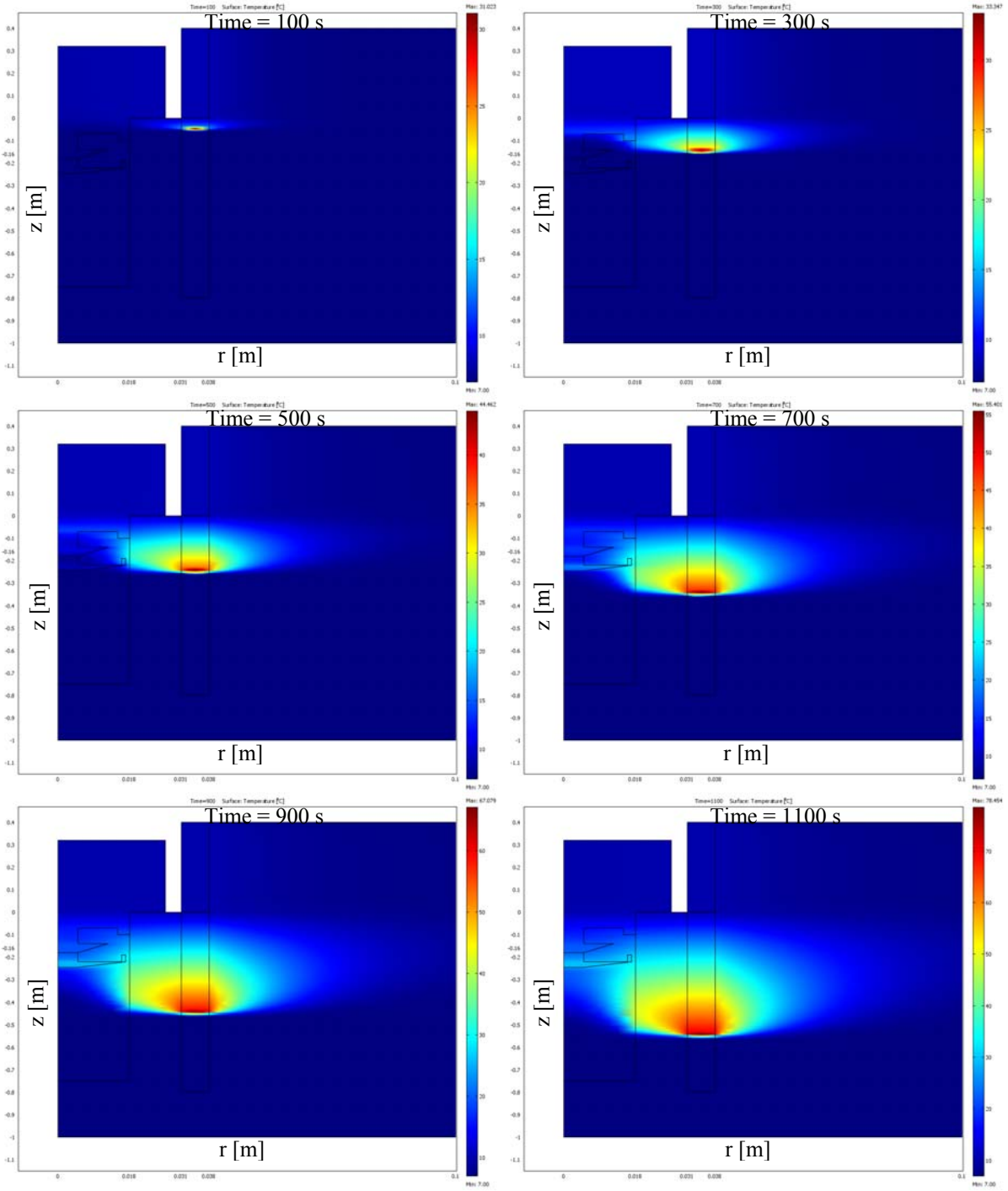


**Figure A. 2 Plots of temperature distributions for different time steps, Simulation with fixed temperature boundary condition on the drill bit.**

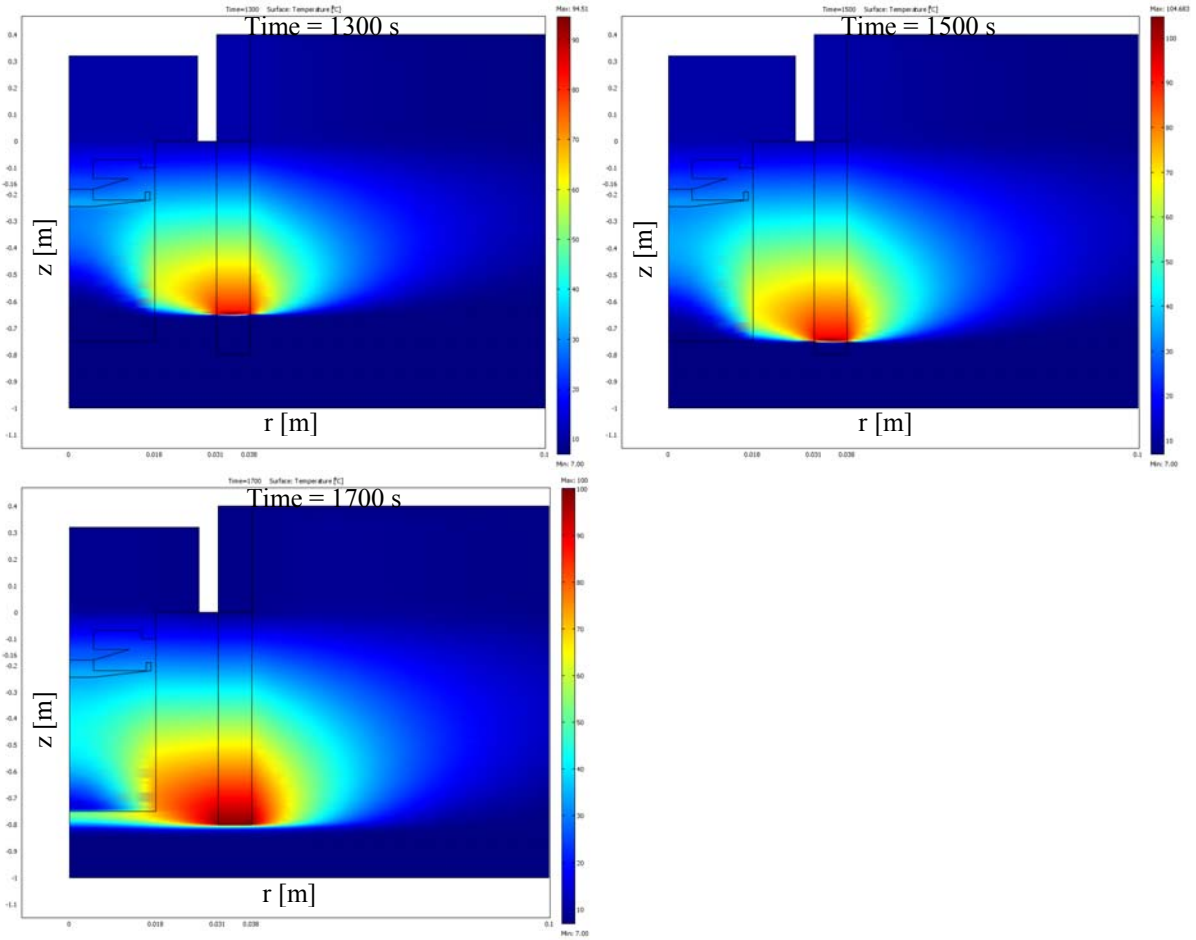


**Figure A. 2 (Continued).**

# Appendix B

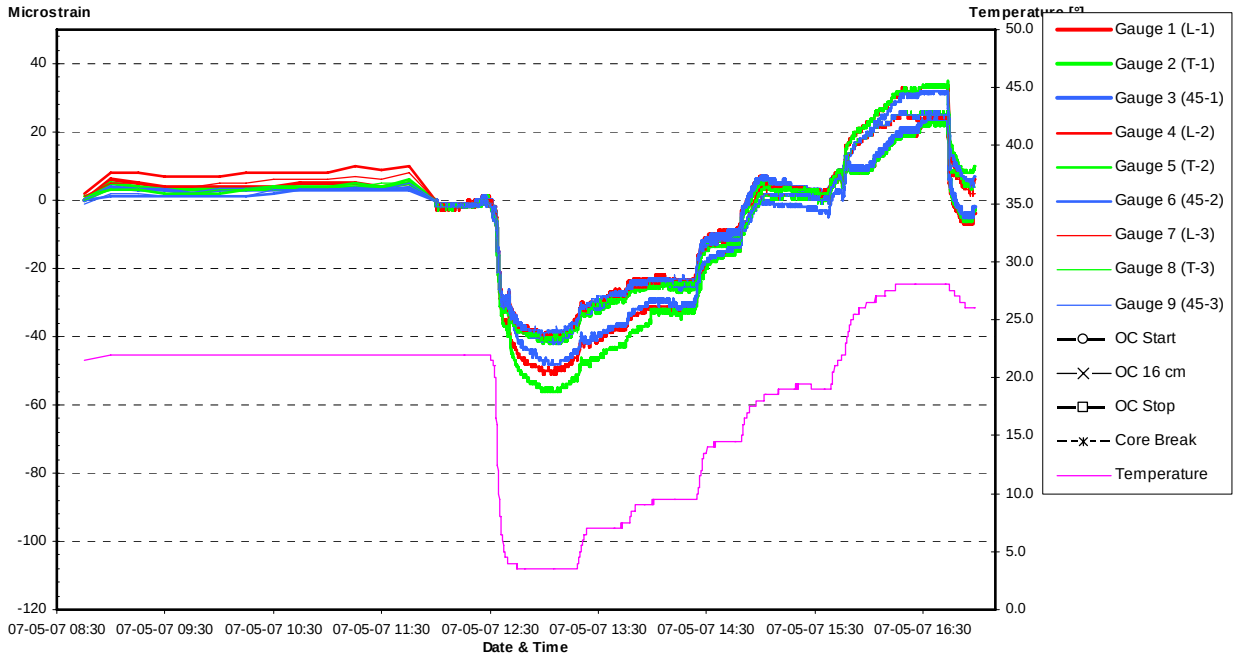


**Figure B. 1 Raw data chart of recorded strains and temperature during the first stepwise heating of the *Borre* cell.**

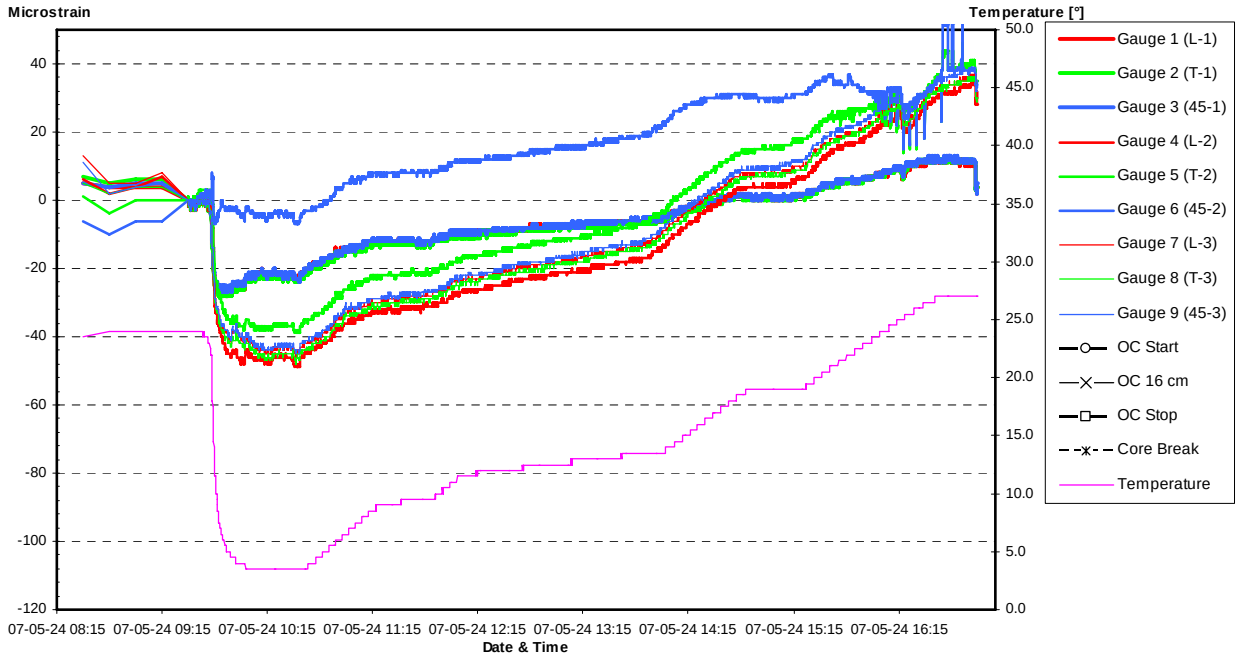


**Figure B. 2 Raw data chart of recorded strains and temperature during the second stepwise heating of the *Borre* cell.**

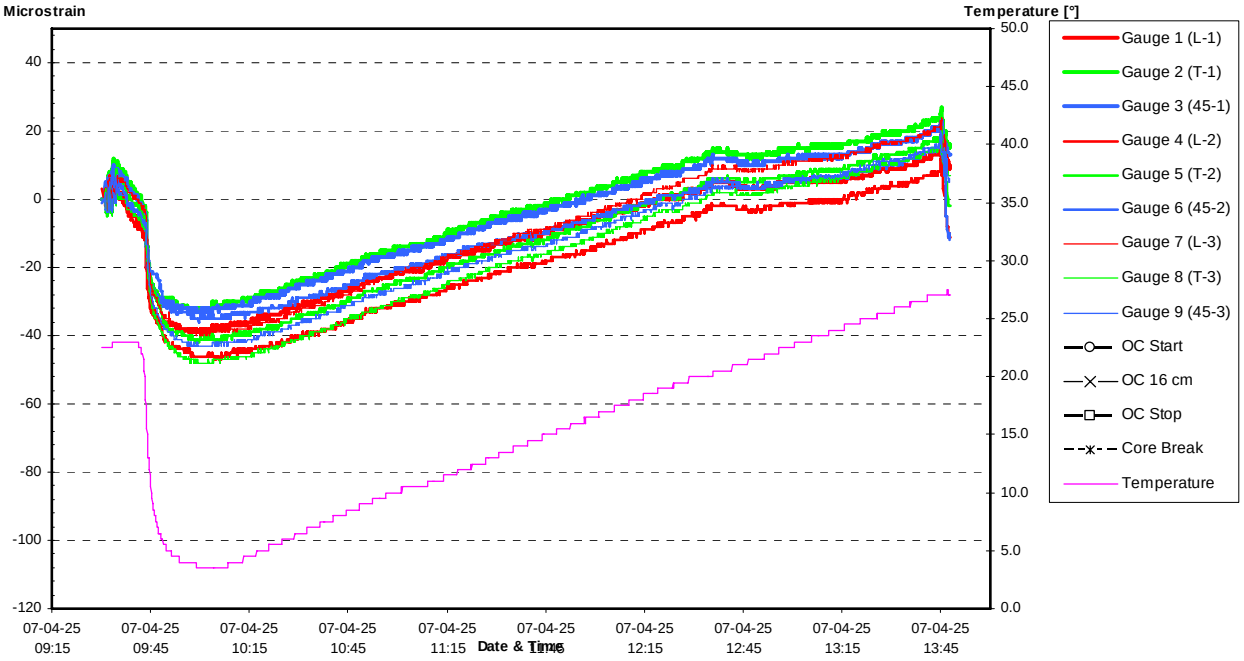


**Figure B. 3 Raw data chart of recorded strains and temperature during the first continuous heating of the *Borre* cell.**

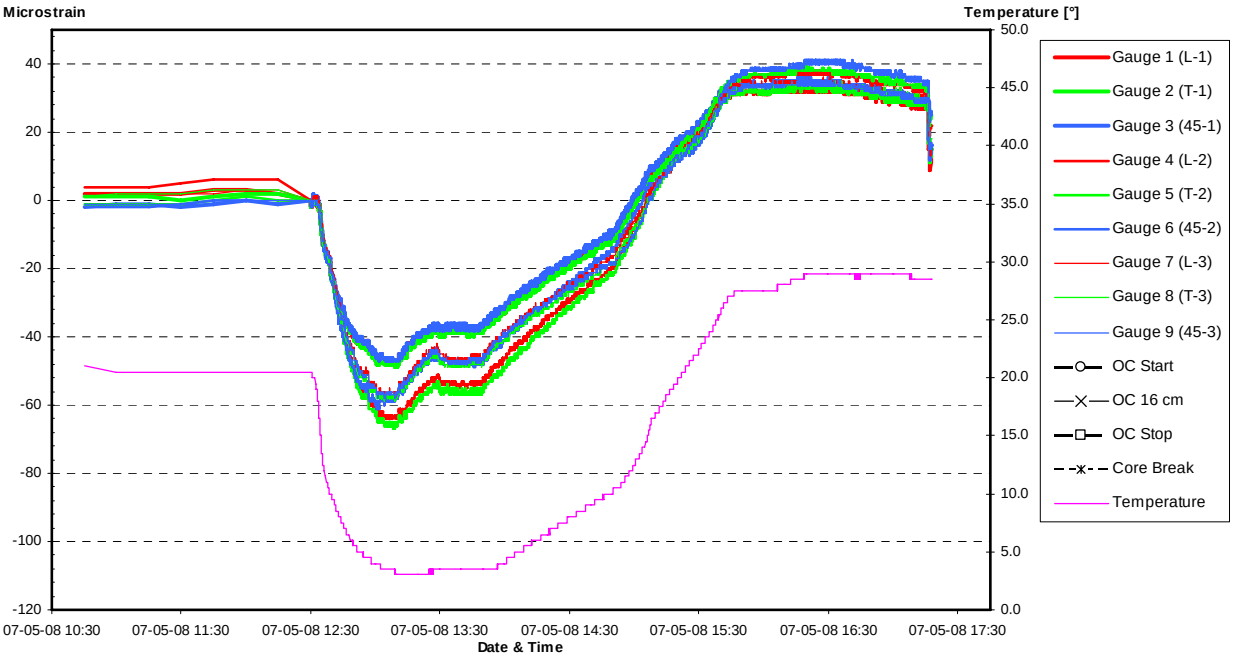


**Figure B. 4 Raw data chart of recorded strains and temperature during the second continuous heating of the *Borre* cell.**

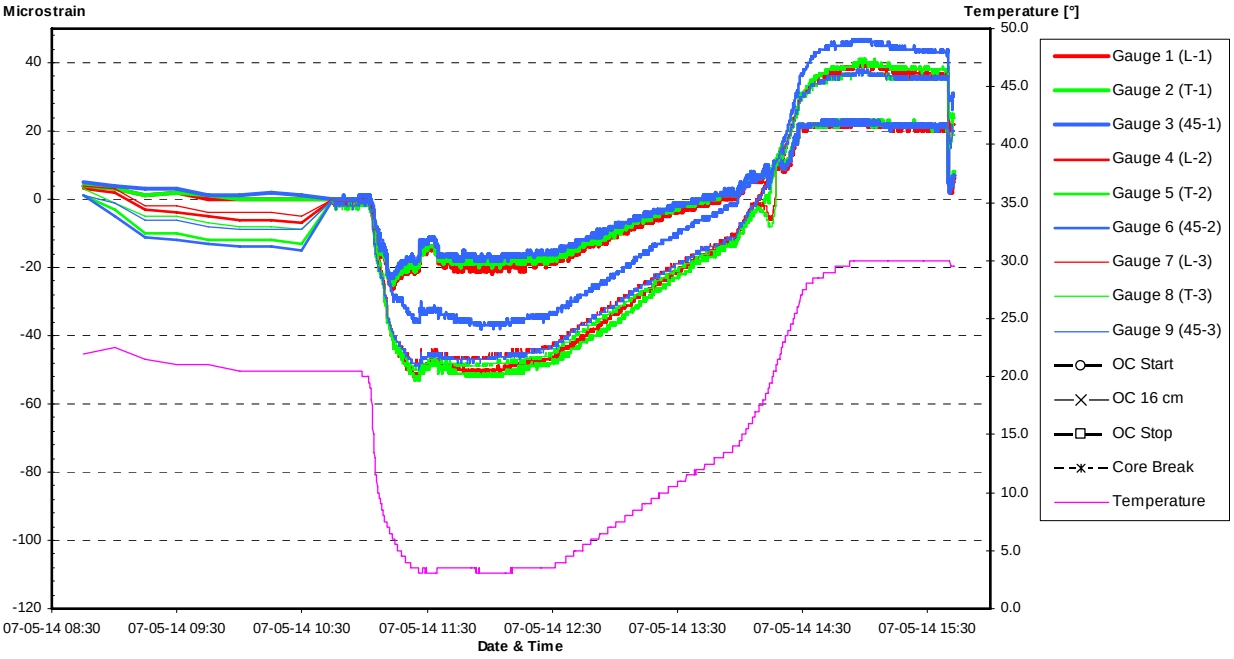


**Figure B. 5 Raw data chart of recorded strains and temperature during the third continuous heating of the *Borre* cell.**

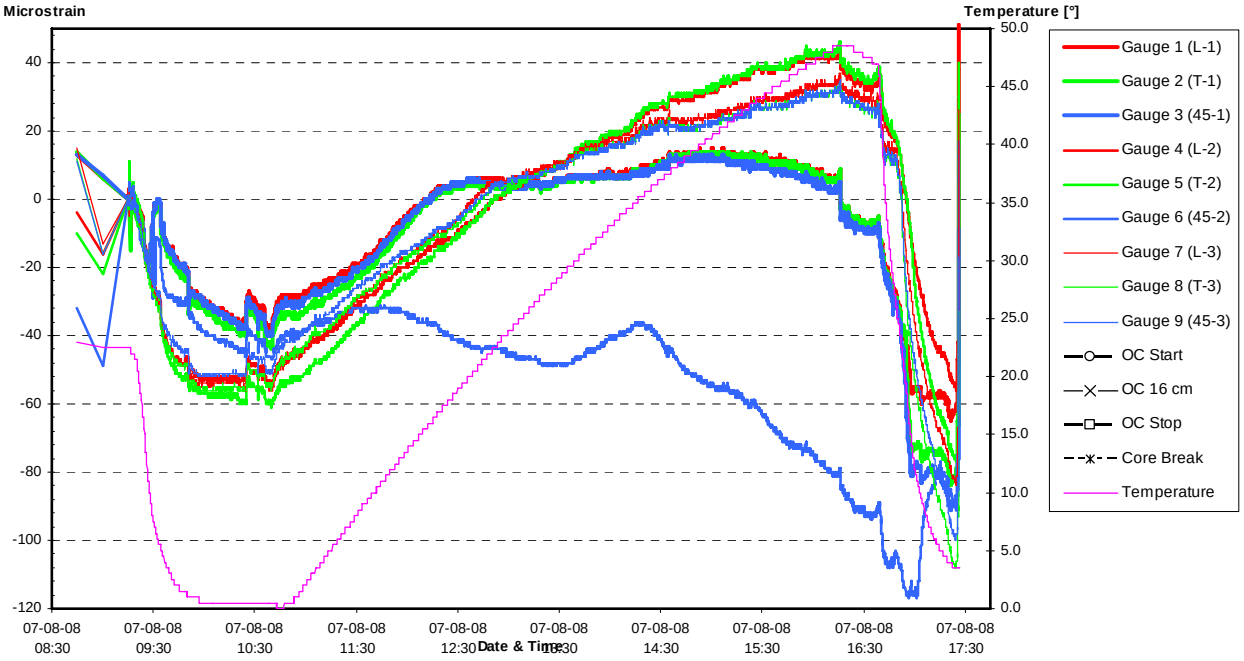


**Figure B. 6 Raw data chart of recorded strains and temperature during the fourth continuous heating of the *Borre* cell.**

# Appendix C

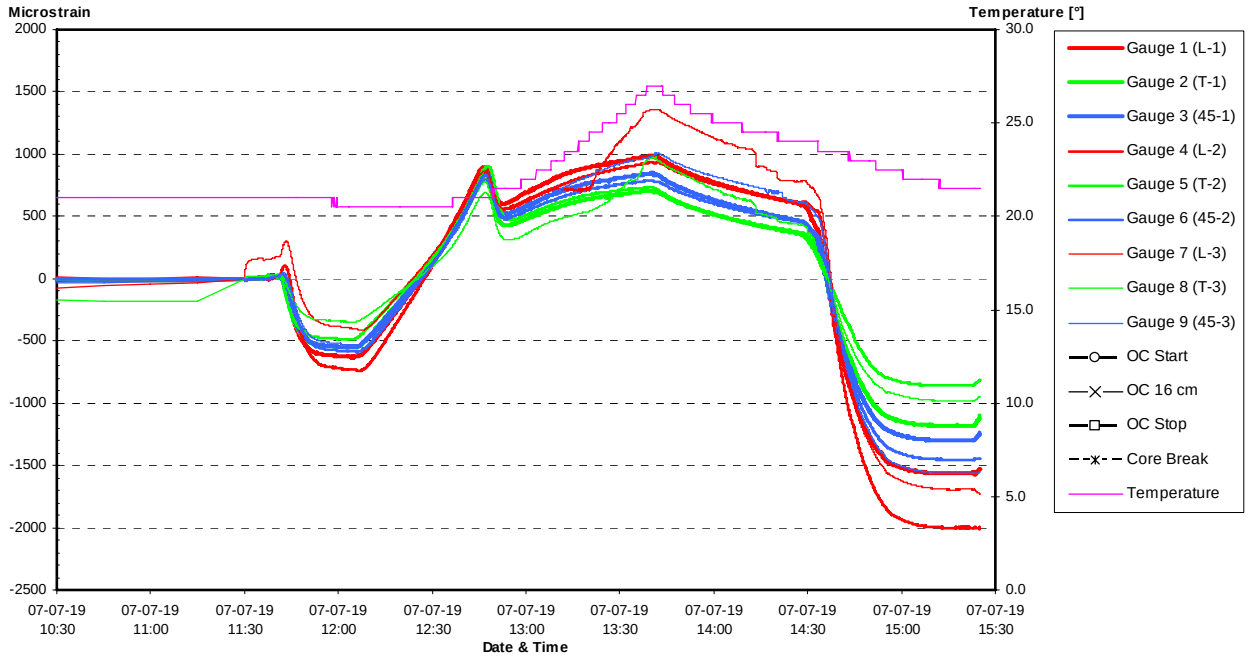


**Figure C. 1 Raw data chart of recorded strains and temperature during the first heating of the glue pot.**

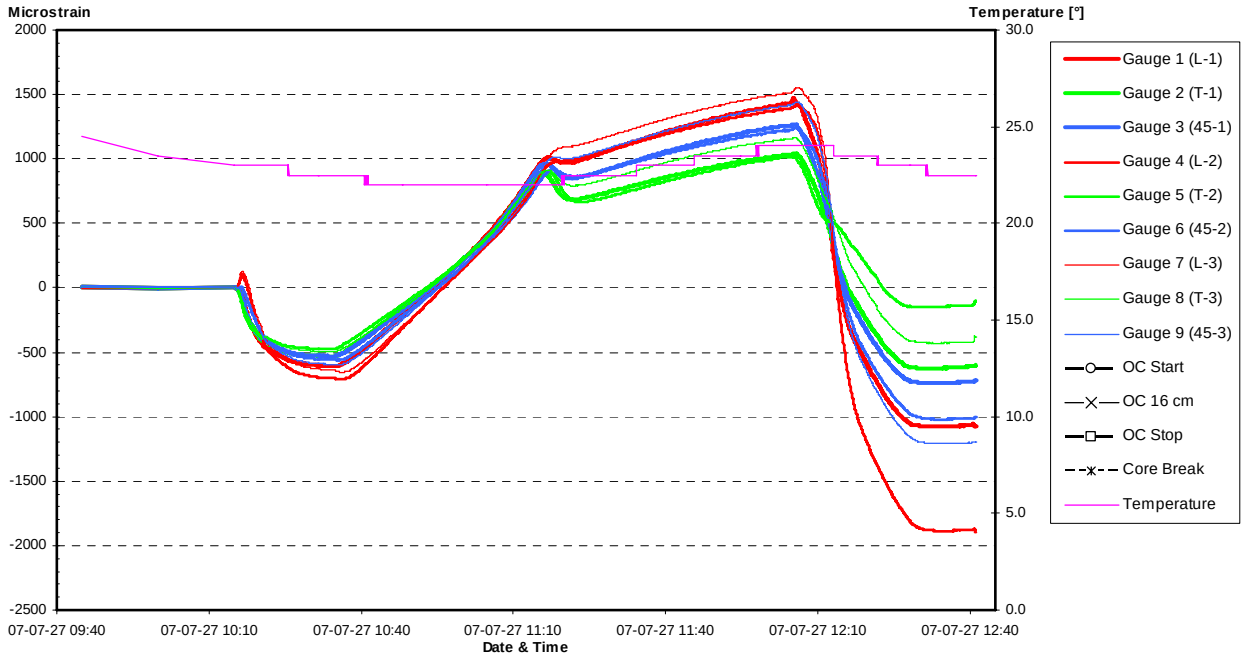


**Figure C. 2 Raw data chart of recorded strains and temperature during the second heating of the glue pot.**

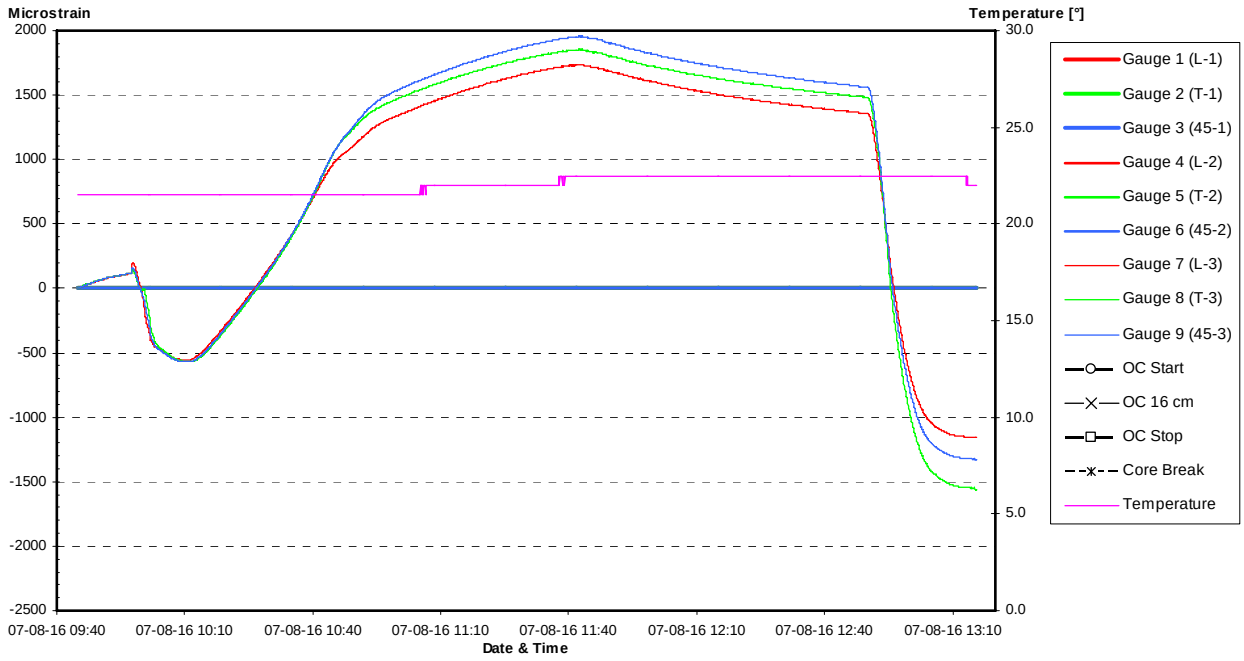


**Figure C. 3 Raw data chart of recorded strains and temperature during the first heating of the glue lump.**

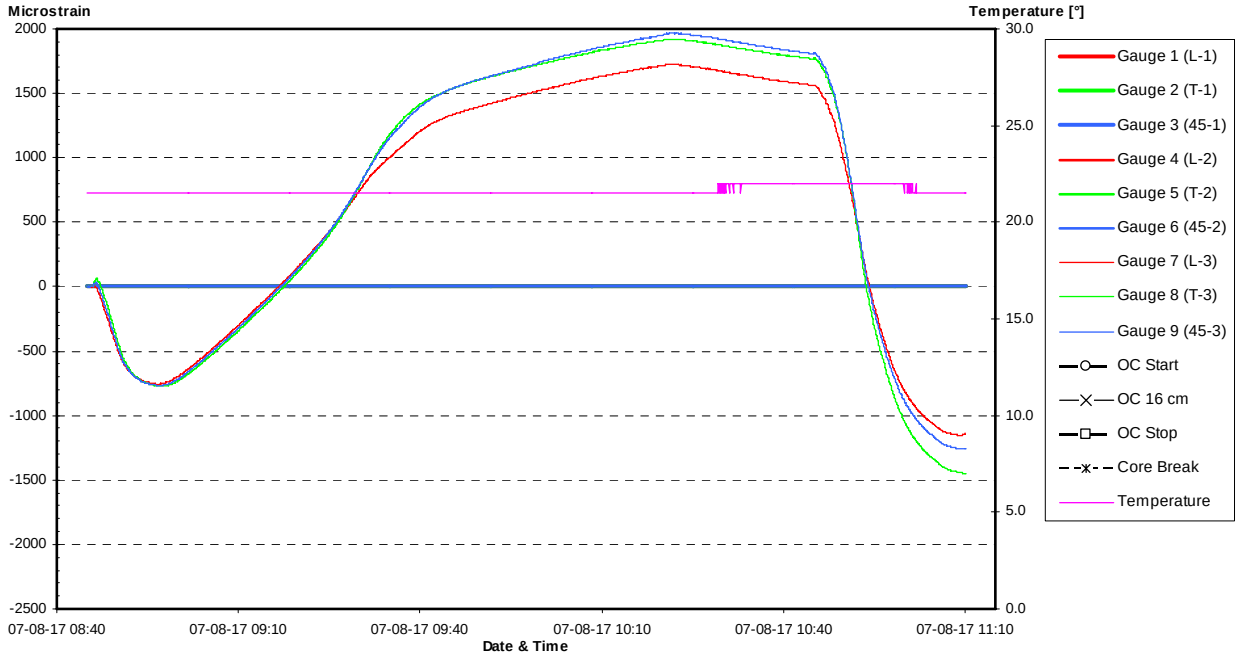


**Figure C. 4 Raw data chart of recorded strains and temperature during the second heating of the glue lump.**

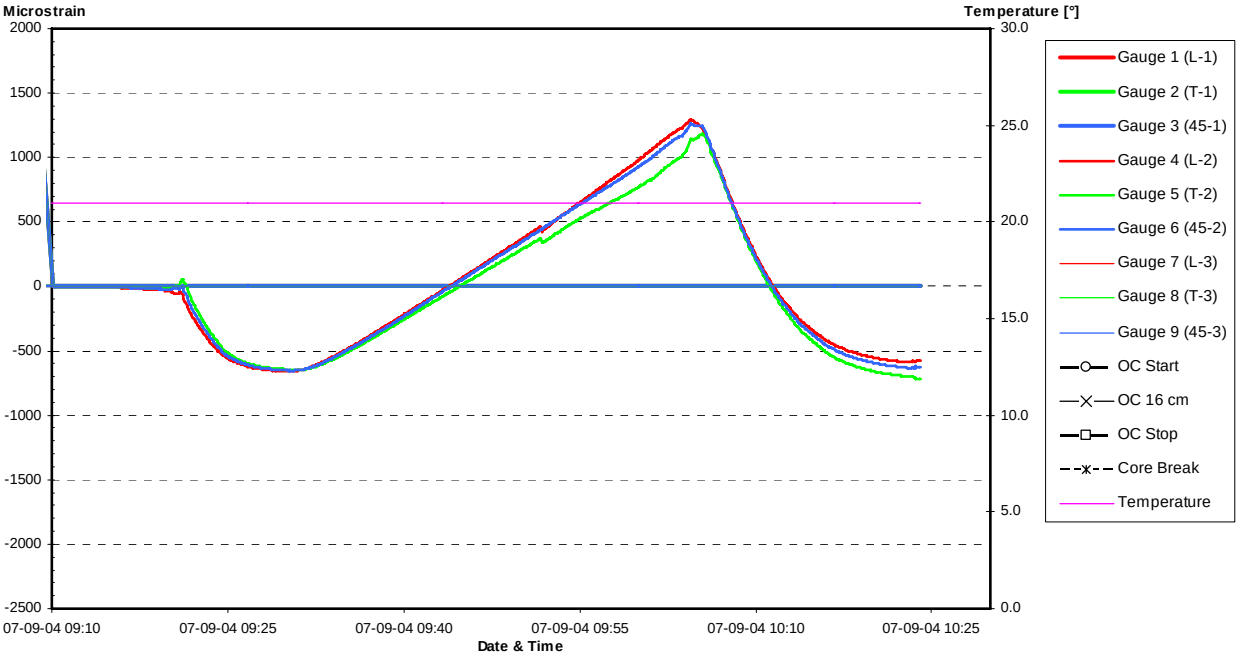


**Figure C. 5 Raw data chart of recorded strains and temperature during the third heating of the glue lump.**

# Appendix D

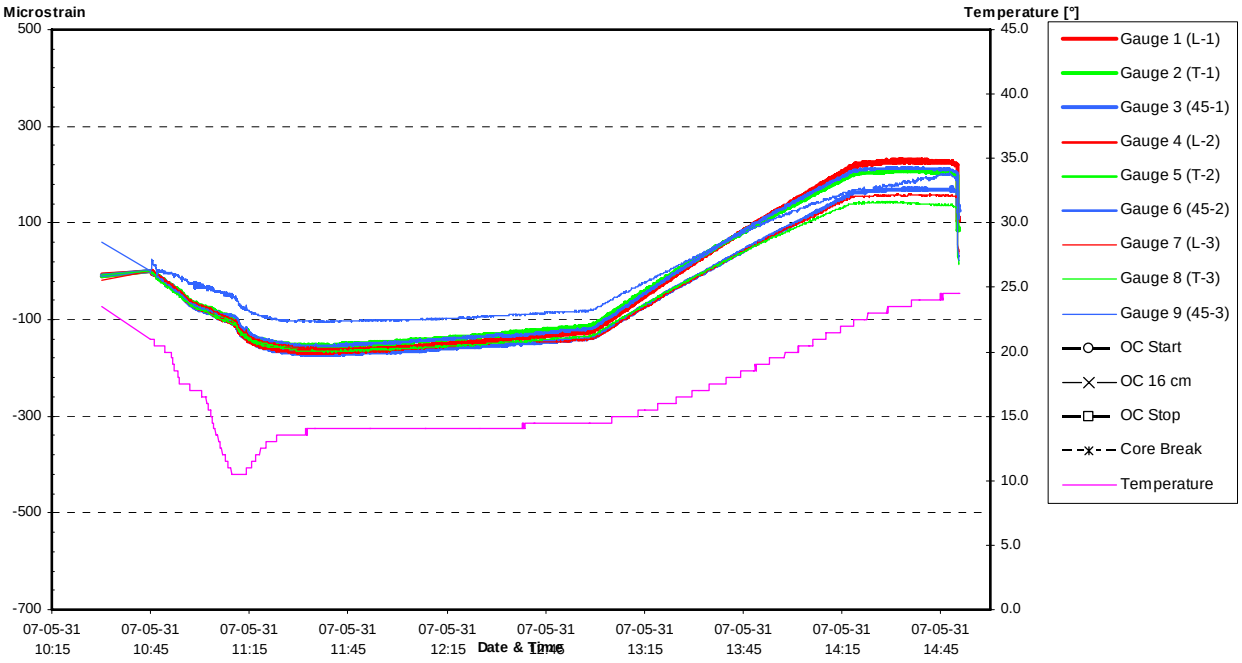


**Figure D. 1 Raw data chart of recorded strains and temperature during the first heating of the new aluminium cylinder, installation A.**

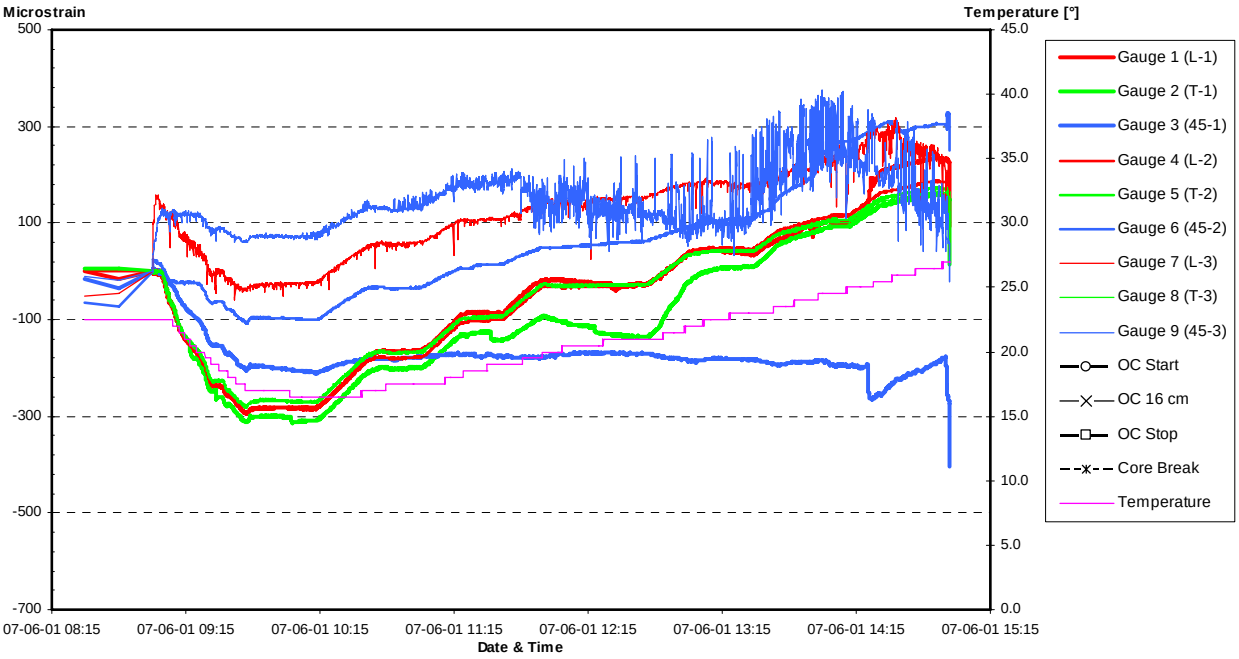


**Figure D. 2 Raw data chart of recorded strains and temperature during the second heating of the new aluminium cylinder, installation A.**

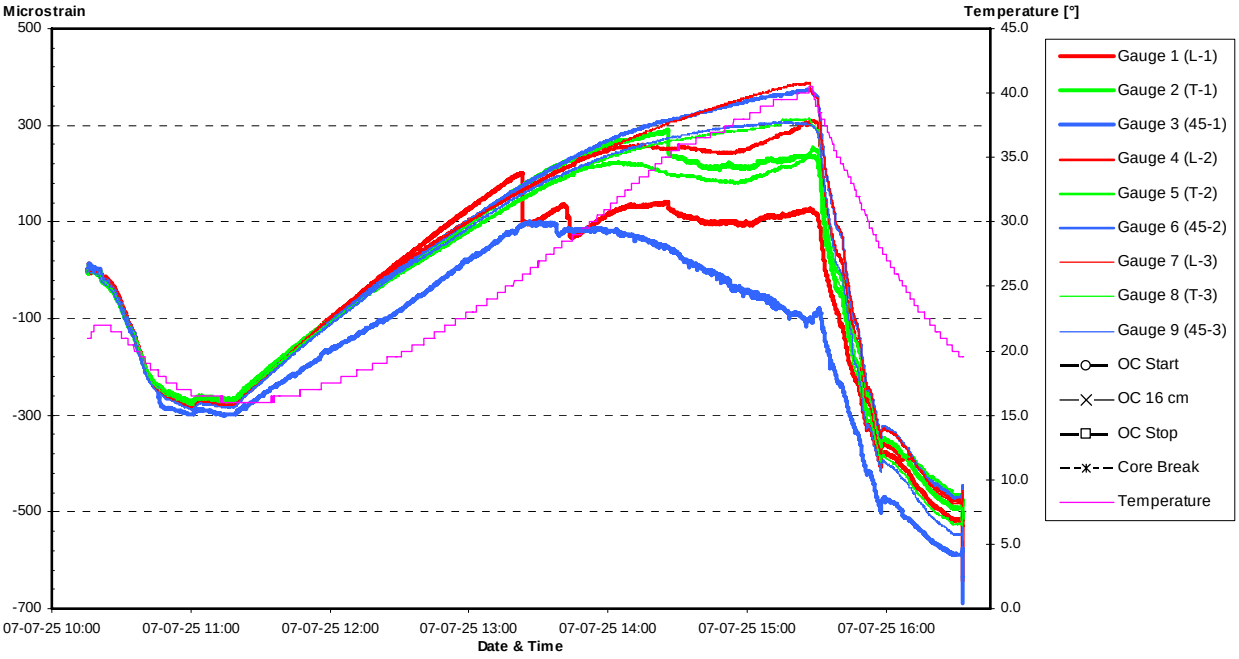


**Figure D. 3 Raw data chart of recorded strains and temperature during the first heating of the new aluminium cylinder, installation B.**

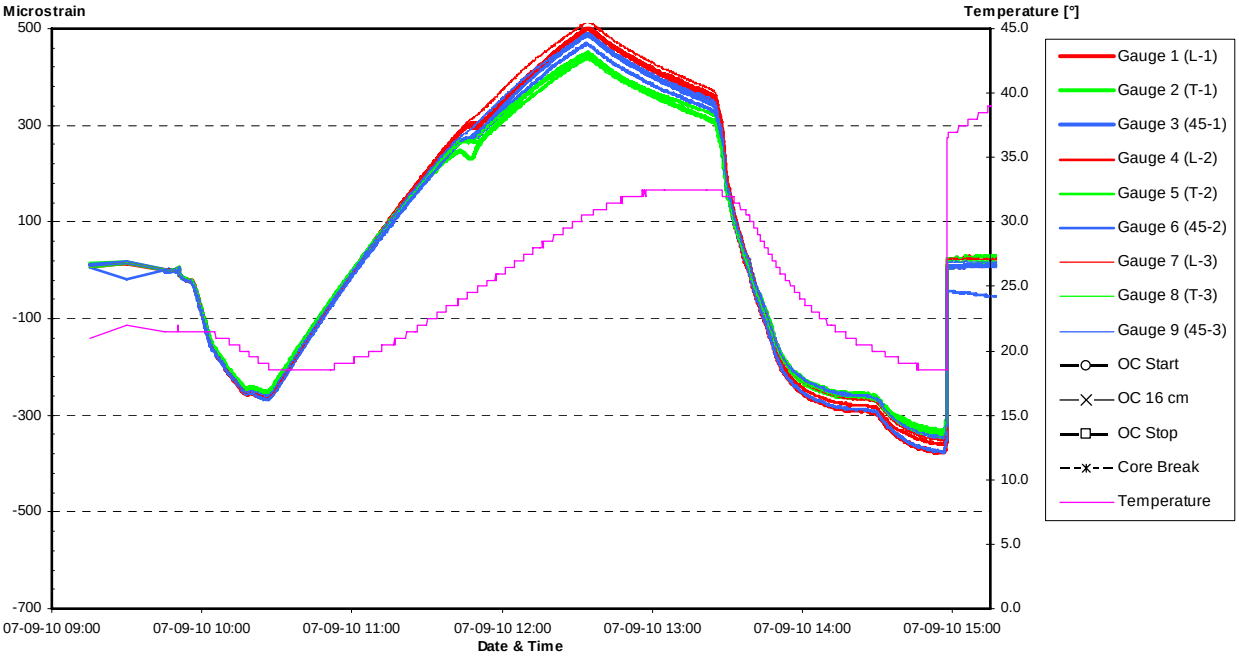


**Figure D. 4 Raw data chart of recorded strains and temperature during the first heating of the new aluminium cylinder, installation C.**

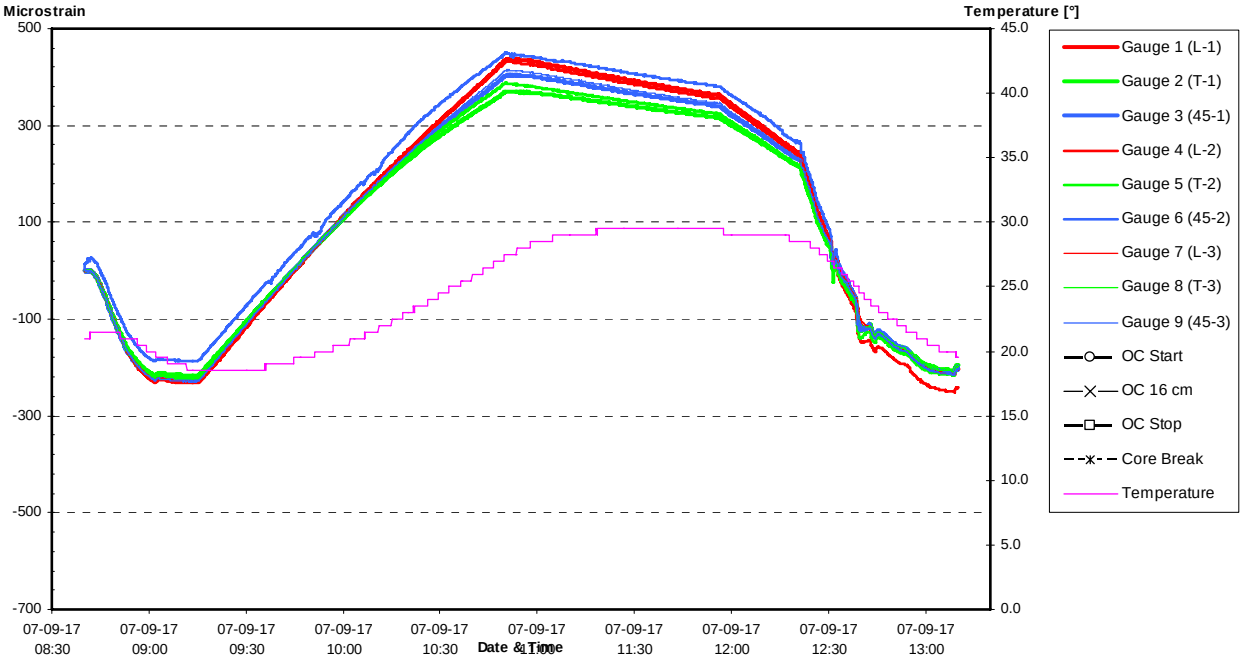


**Figure D. 5 Raw data chart of recorded strains and temperature during the second heating of the new aluminium cylinder, installation C.**

# Appendix E

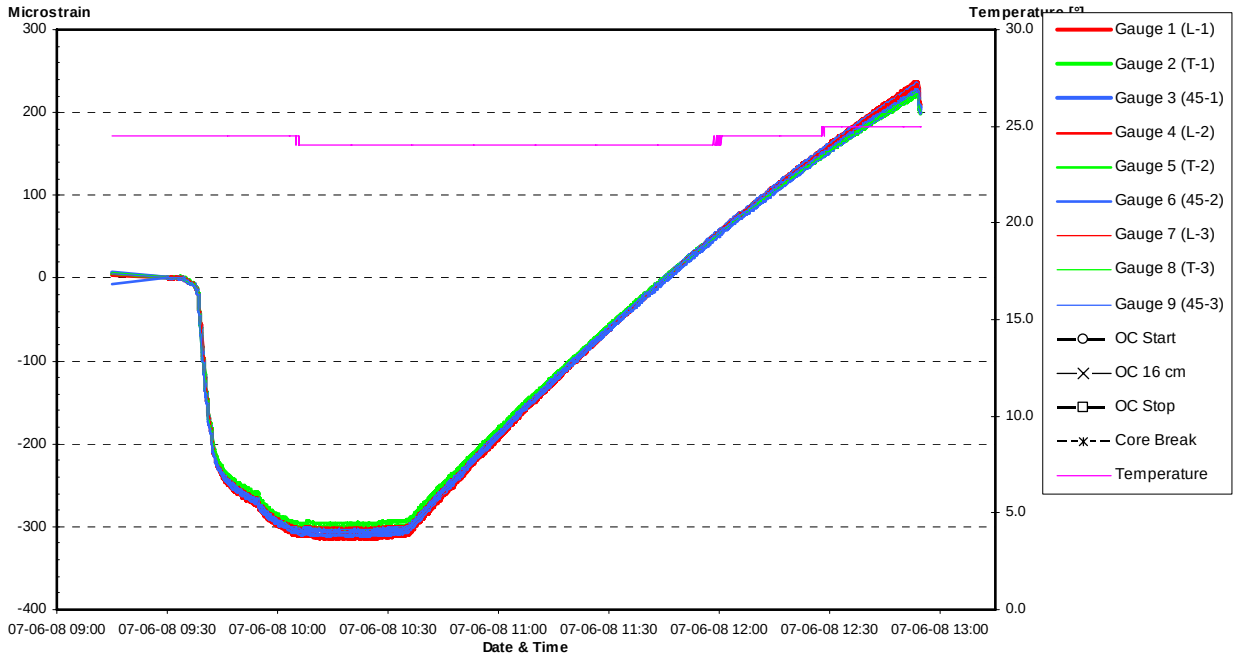


**Figure E. 1 Raw data chart of recorded strains and temperature during the first heating of the old aluminium cylinder.**

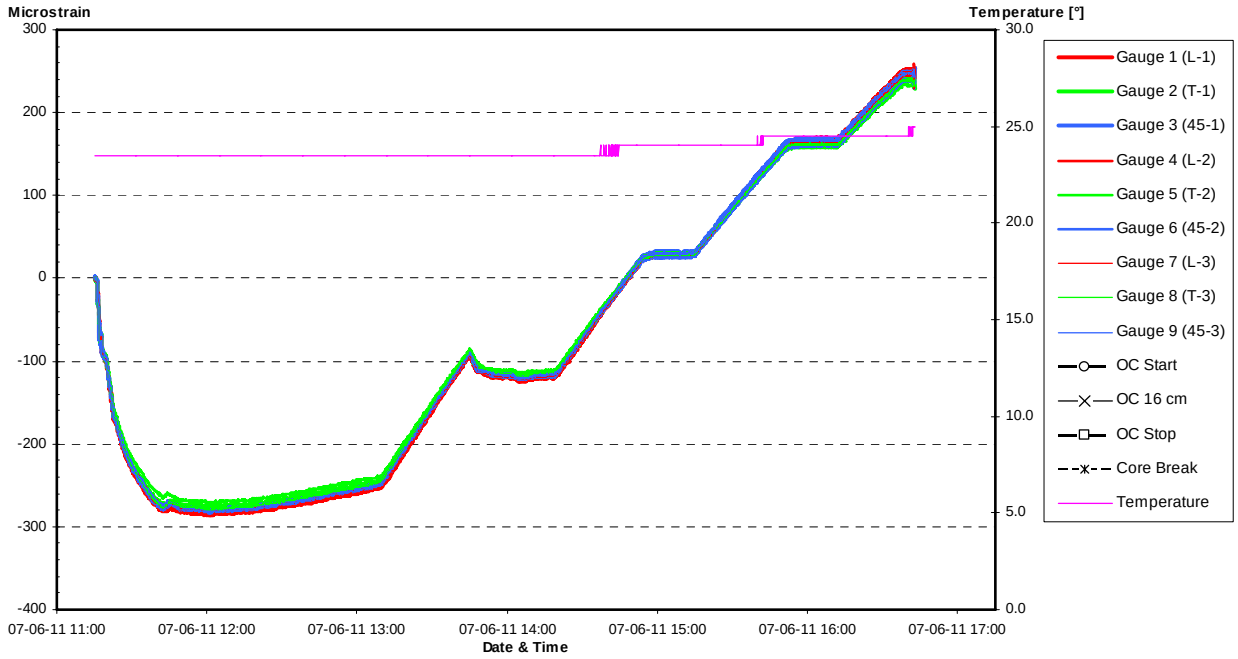


**Figure E. 2 Raw data chart of recorded strains and temperature during the second heating of the old aluminium cylinder.**

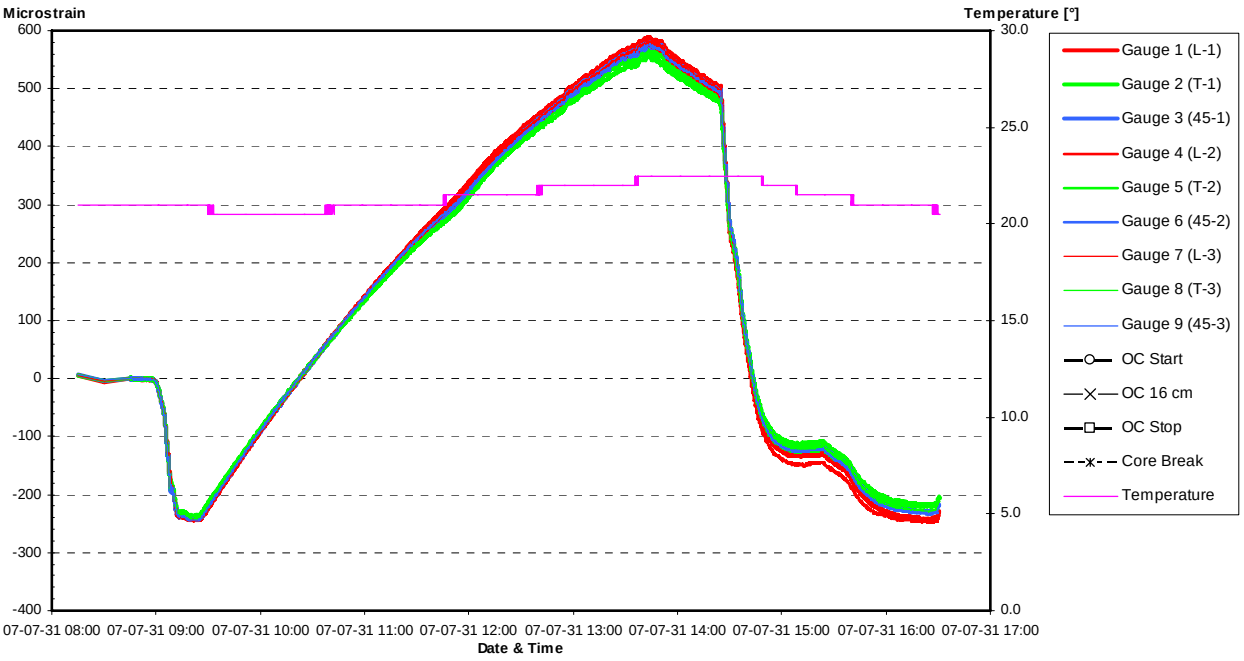


**Figure E. 3 Raw data chart of recorded strains and temperature during the third heating of the old aluminium cylinder.**

# Appendix F

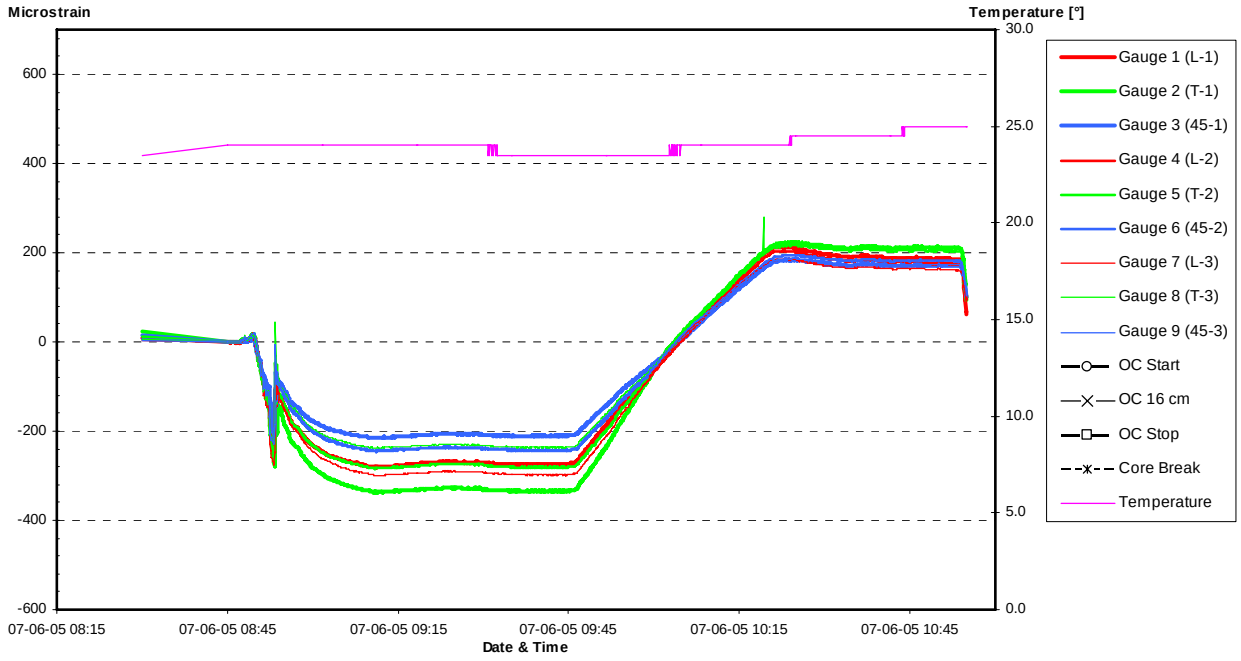


**Figure F. 1 Raw data chart of recorded strains and temperature during the first heating of the aluminium slab.**

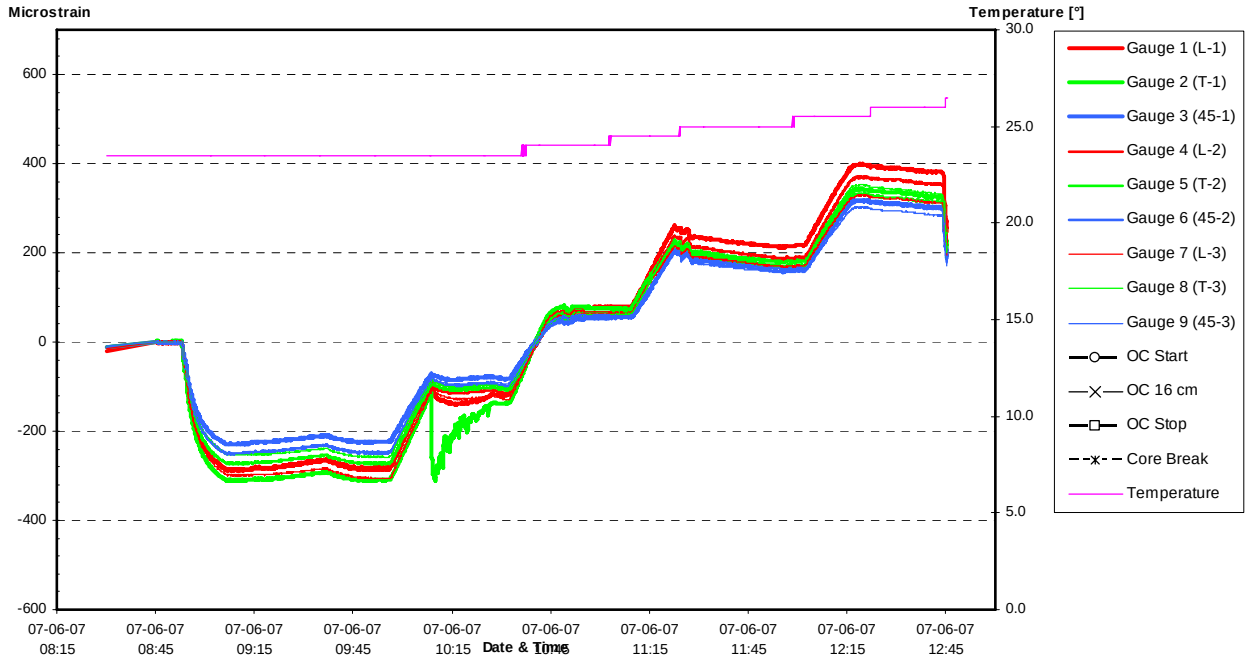


**Figure F. 2 Raw data chart of recorded strains and temperature during the second heating of the aluminium slab.**

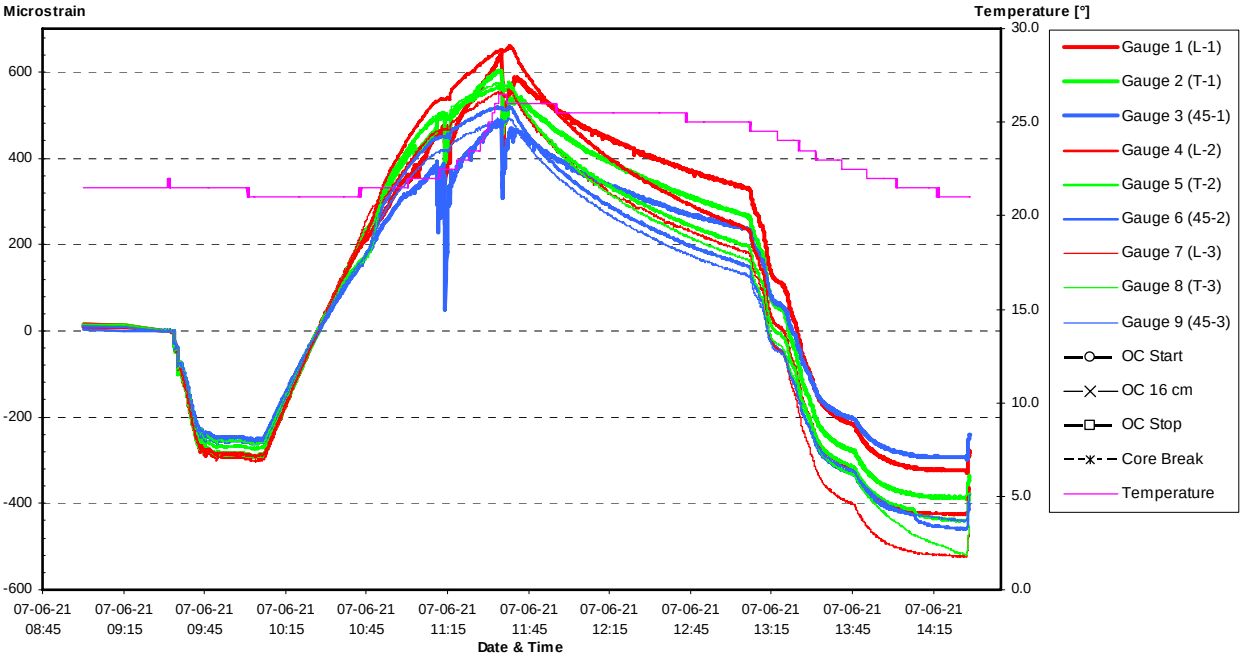


**Figure F. 3 Raw data chart of recorded strains and temperature during the third heating of the aluminium slab.**

# Appendix G

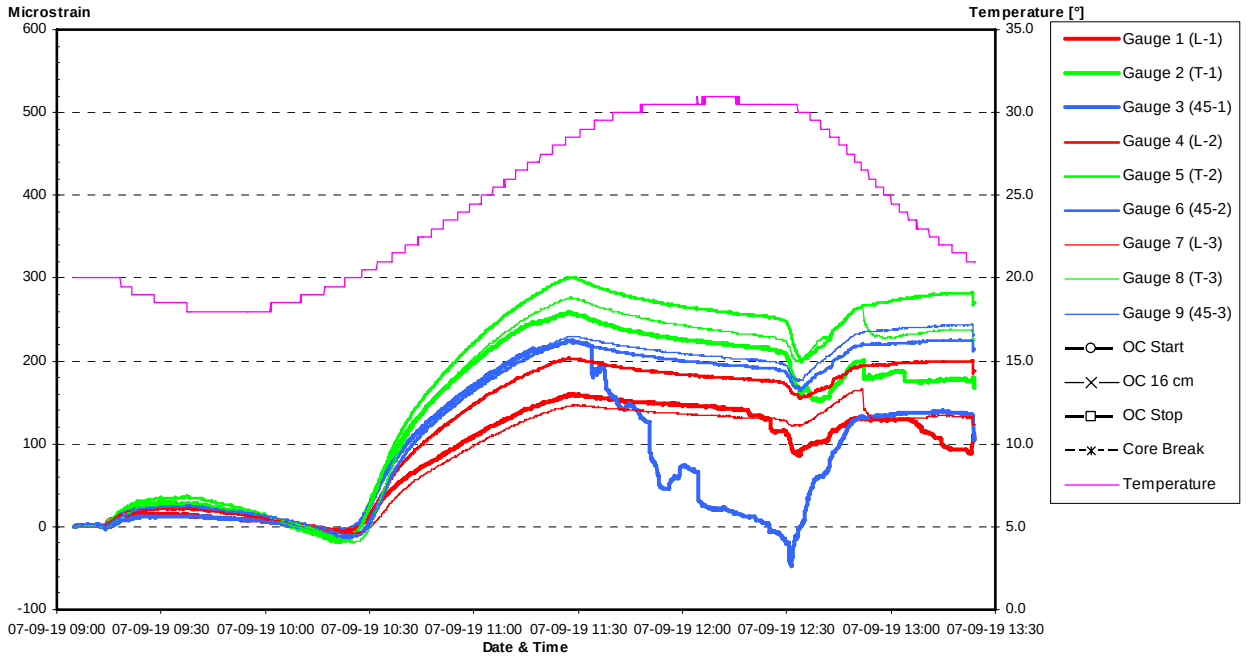


**Figure G. 1 Raw data chart of recorded strains and temperature during the first heating of the rock core, first installation.**

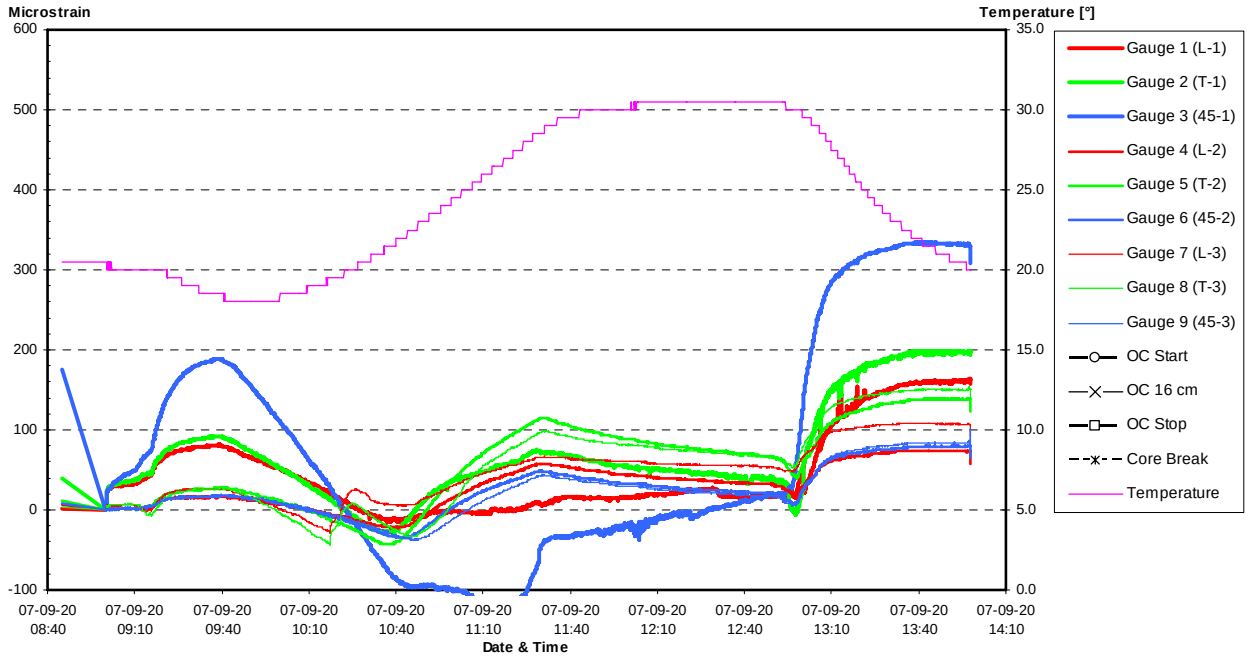


**Figure G. 2 Raw data chart of recorded strains and temperature during the second heating of the rock core, first installation.**

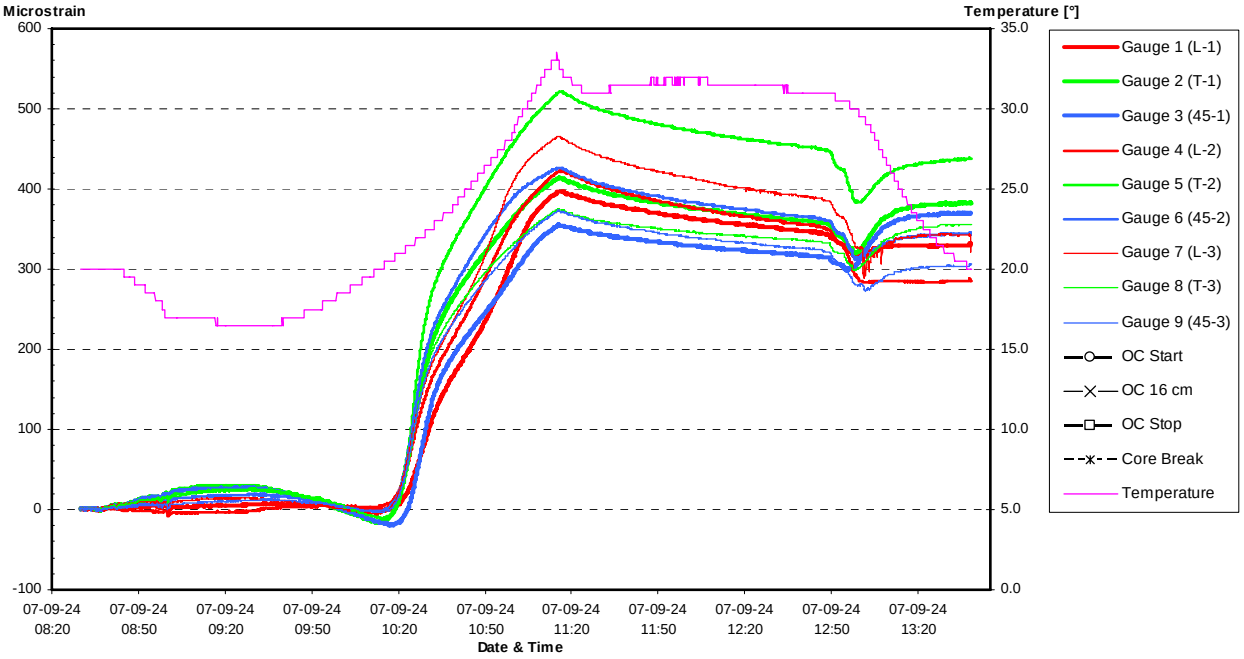


**Figure G. 3 Raw data chart of recorded strains and temperature during the first heating of the rock core, second installation.**